Final Report

Project Title: Reliable, Efficient and Cost-effective Electric Power Converter for Small Wind Turbines Based on AC-link Technology

Covering Period: September 30, 2003 to March 31, 2006

Date of Report: June 20, 2006

Recipient: Princeton Power Systems
501 Forrestal Road
Princeton, NJ 08540
www.princetonpower.com

Award Number: DE-FG36-03GO13134

Contact: Darren Hammell – Princeton Power Systems – (609) 258 5994
Mark Holveck – Princeton Power Systems – (609) 258 5994

DOE Contact: DOE Field Project Officer – Keith Bennett

DOE Golden Field Office
1617 Cole Blvd
Golden, CO 80401
303.275.4700

Working Partners: Finger Lakes Engineering, Northern Power Systems, Bergey Windpower
Cost-Sharing Partners: Finger Lakes Engineering, Northern Power Systems, Bergey Windpower

COMPLETED TASKS:

<u>task 1.1</u>: **Certification Planning**
<u>task 2.0</u>: **Identification of converter requirements**
<u>task 3.0</u>: **System design**
<u>task 3.1</u>: **Power Electronics Components Specifications**
<u>task 3.2</u>: **Design and Modeling of Operational Algorithms**
<u>task 3.3</u>: **Design and layout of control circuit boards**
<u>task 4.0</u>: **Breadboard Prototype Development**
<u>task 4.1</u>: **Manufacture and delivery of power electronics**
<u>task 4.2</u>: **Manufacture and delivery of control boards**
<u>task 4.3</u>: **Integration of controls and power electronics**
<u>task 4.4</u>: **Program the control microprocessor**
<u>task 4.5</u>: **Procurement and installation of testing setup**
<u>task 5.0</u>: **Breadboard Prototype Testing**
<u>task 5.1</u>: **Basic Operational Testing on Static Load**
<u>task 5.2.1</u>: **Generator Control**
<u>task 5.2.2</u>: **Grid Interaction**
<u>task 5.3.1</u>: **Full System Test (Normal Conditions)**
<u>task 5.3.2</u>: **Dynamic Conditions**
<u>task 6.1:</u> **Software, Algorithm Modifications**
<u>task 6.2:</u> **Power Electronics Design Modifications**
<u>task 6.3:</u> **Control Board Design Modifications**
<u>task 7.1:</u> **Power Electronics Manufacture and Delivery**
<u>task 7.2:</u> **Control Board Manufacture and Delivery**
<u>task 7.3:</u> **Integration and Validation Testing**
<u>task 8.1:</u> **Subsystem Testing**
<u>task 8.2:</u> **Full System Testing**
<u>task 8.3:</u> **UL 1741 Testing**
<u>task 9.1:</u> **Site Prep**
<u>task 9.2:</u> **Shipping and Installation**
<u>task 9.3:</u> **Startup**
<u>task 9.4:</u> **Steady-state Testing**
<u>task 9.5:</u> **Testing for Certification Compliance**
<u>Task 10.1:</u> **Analysis of Testing Results**
<u>Task 10.2:</u> **Hardware and Software Modifications**
<u>Task 10.3:</u> **Build Production Prototype**
<u>Task 10.4:</u> **Shipment and Installation**
<u>Task 10.5:</u> **Performance Testing**
<u>Task 9.6.1</u> **Final Project Report**
<u>Task 9.6.2</u> **Final Project Review**

Summary and Major Milestones Achieved

Project Objective: - Design, build, and test a reliable, efficient, 50kW, 480VAC 3-phase grid-tied inverter for small wind turbine applications, based on the AC-link power conversion technology.

Background: - Grid-tied inverter power electronics have been an Achilles heel of the small wind industry, providing opportunity for new technologies to provide lower costs, greater efficiency, and improved reliability. The small wind turbine market is also moving towards the 50-100kW size range. The unique AC-link power conversion technology provides efficiency, reliability, and power quality advantages over existing technologies, and Princeton Power will adapt prototype designs used for industrial asynchronous motor control to a 50kW small wind turbine design.

1. In-house Testing Setup Design and Build
2. C&F Design, Build
3. C&F Modifications for Commercial Acceptance
4. C&F Field Test (Sandia National Lab's Distributed Energy Test Lab)
5. Pre-Production Prototype Build
6. Pre-Production Prototype Field Test (Sandia's DETL)

This contract and continued support from the DOE, National Wind Technology Center, and Sandia National Labs Wind Technology department and Distributed Energy Test Lab have been crucial in bringing our technology from the concept stage to working prototypes. Prototype operation has been verified through testing at Sandia's world-class facilities, and the operation of the technology has been validated. Princeton Power is planning to take the next steps toward commercializing the technology for small wind applications, to join in the efforts to make the economic case for wind power more compelling and more attractive to potential customers.

In particular, we would like to acknowledge the following people for their invaluable efforts in supporting this project:

Mark Rumsey
Trudy Forsyth
Lee J. Fingerish
Keith Bennett
Sigifredo Gonzalez
Juan Ortiz-Moyet

Next Steps
As part of Princeton Power's efforts to commercialize the AC-link^{TM} small wind product, we are planning on shipping the unit to Bergey Windpower's facility in Norman, OK, and to install the converter and run functional tests on the XL50 50kW turbine installed on-site. The installation and testing should take 3-4 days once the converter is on-site. This testing is tentatively scheduled for March 13-15, depending on the availability of the Bergey turbine. Following the testing, we will analyze the results and write a testing report.

We are also talking to UL representatives about testing our motor control product to UL 508c, and our grid-tied products to UL 1741. These listings will both apply to the wind converter, and we hope to have them completed by June 2006.

Related to this project, we recently began development of a grid-tied solar inverter for the 20-200kW power range. We hope to leverage work done on grid-interaction during this project for the solar product also. We also plan to leverage the relationship we developed with Sandia's DETL to perform testing of the inverter prototypes to UL 1741 and IEEE 1547 standards. Due to the close hardware relationship of each AC-link^{TM} product, success in developing and testing the inverter will help to reduce cost and grow the market for the wind converter.

Finally, as part of our internal efforts to commercialize our industrial variable speed motor controller based on AC-link^{TM}, we have launched an ambitious project to reduce the materials cost of a 75kW unit by about 25% in low volumes. This will directly impact the production cost of the small wind converter, allowing it to be produced for less, and making this a more attractive business and market for Princeton Power. This in turn may help attract further investment into the technology and development for the wind market in general.

In summary, we plan to pursue commercialization of this product in conjunction with other programs to leverage the similar hardware topology we can use for each. We still must count on development of a stronger market for small wind turbines in the 20-100kW range, but we think this is likely with continued support from the DOE and if trends in the energy market continue in the same direction.

Detailed Project Activities (Compiled Quarterly Reports)

<u>task 1.1</u>: **Certification planning**

The UL 1741 standard was investigated, two team members attended a relevant IEEE1547 meeting and met with UL representatives. The PPS team has a strong idea of UL 1741 concepts and has a plan to design the converter for UL 1741. During the course of the project, PPS was performing another development project for which a hardware design was generated that enabled us to reduce the materials cost of the converter. Near the end of this project, we switched to the new hardware design. Our plan is to have this new design listed under UL1741 and UL508c (industrial motor drives) by mid-2006.

<u>task 2.0</u>: **Identification of converter requirements**

After several meetings with Northern Power Systems (NPS) and Bergey Windpower, we were able to formulate specifications for the converter. These specifications were drawn up in accordance with requirements described by both Bergey and NPS. The baseline design is for the Bergey XL50 turbine, since this was the closest turbine to commercial feasibility that we were aware of at the time the specification was determined. The operational requirements are fairly similar for all of the turbines we have researched, so adapting the converter to different makes and models should be very straightforward – the converter will be compatible with most turbines.

See Appendix A for the specification of the C&F converter.

<u>task 3.0</u>: **System design**

<u>task 3.1</u>: **Power electronics components specifications**

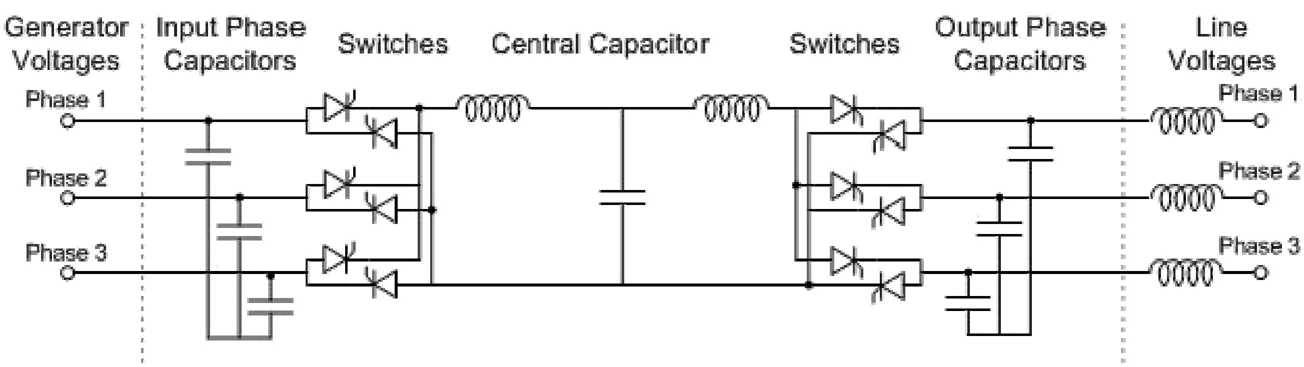

Figure 1 – AC-link™ circuit diagram

In Q4 2003, the PPS team met with both Northern Power Systems and Bergey Windpower to discuss their requirements for a small wind inverter. From these discussions we were able to design the appropriate specifications for this particular design. Bergey Windpower was able to furnish us with their requirements for an inverter which we have used as a starting point for our design.

The general power electronic component specifications were generated by first designing the system to meet the power conversion specification, and then analyzing the conditions under which each component will operate. The values of the capacitances and inductances within the system were produced using AC-link system design software that produces all the required values based on the desired system parameters of voltage and current. These parameters were taken from Bergey's specification.

The rating requirements for all of the power electronic components were generated by using Princeton Power's proprietary AC-link™ modeling software to simulate the operation of the wind power converter in various operating conditions. These simulations produced data that described the voltages and currents experienced by each component. Through analysis of this data, all of the component ratings were generated. The completed specifications were compiled by component for delivery to component manufacturers. These are available upon request.

After the preliminary design review, we were able to better determine the ratings for the major components. The component values for the converter are derived using pre-existing Princeton Power Systems software, which calculates the correct ratings and furnishes operational waveforms that the component must handle. These ratings and waveforms were sent to our manufacturing partners, along with design constraints for each component, and we worked together to come up with appropriate designs. The major components that were specified and designed were:

1. SCRs and SCR bridge (Motors & Controls, Dynex)
2. Filter inductors (NWL Inductors)
3. Filter capacitors (NWL Capacitors)
4. Charging and discharging inductors (NWL Inductors)
5. Central capacitor (NWL)

One of the issues that was prevalent in previous AC-link™ designs was audible noise emanating from the air-core charging inductors. Vacuum varnishing the inductor with an insulating resin reduced the noise but not to desired levels. For the C&F inductor design we are taking the further step of sinking the inductors completely in epoxy which should reduce audible noise further.

<u>task 3.2</u>: **Design and modeling of operational Algorithms**

Princeton Power Systems developed a C++ computer model of its AC-link™ system for use in the design and testing of control algorithms. In small time steps (~1us) the software models the physical state (voltage and current values) of the AC-link™ circuit and the application being simulated. This hardware emulation code receives its control inputs from a control system emulator, also part of the software. At each time step, data is output in a format readable by Matlab for plotting and analysis.

The control system emulator has been designed to mimic the timing and interrupt patterns of the actual DSP. Its variables receive data from the hardware emulator exactly like the DSP receives data from the sensors on the actual system. It then sets hardware variables for switch firing, just as the DSP will fire the SCR switches via the trigger board. This allows the engineering team to perform the majority of development in software on a PC before any operation is attempted on a real hardware system.

The following algorithms were developed for or modified to work on the small wind converter:

1) Synch algorithm for synchronizing the AC-link™ inputs and outputs to the signals from the wind turbine and grid
2) t1 firing time algorithm for allocating the correct amounts of charge to each input and output phase
3) Central capacitor voltage change filter algorithm
4) Inputvar algorithm, for regulating the central capacitor voltage
5) Pulse frequency modulation, for regulating the central capacitor voltage
6) Input and output voltage magnitude filtering algorithms
7) Pulse length prediction algorithms for preventing system faults
8) Inversion control algorithm
9) Outputvar algorithm (for controlling grid-side power factor)
10) Anti-islanding algorithm
11) Wind turbine control (for drawing the desired power from the source)

Each algorithm has been passed through a standard bring up process to get it from conception to operation on the system. Once each algorithm was designed on paper, they were coded into the computer model, tested and debugged. Approximations used in algorithms such as the pulse length prediction algorithm could be tested from a theoretical standpoint in this manner for accuracy. When they performed correctly, the algorithms were ported onto the DSP. Generally this transfer required an algorithm to be optimized, and if certain parts were time-critical, to be divided into process and preprocess code blocks. Once they were implemented in the DSP, the algorithms were tested against the model often by halting the DSP during a real-time run, copying sensor values into the computer model, and running the upcoming algorithms to test for consistency. A logic analyzer was set up to output much of the same data about every pulse that the model outputs into Matlab, for easy comparison. Results between the system and the model were verified.

In Q3 2004, the first version of the operational algorithms was completed and tested on the system. The unit demonstrated power conversion from a variable speed synchronous generator to the power grid, successfully synchronizing with the generator input at speeds from 10-60Hz. To meet strict harmonics requirements it may be necessary to add inversion control to the low level algorithms. Inversion control is a technique, developed under a separate contract, that allows more precise internal power control of the AC-link™ system. The technique was invented by Mark Holveck, and he and Casey Jacobson co-authored a provisional patent for it.

task 3.3: **Design circuit schematics**

The control boards were designed to incorporate all the functionality necessary to control the AC-link™ system, employ high-speed control algorithms, and provide user-interface functionality using just one printed circuit board. To perform AC-link™ control, the boards have current and voltage sensor inputs, analog conditioning circuitry, A/Ds and digital processing in logic, and SCR trigger timers and trigger circuitry. To perform high-speed control algorithms, the boards have a 200 MHz floating-point TI DSP integrated with an FPGA. Interfacing with users and other control systems is provided through analog voltage and current inputs and outputs, digital inputs and outputs, and two serial RS-232 ports for communication with LCDs and keypads, PC-based user interfaces, and expansion communication boards.

task 4.0: **Breadboard Prototype Development**

task 4.1: **Manufacture and Delivery of Power Electronics**

After searching for distributors who were able to design and deliver the major magnetic components, we met with NWL Inductors in Bordentown, NJ, whom we worked with to deliver inductors and capacitors. Lead times for both of these components were about 10 weeks. They arrived in early June, which pushed our C&F (breadboard) delivery date out, but did not affect overall completion of the project.

Figure 2 - SCR Bridge Design #1

The SCR bridge represents a redesign of the existing bridge on our prototype systems, for increased airflow and cooling of the SCRs. Motors & Controls International delivered the bridge to PPS. The bridge uses Dynex TF440 SCRs.

Thermal management is an important issue we addressed on the C&F system with iterative component and packaging designs. The existing package design will allow for sufficient cooling, but future redesigns to lower size will need to focus closely on thermal management issues.

As of Q2 2004, the system had no major design issues, and most components had been procured with ease. However, we have had significant delays with NWL who have been supplying us with inductors and capacitors. The capacitors took over three months to arrive. The final assembly of the unit was completed on July 15th 2004.

<u>task 4.2:</u> **Manufacture and delivery of control boards**

After schematic design, a manufacturability review was performed by Finger Lakes Engineering on the boards to verify that the part footprints were correct, ensure that the signal traces travel at the correct angles and were a minimum distance away from adjoining board items, and a number of other smaller checks. Once the review was finished, the bare boards were manufactured, the parts populated, and basic electrical tests performed. The board was then powered up, the DSP and FPGA programmed, and the functionality of all board subsystems verified using bring-up code and test analog signals.

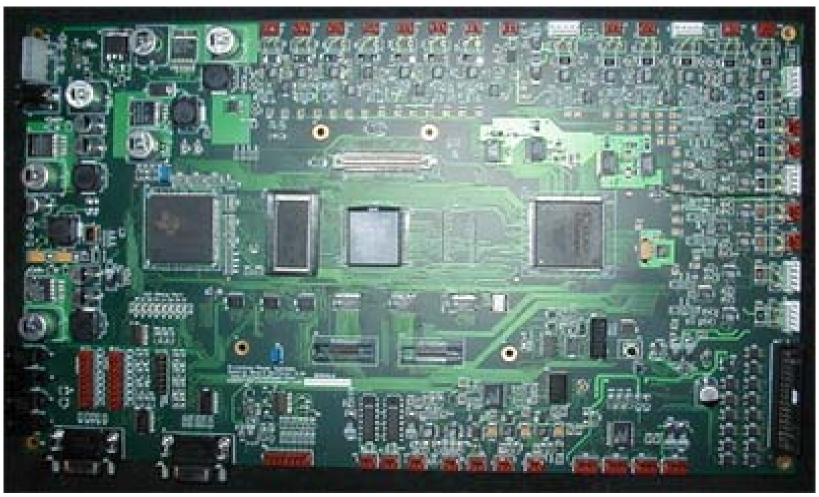

Figure 3 – AC-link™ v2.0 Control Board

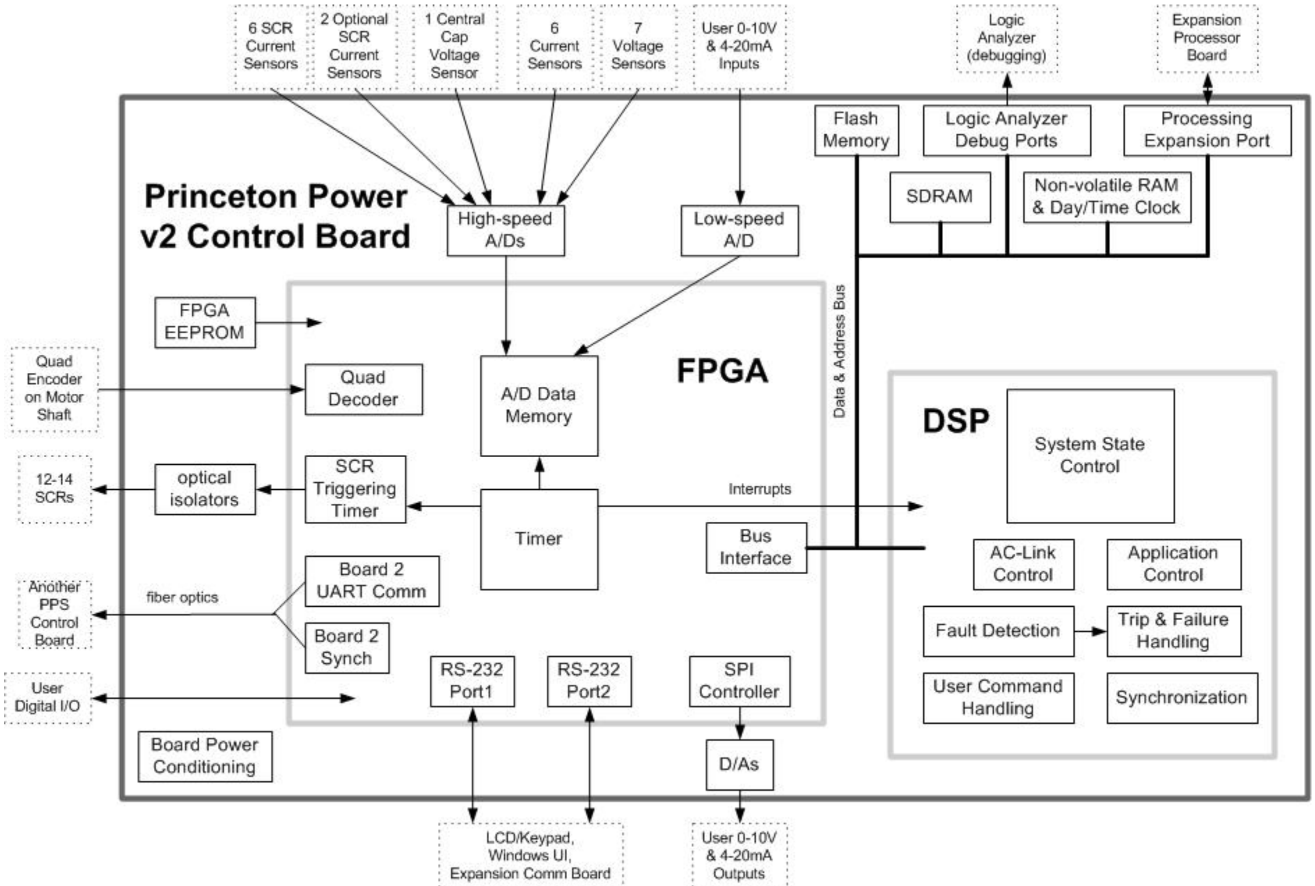

Figure 4 – Block Diagram of AC-link™ v2.0 Control Board

The control boards having been designed by both Princeton Power Systems and Finger Lakes Engineering arrived in January. The v2.0 control board has two microprocessors, an “F.P.G.A” and “D.S.P”. The FPGA is a high-speed chip coded with low-level algorithms (such as data sampling routines) that are required to operate at high speed. The FPGA also controls highly accurate clocks (timers) it uses to signal the other processor (the DSP) to complete a slightly higher-level algorithm. The DSP, though slower than the FPGA, is useful because it is programmed with standard C code and is highly versatile. Following is a list of the major features of the board:

- 200 MHz TI C6713 DSP (center left)
- Xilinx Spartan IIE 300,000-gate FPGA (center right)
- Flash, SRAM, & day/time clock (center)
- Maxim 80C400 Integrated Ethernet Controller with a dedicated WebServer function, 10/100 auto negotiating PHY device, and an RJ45 connector (bottom left)
- RS-232 or RS-485 serial communication capability, for connecting to an LCD or expansion communication board (bottom left)
- Sensor inputs & analog signal conditioning for high-level system input/output voltage & current (top right)

- Sensor inputs & analog signal conditioning for low-level SCR currents & central capacitor voltage (right)
- 0-10V and 4-20mA analog inputs & outputs for interfacing with a user or a third-party control system (bottom)
- Digital input port & digital output port for interfacing with a user or a third-party control system (bottom left)
- 14 optically-isolated SCR triggers (bottom right) capable of connecting to a daughter card for conversion to fiber optic trigger signals
- Fiber optic connectors for connecting additional PPS control boards (bottom left)
- Inputs & analog signal conditioning for temperature sensors (bottom)
- Motor/generator shaft encoder input (bottom)
- Mictor headers for system debugging via a logic analyzer (center bottom)
- Power conditioning (upper left)

The v2.0 control board was tested by Finger Lakes Engineering and worked as required. There are some slight modifications which will need to be integrated in the next revision. The bare board and assembly was manufactured by SWEMCO.

task 4.3 **Integration of Controls and Power**

Since the Power Electronics system was delayed to the middle of July, this task had not been completed within the time expected. However, the integration of controls and power was completed on August 3rd 2004.

task 4.4: **Program the control microprocessor**

Princeton Power completed initial testing of the new v2.0 control system and began algorithm bring-up. The core FPGA firmware, the analog signal conditioning (including sensor inputs, user inputs, and A/D conversion), digital user run/stop and enable control, and the basic DSP software functioned properly. After board testing, Princeton Power began integration of the high-speed algorithms, developed on the AC-link™ model, into the DSP control code. These algorithms include the input & output SCR selection, input VAR calculation, input line synchronization, SCR timing calculation, output frequency control, and system switching frequency control. At this point, the system could run a variable frequency output on both resistive and inductive motor loads from minimum to maximum switching frequency. The main tasks remaining in low-level algorithm work were completion of the inversion control algorithm implementation on the system and the permanent magnet generator model. High-level algorithms controlling interaction with the power grid were also in the design stages.

In Q2 2004, the control microprocessor was programmed with a most recent version of the AC-link™ software. This software allowed for high-speed trips, essentially allowing for quick response times to grid disturbances. In Q3 2004, the control system was programmed with the appropriate software architecture and conversion code to operate the system.

task 4.5 **Procurement and Installation of testing setup**

During Q4 2003, a number of vendors were researched for their ability to design and deliver a testing setup for the converter. We decided to use Motors and Controls International because of their proven ability to develop testing stands for such systems. Princeton Power Systems and M&CIdesigned a 75kW dynamometer-based testing setup, which arrived in Q1 2004 and was electrically connected and calibrated.

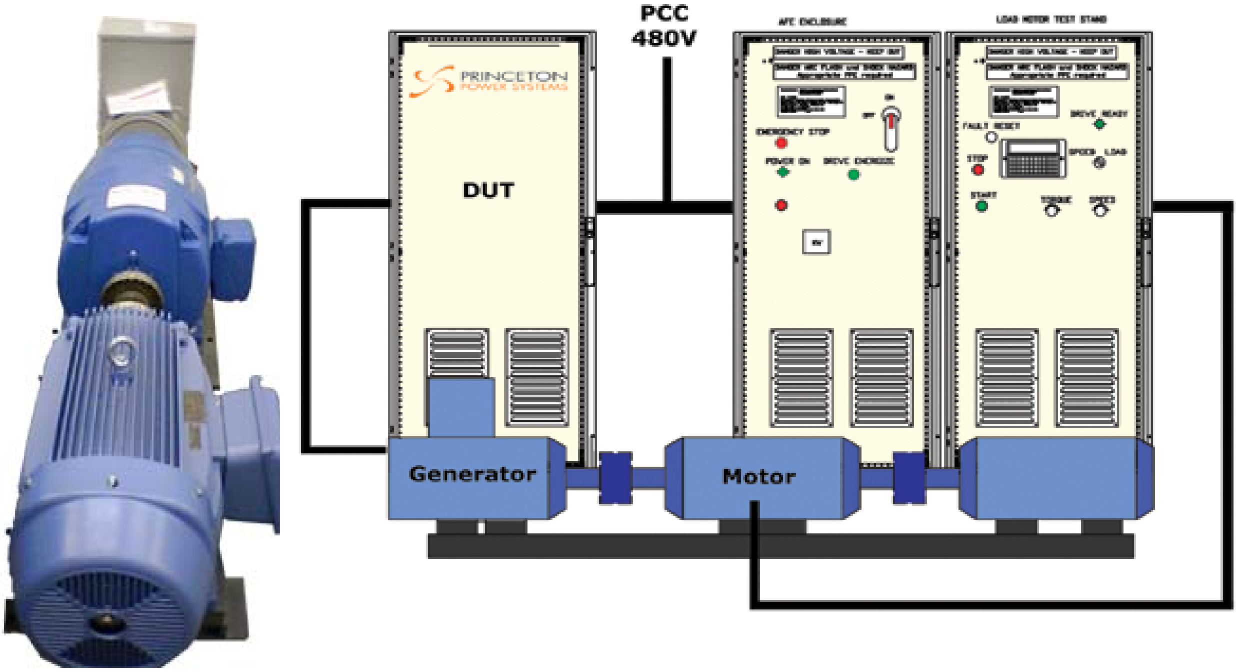

Figure 3 – Dynamometer test setup built by M&CI

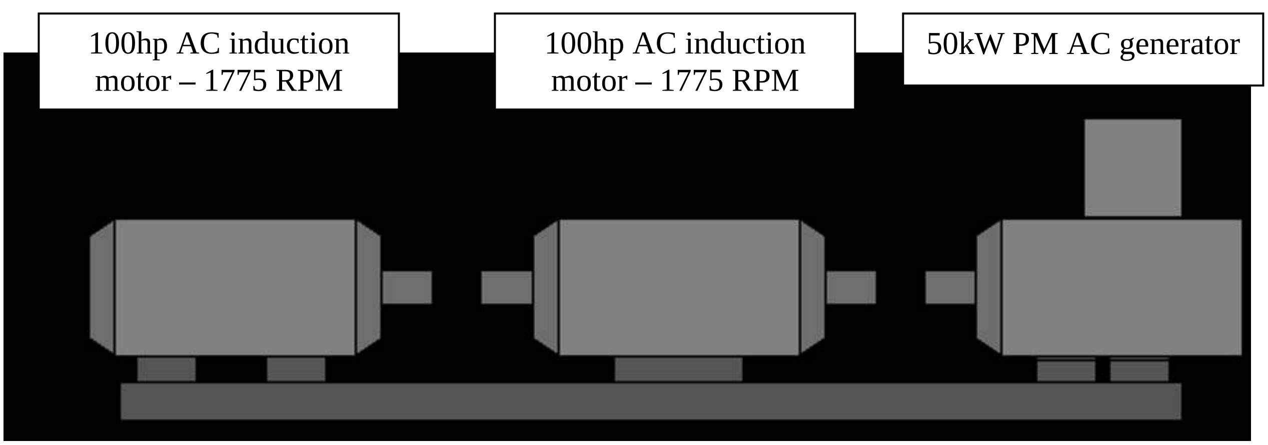

Figure 4 – Conceptual diagram of dynamometer testing setup

As depicted in Figure 3, the testing setup mimics a permanent magnet wind turbine generator. A 100kW motor drive operates a 75kW 3-phase induction motor,which is mechanically connected to a 75kW permanent magnet generator similar to that used by the Bergey turbine and NPS' contemplated design. Depending on the setting of the 100kW motor drive, the PM generator will output variable frequency AC ("wild" AC) to the AC-link™ converter (device under test), which then conditions the power and feeds it back to the utility grid. The net power usage of the system is low, consisting only of losses in each of the components. The testing setup allowed a tremendous amount of control over the testing plan for the converter, and was one of the primary resources for the testing effort.

In Q2 2004, the testing setup was calibrated and tested.

task 5.0: **Breadboard Prototype Testing**

All components for the breadboard prototype (C&F prototype) were procured in a timely fashion and assembled by the Princeton Power team. The passive components, control system and wiring were tested and the system passed.

task 5.1: **Basic Operational Testing on Static Load**

The input of the AC-link™ converter was connected directly to the output of the testing generator, while the output of the converter was connected directly to a resistive load bank. The generator was driven by the dynamometer test setup at various frequencies. It was first verified that the converter control system could synchronize with the generator frequency, even under rapidly changing conditions. Then, the converter was activated and commanded to feed constant power into the resistive load, drawing this power from the generator. The generator was run at various speeds between 30Hz output and 60Hz output.

The converter successfully maintained the commanded power output as the generator frequency was changed. The frequency of the converter was ramped at a maximum rate approximately equivalent to the maximum requirement specified (~25Hz/s). Power output was constant throughout the ramping.

task 5.2.1: **Generator Control**

The converter demonstrated variable torque capability for controlling the generator. It was then programmed with a torque-speed curve similar to those provided by Bergey Windpower. This results in the generator settling at different equilibrium speeds determined by the curve when it is driven at varying torques by the dynamometer and power is drawn from it by the converter.

task 5.2.2: **Grid Interaction**

At first, the outputVAR algorithm was used to feed power from the generator into the grid.

It was difficult at first to evaluate the current harmonics of the converter because of harmonics that were already present in the system due to the generator in the testing setup. The figure below shows the input and output currents of the converter when it was converting power from the generator at 40Hz to the power grid at 60Hz. The obvious 5th and 7th harmonics are caused by the generator.

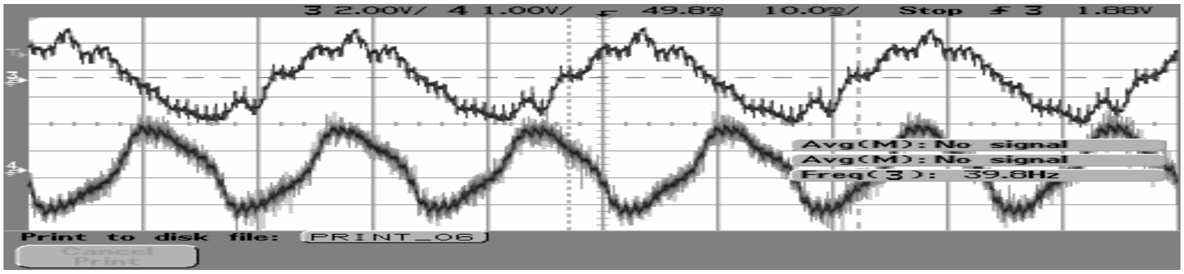

Figure 5 - 40Hz Input Generator Current and 60Hz Output Grid Current of the AC-link™ converter

Conversations with Lee Fingerish helped to identify the causes of the harmonics, and to determine that they were 'normal' for this type of permanent magnet generator. Given this information, it was necessary to incorporate some harmonic-damping algorithms in order to get the system to operate properly with the high harmonic content of the generator.

task 5.3.1: **Full System Test (Normal Conditions)**

task 5.3.2: **Dynamic Conditions**

In Q3 2004, various edge conditions were tested that showed how the system will shut down safely in these events. Due to the nature of some of the edge conditions, some could only be tested by simulating the condition in computer software rather than running the test on the hardware. In these cases the control system proved that it was capable of shutting down the system and ensuring that a dangerous condition would be averted. This will need to be tested further but most likely will undergo extensive testing once the product is either field tested or sent to UL for qualification.

task 6.1: **Software, algorithms modifications**

In Q4 2004, the inversion algorithms were implemented on the model and were ready for porting to the DSP. They were shown to operate well enough to improve upon VAR mode harmonics, even when commutation inductance was left at the large levels used for thyristor dI/dt protection.

The main point behind incorporating the inversion control was to interact with the harmonics being created by the generator, and to allow greater control for such purposes as anti-islanding protection. The goal is for grid-side harmonics to remain under acceptable levels according to UL 1741 regardless of the generator harmonic levels. The inversion control method was developed under a separate contract and had been proven to be effective at damping harmonics. However, it also lowers conversion efficiency slightly since it requires the firing of an additional switch during each charge/discharge process. This efficiency decrease was seen as necessary in order to operate with the harmonic levels present, though we have since thought of some techniques that may allow the converter to run without inversion control through much of its power range, and dynamically incorporate inversion control only when necessary. This would raise the efficiency of the system.

task 6.2: **Power Electronics Design Modifications**

The original C&F unit was designed for a nominal generator voltage of 480V, and was constructed using the bridge design in Figure 2, and the TRANEX thin foil inductor (See Appendix B).

The new modified C&F system was redesigned with an existing generator voltage in mind, which requires a higher kVA rating. The charging inductors were redesigned to meet the proper specification, still using the air core thin copper foil design. No other major changes were made to the power electronics design. The new system was packaged in the same enclosure as the C&F unit, though the new components would make size reductions possible on future revisions.

In Q1 2005, the scope of this task was increased to incorporate a set of extra functionality that is being partially funded through other, related projects.

A project was undertaken to design an LCD/keypad interface for the unit, in order to provide field programmability and access to parameters. In concurrence, a communication protocol based on MODBUS was implemented to enable access via a laptop and Ethernet cable. This contract was asked to cost-share a portion of the design work, since the LCD/keypad will also be useful for all AC-link™ products.

In Q2 2005, the LCD keypad hardware was delivered and underwent initial testing. The software for the LCD unit was completed by mid-August. MODBUS via the webserver was also successfully developed.

Figure 6 – LCD/keypad mounted on the cabinet

Figure 7 – Close-up of the LCD/keypad

A great deal of effort was also put into redesigning the internal charging inductors in order to reduce cost, size, audible noise, losses, and radiated emissions. The air core, copper-foil-wound design in use on the C&F and Modified C&F systems worked operationally, but were inefficient, noisy, and large. Several prototype inductors were purchased and tested, including:

- copper foil-wound sunk in epoxy
- Nanocrystalline core, litz wire wound (MK magnetics core, wound in-house)
- Nanocrystalline core, litz wire wound (assembly supplied by VAC)
- Sendust core, litz-wire wound (cores from Arnold Magnetics, wound in-house)

See Appendix B for a brief summary of various prototype inductor designs that were built and tested.

The nanocrystalline core, litz-wire wound design constructed in-house using a core from MK Magnetics was the best design known at the time of constructing the pre-production prototype. The core material is expensive, but has low losses, is small, and eliminates radiated emissions. It also requires a gluing step in the manufacturing process, which takes time and must be done in-house. This design was used with success in the pre-production prototype.

However, a new revision of the AC-link™ hardware platform will use Sendust cores, which were recently found to perform as well as the nanocrystalline design, but are much less expensive and easier to assemble. This design will save significant materials cost. However, the discovery and analysis was made too late to include it in the pre-production unit delivered to the DOE under this contract.

task 6.3: **Control Board Design Modifications**

The trigger system was redesigned to use fiber optic triggering. This new method solved spurious triggering problems seen on prototype units and is a step towards meeting UL safety standards. The voltage sensor board was also redesigned to meet UL safety requirements. An I/O board was designed and added to the system to provide isolation on user digital I/O signals. Lastly, a small design revision was done on the main control board to fix errata in the user interface hardware.

PPS major software development effort was redesigning the control code software architecture to improve the timing of real-time code execution and provide more flexibility with I/O configuration and communication protocol implementation.

Automated, high-speed protective trips were implemented in FPGA firmware, automated commutation inductance measurement software was developed for faster system bring-up, and data logging code was implemented for remote diagnostics purposes. To facilitate development of anti-islanding software and turbine control software, phase and synchronization software was implemented for all input & output current & voltages.

task 7.1: **Power Electronics Manufacture and delivery**

In Q4 2004, we started to order the parts for the units. There were substantial lead times on some of these parts but they were ordered early enough to ensure a time buffer.

Due to a no-cost extension to the contract in Q1 2005, the units were put on hold for assembly and check-out until a later date.

In Q2, one prototype unit was completed and ready for bring-up. One of the units was scheduled for shipment to Sandia's Distributed Energy Testing Lab (DETL) in late August, and the other remained at PPS. This unit had not yet incorporated the new LCD keypad.

task 7.2: **Control Board Manufacture and Delivery**

In Q4 2004, PPS completed assembly and testing of the v2.1 control boards, v1.0 optical trigger card, v1.0 trigger daughter cards, v1.1 sensor boards, and v1.0 I/O boards. Parts procurement and assembly began for the boards that underwent revisions to meet UL requirements and fix errata discovered during testing: v2.2 control board, v1.1 optical trigger card, and the v1.2 sensor board.

In Q3 2005, several work paths came together, and several major project tasks were completed, including the following:

task 7.3: **Integration and Validation Testing**
task 8.1: **Subsystem Testing**
task 8.2: **Full System Testing**
task 8.3: **UL 1741 Testing**
task 9.1: **Site Prep**
task 9.2: **Shipping and Installation**
task 9.3: **Startup**
task 9.4: **Steady-state Testing**
task 9.5: **Testing for Certification Compliance**

The prototype unit was built and tested at PPS, then shipped to Sandia's Distributed Energy Technology Laboratory where it was further tested according to standards and methods developed by the DETL for compliance with UL 1741 and IEEE 1547. Finally, a new plan for further modifications and building a revised pre-production prototype to undergo a final set of testing both at Sandia and on a turbine at Bergey's facility in Norman, OK, was developed.

Figure 8 – Prototype AC-link^{TM} unit with measuring equipment

Manufacture and In-house Testing

The full power electronics and control system for the modified C&F AC-link^{TM} unit were manufactured at PPS' lab and underwent a variety of tests. The testing focused on 1) power electronics and thermal properties, and 2) wind turbine control software functionality.

In order to test the power electronics, a make-shift environmental chamber was constructed at PPS. We took a 3-walled corner of our lab space and constructed a plastic sheet as the fourth wall with a cut-out for an industrial fan at the bottom. The converter was placed in the chamber with several temperature sensors and other measurement signals coming out through the plastic sheeting. The exhaust fan was designed into an automated circuit that can sense the ambient temperature inside the room and automatically adjust the fan speed to maintain a constant ambient temperature in the chamber. Several tests were run on the converter running for 3+ hours at 20, 30 and 40 degrees centigrade. The temperatures of the heat sinks and other major components were measure to assure that thermal runaway would not occur.

The wind turbine control functionality was tested using our dynamometer test stand and permanent magnet generator. Several basic tests were conducted varying the input frequency of the PM generator to test whether the converter followed it programmed power curve. The converter passed the internal tests with minor software adjustments.

<u>Testing at Sandia's Distributed Energy Testing Lab</u>

Mark Rumsey introduced PPS to the capabilities of Sandia National Lab's Distributed Energy Testing Lab (DETL), and we decided to pursue this as a way to test the more complex grid-tied functionality that we could not test in-house. Sigifredo Gonzalez and Juan Ortiz-Moyet were our primary contacts at the DETL (along with Mark) and helped us organize the schedule and testing protocol.

The DETL is set up primarily to test solar equipment, including grid-tied inverters, and as such is very experienced with the latest standards and testing procedures for grid connectivity. This portion of inverter functionality is analogous to the functionality required of a grid-tied wind converter in terms of such things as anti-islanding, tripping on grid voltage fluctuations, etc. Our goal is to make the wind converter conform to UL 1741 specifications, as well as IEEE 1547. Though traditionally used mostly for solar equipment, the ability to "fit" a wind converter into these guidelines will make it that much easier to bring grid-connected wind turbine testing and operation into the mainstream. The DETL's experience with this type of testing, combined with our knowledge of wind turbine converters, made this an ideal partnership for testing a wind turbine converter using facilities, equipment and procedures traditionally used for solar equipment.

The input power side of a wind converter is clearly much different than for a solar inverter, so this is where the team of PPS and the DETL were really breaking new ground in terms of testing using the DETL's facilities and equipment. The DETL recently installed a Pacific Power Source capable of varying output frequency, voltage, and supplied current, in order to simulate a small wind turbine generator. The AC-link™ converter was modified to operate with a power curve that was compatible with the Pacific's capabilities (equivalent to reprogramming the AC-link™ converter to work with a different turbine), and multiple tests were run over a 3-day period.

See Appendices B and C.

Testing Results
Most of the tests run were geared towards analyzing the AC-link^{TM} converter's ability to meet the grid-interconnection requirements of UL 1741 and IEEE 1547. The converter performed well enough that it should have no problem passing the critical functional portions of each of these standards. In fact, much of the data gathered will be used to relax some of the algorithms since they exceeded the test criteria by a wide enough margin that they can be relaxed quite a bit while still passing.

Three critical areas were identified where further development should be focused: 1) efficiency over the full operating range, 2) audible noise, 3) standby losses. Our knowledge of the converter's functional capabilities as discovered during the tests at the DETL allowed us to modify software and hardware over the next 2-3 months to optimize the system according to these three criteria.

Production Prototype Testing
In the fourth quarter of 2005, a pre-production prototype AC-link^{TM} converter was built and tested, based on a new hardware platform developed for our line of commercial motor drives. The new design includes nanocrystalline-core inductors that provide greater efficiency, smaller physical size, lower noise, and lower radiated emissions. The converter included hardware and software modifications based on the analysis of testing results from the testing done at the DETL in the 3rd quarter.

Several software modifications were made to increase the efficiency of the system while performing according to the IEEE 1547 guidelines, particularly in regards to anti-islanding protection. The previous testing at the DETL had identified several areas where the searching algorithms could be "relaxed", and still perform according to the IEEE 1547 anti-islanding guidelines, resulting in efficiency gains for the converter. These changes were implemented in the software.

The new hardware was programmed with the revised code and shipped to Sandia to undergo performance testing. The unit was shipped on November 30th, and testing began on December 12th. Detailed thermal imaging tests were conducted again -- results can be seen in the comprehensive testing report included as Appendices D and E.

NOTE ON CANCELLED TASKS 10.6 and 10.7:
The tasks under this project involving field testing on the Bergey 50kW wind turbine were cancelled due to the unavailability of the 50kW turbine for testing during the timeframe of the project. At the conclusion of this project, the timeframe for availability of the turbine was still uncertain, and the technical project team therefore deemed it sufficient to perform a second round of testing at the DETL which would provide similar results to field testing on the turbine.

Patents:
A provisional patent application for the “VAR Control Method”, has been filed with the USPTO and been given case number 60,650,210. The patent is not a “subject invention” since it was developed under a separate contracted effort.

Publications / Presentations / Travel:
DoE – Boulder, Colorado – Preliminary Design Review
March 1st, 2004
3 People (Bijan Treister, Mark Holveck, Darren Hammell)

Chicago, IL – AWEA Global Windpower 2004
March 28th – 30th,2004
Darren Hammell
Poster Presentation: “AC-link Power Converter for Small Wind Turbines”
(not paid for by DOE)

DoE – Boulder, Colorado – Concept & Feasibility System Testing Review
October 25th, 2004
Bijan Treister, Mark Holveck Darren Hammell

London, UK – EWEA European Wind Energy Association 2004 Conference
November 22nd – 25th
Darren Hammell
Poster Presentation
(not paid for by DOE)

Albuquerque, NM – Sandia National Lab, Distributed Energy Technology Lab
September 11th – 14th
Darren Hammell, Mark Holveck, Casey Jacobson
Operational testing of the prototype AC-link converter at the DETL facilities.

Albuquerque, NM – Sandia National Lab, Distributed Energy Technology Lab
December 12th – 14th
Darren Hammell, Mark Holveck, Casey Jacobson
Operational testing of the production-prototype AC-link converter at the DETL facilities.

Major Task Schedule

Task Number	Task Description	Task Completion Date				Progress Notes
		Original Planned	Revised Planned	Actual	Percent Complete	
1.1	Certification Planning	1/1/04		1/1/04	100%	Completed
2.0	Identification of converter requirements	11/1/03		11/1/03	100%	Completed
3.1	Power Electronics component specifications	11/21/03		11/21/03	100%	Completed
3.2	Design and modeling of operational algorithms	2/17/04		2/17/04	100%	Completed
3.3	Design and Layout of Control Circuit Boards	2/17/04		2/17/04	100%	Completed
4.1	Manufacture and delivery of power electronics	05/28/04		07/16/04	100%	Completed
4.1	Manufacture and delivery of control boards	05/28/04		07/16/04	100%	Completed
4.3	Integration of controls and Power	06/11/04		07/26/04	100%	Completed
4.4	Program the control microprocessor	04/02/04		06/11/04	100%	Completed
4.5	Procurement and installation of testing setup	04/27/04		06/01/04	100%	Completed
5.1	Basic Operational Testing on Static Load	7/2/04		07/26/04	100%	Completed
5.2.1	Generator Controls	7/23/04		08/20/04	100%	Completed
5.2.2	Grid Interaction	8/13/04		09/13/04	100%	Completed
5.3.1	Normal Conditions	8/13/04		09/13/04	100%	Completed
5.3.2	Dynamic Conditions	10/8/04		10/8/04	100%	Completed
6.1	Software, algorithms modifications	11/12/04	7/31/05	7/31/05	100%	Completed
6.2	Power Electronics Design Modifications	11/12/04	7/31/05	7/15/05	100%	Completed
6.3	Control Board Design Modifications	11/17/04		06/11/04	100%	Completed
7.1	Power Electronics Manufacture and delivery	1/19/05	7/15/05	7/15/05	100%	Completed

Task Number	Task Description	Task Completion Date				Progress Notes
		Original Planned	Revised Planned	Actual	Percent Complete	
7.2	Control Board Manufacture and Delivery	12/8/04	7/1/05	7/1/05	100%	Completed
7.3	Integration and validation testing	2/16/05	8/15/05	8/5/05	100%	Completed
8.1	Sub-System Testing	3/2/05	8/15/05	8/10/05	100%	Completed
8.2	Full System Testing	4/13/05	8/20/05	8/26/05	100%	Completed
8.3	UL 1741 Testing	5/18/05	8/15/05	9/14/05	100%	Completed
9.1	Site Prep	5/24/05	9/6/05	9/5/05	100%	Completed
9.2	Shipping and Installation	6/2/05	8/29/05	9/9/05	100%	Completed
9.3	Startup	6/16/05	9/6/05	9/12/05	100%	Completed
9.4	Steady-state testing	7/7/05	9/7/05	9/13/05	100%	Completed
9.5	Testing for certification compliance	9/8/05	---	9/14/05	100%	Completed
9.6.1	Draft Final Project Report		2/15/06	2/22/06	100%	Moved up by 1-month
9.6.2	Final project Review	9/30/05	2/24/06		0%	Moved up by 1-month
10.1	Analysis of Testing Results	10/10/05	11/1/05	11/1/05	100%	Completed
10.2	Hardware and Software Modifications	11/15/05	11/18/05	11/18/05	100%	Completed
10.3	Build Production Prototype	11/15/05	11/14/05	11/14/05	100%	Completed
10.4	Shipment and Installation	11/28/05	11/30/05	11/30/05	100%	Completed
10.5	Performance Testing	12/15/05	12/16/05	12/16/05	100%	Completed
10.6	Shipment to Bergey Windpower	1/16/06	---	---	---	CANCELLED
10.7	Functional Testing	2/3/06	---	---	---	CANCELLED

Appendix A – Small Wind Converter Specification (C&F unit)

AC-link 480-75WIND	
Rated Capacity	75 kVa
Applicable generator	50kW @ 320V 75kW @ 480V
Switching Freq.[1]	500 Hz to 2400 Hz
Efficiency	94% (@ 50kW, 320V)
Overload Capability	125% for 1 minute
Rated Input voltage/freq	0 - 700V / 0 – 200 Hz
Slew Rate	25Hz / sec
Max. produced $\frac{dV}{dt}$	5V/μs
Max cable length to generator	10,000 ft (est.)
Rated Output voltage/freq.	480V± 10% / 60Hz ± 5%
Max. cable length to xformer	10,000 ft (est.)
Standards Compliance	UL 1741 (pend), IEEE 1547
Installation	Stand alone
Audible noise	< 80 dB at 1m
Protective enclosure	NEMA 1
Weight	600 lbs
Dimensions	24" x 30" x 60"
Cooling Method	Forced air-cooled, redundant fans
Color	Standard
Conditions	Indoors (outdoor available)
Max. Humidity	95% (no condensation)
Temperature	-10C – 40C, space heater available

Control Features	
Power curve	Programmable I vs. V curve – up to 128 points
Cut-in speed	Programmable – 0 to 200Hz
Protection	Automatic over-current protection – programmable current limit
Retry	User Configurable
Power	Dual-source control power[2]
Faults	Over Speed, Overload, Grid Failure, Over Temperature, etc
Failures	Device Failure, Control Failure
Fault History	Past 10 Faults are stored - Included data: Turbine RPM, Output Current, Output Power, 3-phase grid RMS Voltage, Input Voltage Magnitude, Recent Run Time, Accumulated Run Time

[1] The switching frequency is controlled internally by the converter
[2] In the event of grid failure, the control system will be powered off of the generator side

Appendix B – Prototype Charging Inductor Designs

Because of component cost and lead time requirements, it was initially determined that charging inductors for commercial VSD's should avoid litz wire or expensive core materials. We decided to try to develop a foil inductor design that would function without excessive losses due to skin factor, proximity effect, eddy current heating, and other problems associated with foil designs.

Prototype 1: Stacked Rolled Foil Inductor

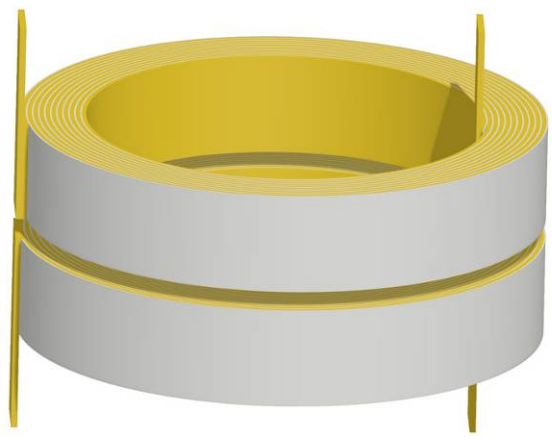

Description:

Each inductor consists of two inductively coupled coils of copper foil stacked on top of each other and wired in series. The foil used is 0.09" thick x 2.00" wide. The overall dimensions including a 0.375" spacing between coils are 10.5" outer diameter, 7.875" inner diameter, and 4.375" height. There are 10.5 turns in each coil and each turn is separated by 0.03125" of silicone rubber. The total length of copper foil is 50.14 feet, with a weight of 34.87 lbs.

Advantages:

- Simple to Manufacture
- More reliable than litz wire
- Low voltage potentials between turns
- Short lead time
- Wide operating temperature range – no magnet wire insulation to melt.
- Smaller than litz wire inductor designs.
- Can be compression wound for reduced acoustic noise

Test Results:

This inductor was briefly tested on 9/26/04. After 2 minutes of operation, the test was terminated since the core of the inductor had exceeded 200 Degrees C. The outer surface had increased only 20 degrees over ambient. This interior heating was most likely the result of induced eddy currents in the extremely intense field region at the core of the inductor. Losses were estimated to be approximately 1000 watts. Although this is only slightly greater than the allowable threshold of 750 watts, the localized heating would exceed the maximum allowable operating temperature of the insulation material.

Prototype 2: Inter Wound Rolled Foil Inductor

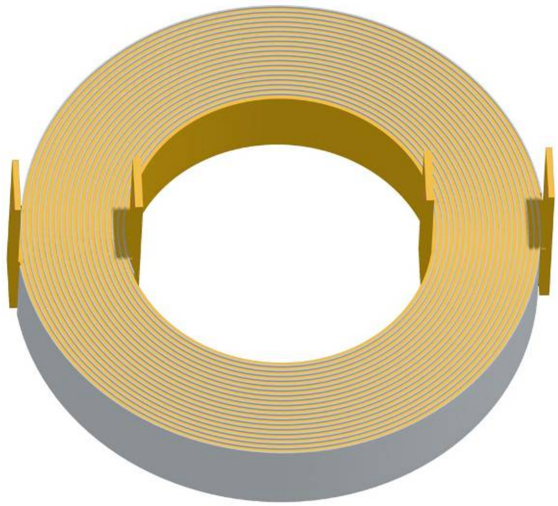

Description:

Both coils of the inductor are wound in parallel separated by a layer of silicone rubber. The foil used is 0.09" thick x 1.875" wide. By winding the coils simultaneously, a high coupling ratio of nearly 6 is achieved; double the ratio of the stacked coil. Each coil consists of 9.5 turns. The spacing between any two adjacent windings is 0.03125", with silicone rubber filling the gap. The outside diameter is 11", and the inside diameter is 6.5". The overall height is 2". The total length of copper used is 43.6 feet, and the weight is 28.45 lbs.

Advantages:

- Relatively easy to manufacture
- Uses the least amount of copper, lightest weight design, lowest material cost
- Smallest form factor of any design, uses a more efficient coupling factor
- More reliable than litz wire
- Short lead time
- Wide operating temperature range – no magnet wire insulation to melt.
- Can be compression wound for reduced acoustic noise

Test Results:

This design was tested on 8/26 @ 235 ARMS @ 3khz in 20 degree C ambient still air. The inductor outer layers remained quite cool, only reaching 45 degrees C after 5 minutes. The inner coils, however, exceeded 200 degrees C, most likely due to induced eddy current heating from the much stronger internal field. Losses were estimated to be approximately 1800 Watts.

Prototype 3: Edge-wound Copper Strip Inductor

(4 used per system, in pairs)

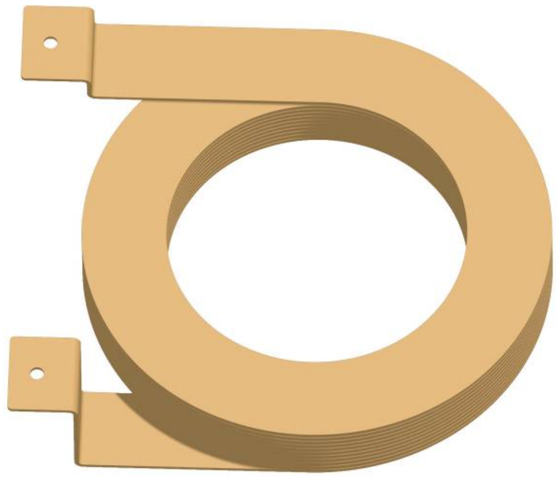

Description:

This inductor is wound on edge using a special mandrel drawing process. It has the advantage of having nearly perfect thermal conductivity to the outer surface for cooling, and it allows much more copper to be wound in a given volume compared to litz wire. The outer diameter is 12.5" with an 8.00" inner diameter. Each coil is 2" tall; the series coupled pair would be about 4.5" tall. 10.5 turns of copper strip 2.25" wide and 0.125" thick are used in each coil segment (21 turns total per inductor). 56.3 feet of copper are used with a total weight of 57 lbs for a pair of two. One interesting benefit of this inductor is its ability to be tuned to an exact inductance. By compressing or stretching the helical spring coil, the inductance of a pair can be infinitely varied from 20 uH to 150 uH. This would allow one production design to be used for a wide range of drive voltages and horsepower ratings.

Advantages:

- High reliability
- Large surface area for cooling
- Wide operating temperature range – no magnet wire insulation to melt.
- Inductance can be adjusted to exact values
- Can be adjusted for use in multiple system configurations
- Low Voltage potential between turns

Test Results:

This design was tested on 8/19 @ 235 ARMS @ 3khz in 20 degree C ambient still air. The inductor became extremely hot in a short period of time. Losses were estimated at 2600 Watts, about 66 times the DC resistance losses. We believe the majority of loss was due to inductive eddy current self heating. Since edge wound coils have the copper conductor aligned perpendicular to the field, eddy currents are free to flow without restriction.

Prototype 4: Long Thin Foil Inductors

(Passed Testing on 8/27/04)

Figure 1 - Thin Foil Inductor (TRANEX)

Description:

This inductor consists of a much thinner foil of approximately 0.021” thick and 6” wide. It is rolled up with 0.005” paper as an insulator between the coils. Approximately 30 turns are used, and the finished inductor is about 9” in diameter and 7” tall. 4 individual coils are used per system.

Advantages:

- High reliability
- Large surface area for cooling
- Wide operating temperature range – no magnet wire insulation to melt.
- Low Voltage potential between turns
- Reduced interior field intensity

Disadvantages:

- Larger than other designs, forces the inductors to be very near the walls of the cabinet.
- Will cause induced losses in the cabinet walls.
- The thinner foil vibrated more freely than the thicker foil designs, they are noisy – over 110 dB.
- Their long solenoid length causes their magnetic field to extend a considerable distance outside the enclosure.

Test Results:

This design was tested on 8/27@ 235 ARMS @ 3khz in 20 degree C ambient still air. The inductor became hot, but was able to stabilize at 145 degrees C, meeting the thermal requirements. Losses were estimated at approximately 400 watts per inductor. This inductor uses much thinner copper foil, so the induced eddy current losses are greatly reduced. They also behave more like an ideal solenoid inductor, and the field remains more parallel to the coil axis than other designs.

These inductors are capable of meeting the specifications without overheating, but they are not the ideal long term inductor solution. They are louder than most other designs, producing approximately 95-115 dB of acoustic noise. They also occupy a larger volume, and will impede the transition to a smaller enclosure.

Prototype 5: Epoxy Potted Litz Wire Inductor

Description:

This design consists of a 2/0 30gauge stranded litz wire coil potted in a silicone rubber epoxy. The outer diameter is 11 inches, and the height is 8 inches.

Advantages:

- Low Proximity effect and skin effect losses

Disadvantages:

- Expensive
- Long Lead times
- Difficult to wind and pot
- Numerous manufacturing inconsistencies possible
- Litz wire has a maximum operating temperature of 155 degrees Celsius
- The core to surface conductivity is 500 times slower than the copper foil designs.

Test results:

The Epoxy Potted Litz wire inductors were tested several times in August and September of 2004. As expected, they were very efficient and did not seem to have any losses from factors other than the DC copper resistance. They heated up slowly, and eventually stabilized with a surface temperature of approximately 135 degrees C. We were unable to directly measure the internal coil temperature, but it theoretically would have been in excess of 155 degrees C. Although this is not an excessively high temperature for power electronics, the litz wire insulation must be kept below 155 degrees C. Because of the slow thermal transfer between core and the outer surface, they do not adequately cool despite their low losses.

The potted litz inductors were quieter than other designs tested due to the rubber dampening. They produce approximately 70-80 dB of acoustic noise, significantly less than the 100 dB+ emitted by other designs.

Appendix C – Operational Testing Results from Sandia Testing September 2005 (Modified C&F)

September 12-14, 2005

PPS Engineers: Mark Holveck, Casey Jacobson

<u>1) Power sweep capture</u>
- Pacific Vsource on input (gen side)
- 480V grid on output
- Current speed curve programmed to be 0A @ 47Hz to 109A @ 60Hz
- Voltage level on Pacific set to 450VAC (freq. independent)
- Freq. on Pacific set to 47Hz
- AC-link started
- Data recorded for at least 1 min at a variety of input frequencies (Pacific frequency step-increased by increments of .5 or 1Hz until reached 59.5Hz, at which point the converter was drawing 50kW from the Pacific.

<u>2) Input overvoltage test</u>
- Converter left running from the power sweep test
- Freq. on Pacific reduced to 55Hz in order to reduce converter power level to about 35kW
- Voltage on Pacific increased in about 10V increments until the input voltage was about 550VAC
- Output voltage (grid) remained at 480VAC
- By 550VAC, the power throughput of the converter had increased to about 44kW
- This demonstrated that the software handled a higher input voltage than output voltage

<u>3) Over/under voltage test</u>
- The Pacific was connected to the output, so utility fluctuations could be simulated
- Since no inductor was available to simulate the stator inductance of a generator, we could not use the grid as a simulated generator source.
- Instead, we programmed the converter to draw 0 current from the input, and just left the input disconnected from anything.
- The Pacific was set to 480VAC/60Hz
- The converter was run drawing zero power (drawing losses from the Pacific)
- The Pacific voltage was increased to about 8% over nominal, then increased slowly in 1 volt increments until the converter tripped offline due to grid overvoltage
- The converter tripped offline at about 1 to 1.5 volts above the setpoint
- The Pacific voltage was then decreased to about 10% under nominal, then decreased slowly in 1 volt decrements until the converter tripped offline due to grid undervoltage.
- The converter tripped offline at about 4-5 volts below the setpoint
- The setpoint in the code was increased by 5 volts
- The undervoltage test was repeated
- The converter tripped offline at about 1 volt below the setpoint

<u>4) Over/under frequency test</u>

- The Pacific was set to 480/60Hz
- The converter was turned on in the same mode as for the over/under voltage test
- The Pacific frequency was incremented by .1Hz until it reached 60.5Hz.
- Within a fraction of a second of the Pacific being commanded to output 60.5Hz (adjusted up from 60.4Hz), the drive tripped offline due to grid over-frequency
- This test was repeated with identical results
- The Pacific frequency was set to 59.6Hz
- The converter was restarted
- The Pacific frequency was decremented by .1Hz until it reached 59.3Hz.
- The converter remained running at 59.3Hz
- The Pacific frequency was decreased to 59.28Hz
- The converter tripped offline due to grid under-frequency within a fraction of a second
- The grid under-frequency trip level was increased by .03Hz in the control system
- The under-frequency test was repeated
- The converter tripped offline within a fraction of a second of the Pacific frequency being set to 59.3Hz

- The anti-islanding algorithm was turned back on
- The over-frequency test was repeated with identical results as the first over-frequency test
- The under-frequency test was repeated, but the converter repeatedly experience internal stability problems below 59.5 Hz, and the test could not be completed
- This instability is attributed to the fact that the converter has no input power source, and was therefore operating under contrived conditions.

<u>5a) Anti-Islanding test (half-power)</u>
- The Pacific was connected to the input of the converter
- The utility 480VAC was reconnected to the output
- The Pacific was set to 450VAC, 53Hz
- The converter was reverted back to its original code that follows the 47-60Hz power/frequency curve, and anti-islanding was deactivated
- 53Hz on the input resulted in about 22kW output to the grid, which is about half power
- Parallel C, L, and R loads were added in parallel to the grid connection until the measured kW and kVAR were within about 300VA of zero
- The grid connection was then opened, islanding the converter and C, L, and R loads
- The L load was tweaked until the stable operating frequency of the islanded converter and loads was 60Hz (it was 60.1Hz before the final tweaking)
- The converter was stopped, the utility re-connected, and anti-islanding activated with a 1 degree sweep setting. Grid frequency trip values were set wide to 57.33 and 62.5Hz
- The converter was run, islanded, and the frequency sweep that resulted from the anti-islanding was recorded
- This test was repeated for 3, 3.3, 3.5, and 4 degrees of anti-islanding with the following results:

1 degree:	59.85 - 60.13Hz
3 degree:	59.44 - 60.52Hz
4 degree:	58.10 - 61.90Hz
3.5 degree:	58.72 - 61.27Hz
3.3 degree:	58.40 - 61.57Hz

<u>5b) Anti-Islanding test (full-power)</u>
- Anti-Islanding software was disabled, converter restarted with utility active
- Pacific frequency was incremented until power output was around 44kW
- C, L, and R loads were re-tuned, the system was islanded, the loads tweaked again.
- The converter was shut down
- The converter was reprogrammed to gradually increase the anti-islanding sweep delta
- The converter was run, islanded, and the output frequency was monitored. The data was saved in the hyperterminal file

<u>5c) Anti-islanding test (1/4 power)</u>
- Test procedure from 5b was repeated with the pacific frequency set to 50Hz to get approximately 1/4 power output
- It was not possible to get the loads configured for a Q factor of 2.5 at this power level because of the amount of capacitance in the output of the AC-link converter. The minimum Q that was possible was about 5.

- The grid frequency trip levels were set back to normal, the anti-islanding sweep degrees was set to 3.3
- The converter was run and then islanded
- The converter tripped offline within a fraction of a second of the grid contactor opening

<u>5d) Anti-islanding test (1/2 power, again)</u>
- The pacific was set back to 53 Hz to produce half power again
- Anti-islanding was disabled in the converter
- The load was matched, the converter was islanded, the load tweaked (attainable Q was slightly higher than 2.5)
- The converter was re-programmed to do the anti-islanding sweep
- The converter was started, islanded, and the the sweep data was recorded by hyperterminal

- Anti-islanding was reactivated, with the sweep degrees set to 3.3
- The converter was run, and then islanded
- The converter tripped offline within a fraction of a second of the grid contactor opening

<u>6) High-efficiency sweep</u>
- The converter was programmed to run with uni-lateral outputvar, and with a minimum pulse frequency of 400Hz
- The converter was run, and the Pacific was set to 450V, and the frequency was incremented in 1Hz increments from 48Hz to 58Hz

Appendix D – Thermal Imaging Testing Results (Modified C&F)
NOTE: The report has been edited in order to save space; some images have been removed and compressed. The report containing all images at full resolution is available upon request.

Thermal Imaging Test

of the

Princeton Power Systems

Prototype Wind Power Converter

Performed at:
Distributed Energy Technology Lab (DETL)
Sandia National Laboratories
Albuquerque, NM

Test performed by:
Mark A. Rumsey and Sigifredo Gonzalez
Sandia National Laboratories
Albuquerque, NM
505-844-3910, 505-845-8942
marumse@sandia.gov, sgonza@sandia.gov

Test performed on:
October 7, 2005

Report date:
October 14, 2005

Table of Contents

Important Notes concerning Infrared Thermography Imaging

An infrared (IR) thermography camera detects and images thermal radiation. The detected thermal radiation can come from several sources. What is desired is to detect only the radiation emitted from the surface. However, the IR camera will also detect radiation reflected off the surface, radiation transmitted through the object (unless it is opaque), and the radiation generated from within the camera optics and detector. In addition, the radiation that reaches the camera is influenced by several factors, such as, the surface temperature, emissivity of the object, radiation wavelength, air temperature and humidity, and the distance between the camera and object. The IR camera corrects itself for any internal radiation generated. If the IR camera is provided with and can measure all the other factors, and the thermographer minimizes the reflected radiation, only then an accurate surface temperature can be calculated based on the radiation detected. Needless to say, an accurate temperature reading can be very difficult to obtain; the IR camera and thermographer can be easily fooled.

Generally, the higher the emissivity of a surface (which means less reflected radiation), the more accurate the calculated temperature is a representation of the surface temperature. Shiny surfaces can have a higher proportion of reflected radiation (to emitted radiation) which makes an accurate calculated "temperature" very difficult to obtain.

Fortunately, for a qualitative evaluation and the environment (materials, temperatures and humidity) found in the DETL, the only variable that was critical to know was the surface emissivity. Below is a table showing the emissivity of the surfaces encountered and observed during the thermal tests of the Princeton Power Systems Wind Converter.

Material	Emissivity (at various IR wavelengths)
Perfect reflector	0.000

Shiny aluminum	0.04	
Polished copper wire	0.05	
Plastic electrical tape	0.85	
Ceramic packaging on electronics	0.85	(rough silica)
Epoxy printed circuit board	0.91	
Human skin	0.98	
Perfect emitter (or absorber)	1.000	(often called a blackbody)

If the surface of the test specimen is not known, a common practice by thermographers is to prepare the surface with paint or tape with a known emissivity. The temperature of the object in question is then measured by measuring the temperature of the surface of the tape or paint using the IR camera. (Of course, this is assuming the tape or paint has a significantly lower thermal mass then the underlying structure.)

We obviously can not see infrared radiation. So when the camera shows an IR image, what color do you use to show the image? The authors chose a rainbow color palette because blue subjectively implies cool and red hot.

Important note: the emissivity setting in the IR camera was set to a constant of 0.96, even though a better emissivity setting would have been 0.85. In any case, this was the emissivity used throughout the test in the calculation of all the temperatures in the thermal images. This also implies all objects in the image have the same emissivity, which generally is not true. However, the objects that we intended to observe did have approximately the same emissivity (~0.85).

For each image, printed in this report, the authors tried to fix the temperature range (color table) so the reader could easily see temperature differences and trends between images by matching colors. However, different images may not show the same temperature range (or color range), so please check the temperature scale before visually comparing colors.

There were several visible and IR image files created in the course of this test. The saved image files have been burned to a CD-R, and will be provided to the Princeton Power staff.

Also on the CD-R are two freeware programs called ThermaCAM Explorer 99 and ThermaCAM QuickView; both are provided free by FLIR Systems, Inc., on their web site (http://www.flir.com). (Double-clicking on the TCEXPSETUP.EXE file icon will install the ThermaCAM Explorer 99 program. Unzipping and double-clicking on SETUP.EXE will install ThermaCAM QuickView.) Both programs can be used to post-process the original IR image files[3] acquired by the FLIR cameras. Both programs allow the user to vary the color palette and temperature range for each image. (The temperature (color) range is easier to set with ThermaCAM Explorer 99. The ThermaCAM QuickView has a very nice tool called the "Flying Spot" where any temperature in the image can be read.) The authors encourage anyone interested in the IR images in this report to exercise the two programs with an original IR image. Changing

[3] The JPG images created by the FLIR ThermaCAM P60 camera have FLIR-embedded information that is used by the ThermaCAM software. When a post-processed JPG image is created and stored the FLIR-embedded information disappears. In other words, only original camera-generated and stored images can be post-processed with the ThermaCAM software.

the color palette, temperature scale and range can bring out very interesting and subtle detail that can't be captured in just one image.

Test Objective

Disclaimer: The Princeton Power technical staff is obviously intimately familiar with every component in this wind converter. For this reason the authors deemed it un-necessary to point out the various wind converter items. However, these items can be difficult to identify in the IR images. Contact the authors if there are questions.

The main objective of this test was to provide a qualitative evaluation of the heating dynamics, for a duration of at least an hour, of the Princeton Power System's prototype wind power converter.

Test Equipment

Item to be Tested

Princeton Power Systems Wind Power Converter, prototype #1(?)

Wind Power Converter Input

Pacific Power Source, Model MS 3060
http://www.pacificpower.com/products/ms-series.htm

Wind Power Converter Output Load

Wind power converter output was connected to the utility grid

Thermal Imaging Cameras

FLIR ThermaCAM P60 Infrared Thermography Camera, P/N 1195342
(Property of the SNL Solar System Department, 6216, S/N 21802894)
IR Wavelength Range: 7.5 to 13 micrometers (considered long-wave IR)
Uncooled Focal Plane Area (FPA) size: 320 pixels by 240 pixels
Temperature Accuracy: +/- 2 ºC (+/- 3.6 ºF)
Thermal Sensitivity is 0.06 ºC (0.11 ºF) at 30 ºC (86 ºF)
http://www.flirthermography.com/cameras/camera/1016/

Time References

Mark's digital watch
FLIR ThermaCAM P60 IR camera has an internal clock
(Mark's watch and the IR camera were manually set to WWV time to within +/- 2 seconds.)
Note: The creation time of the post-processed image files (generated by a PC) probably deviate from WWV time.

Image Editing Software

ThermaCAM Explorer 99, Oct 2003 edition, provided free by FLIR Systems, Inc.
PrintKey, version 3.08 (screen capture)

Test Item Connection

Test Setup

One test was conducted to determine the heating dynamics of the wind power converter. The Pacific Power Source provided a constant 20 kilowatts of 3-phase power to the Princeton Power Systems wind power converter for over an hour. The 3-phase output of the wind power converter was tied to the utility grid. A simple graphic showing the test setup is shown in Figure 2.

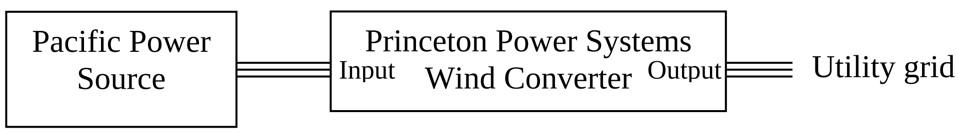

Figure 2: Graphic showing the test setup.

Infrared Image Files

Because some of the parts in the converter were made of shiny metal we used plastic electrical tape (as a surface with a known high emissivity) to monitor the temperature of the metal surfaces.

The IR image color palette, temperature scales and ranges were post-processed using ThermaCAM Explorer 99. The final image was screen captured, using PrintKey, to obtain the color image and the color-to-temperature scale. (The ThermaCAM software does have an image post-processed storage capability, but the color-to-temperature scale is stripped off the final stored image.)

All the original visible-light image files have a filename of DSCN00NN.JPG, where NN is from 45 to 80 (not all images were kept). All post-processed image files have the letters “a” or “b” appended to the filename, for instance, DSCN0063b.JPG.

All the original infrared image files have a filename of IR_00NNN.jpg, where NNN is from 013 to 105 (not all images were kept). All post-processed image files have the letters “a” or “b” appended to the filename, for instance, IR_0045a.jpg.

The thermal test started at the DETL at 1:33:00 MDT, and ended at 2:47:25 MDT. A timeline graphic showing the relative time between major events of the test is shown in Figure 3.

Sequence of Events

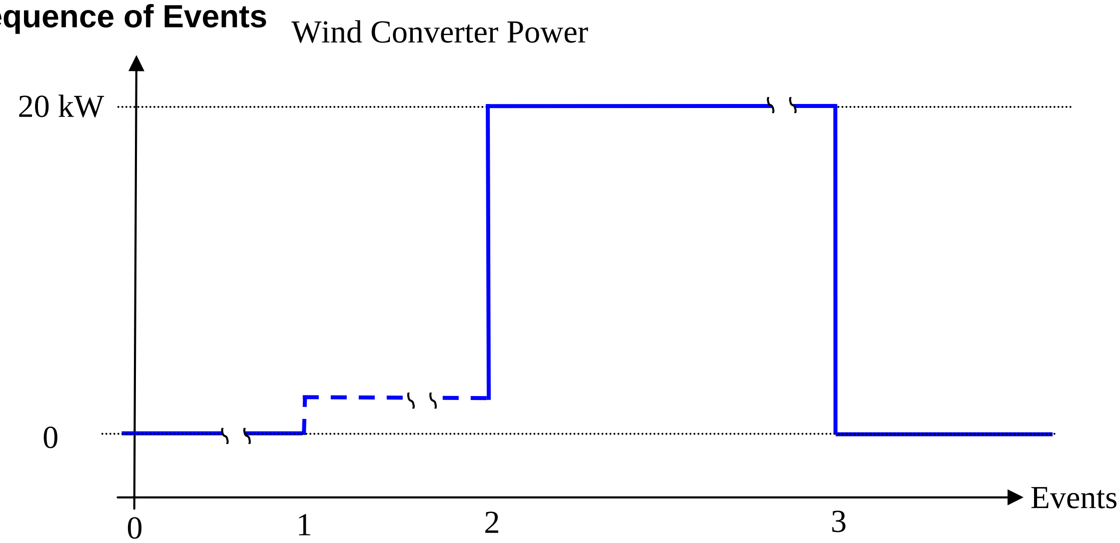

Figure 3: Graphic showing a timeline of the thermal test.

Event 0 Time: before 1:33:00 MDT. The wind converter was completely disconnected from any input power, and had been for several hours. The internal components of the converter were all at the same temperature as the surrounding environment. Sig took visible-light images of the converter interior and control board, and Mark took a series of IR images of the converter interior and control board.

Event 1 Time: 1:33:00 MDT. Three-phase 480-VAC power was applied to the wind converter, but the wind converter was not turned on. However, applying power to the converter does apply power to the control board. Mark took a series of IR images of the control board.

Event 2 Time: 1:38:06 MDT. The wind converter was turned on with 20-kVA of power being applied to the input from the Pacific Power Source. Mark took a series of IR images of the converter interior and control board.

Event 3 Time: 2:47:25 MDT. The wind converter was turned off and the 480-VAC was disconnected from the input. A few IR images were taken after the converter was turned off.

Visible Light Images

Several visible light images are included here to give the reader some idea as to what is in a corresponding IR image. In particular, plastic electrical tape was placed on several shiny metal surfaces in the converter to enable the IR camera to read accurate surface temperatures. The IR images of the wind converter under ambient conditions (hopefully and intentionally) show very little detail. The authors noticed that the printed IR images of the wind converter under ambient conditions show even less detail.

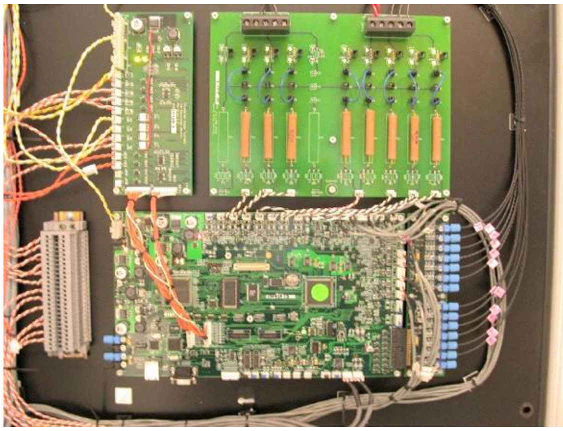

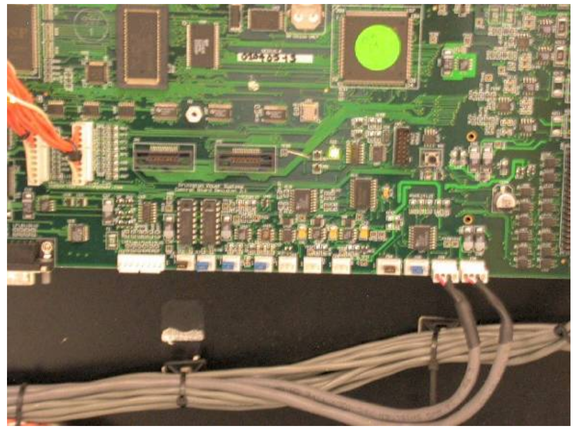

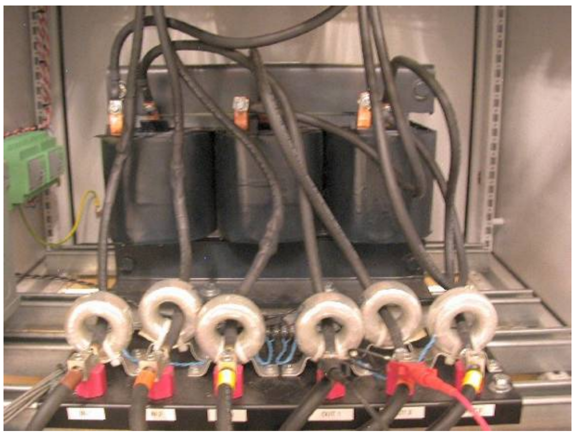

Plastic Electrical Tape

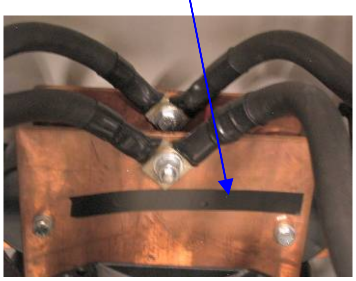

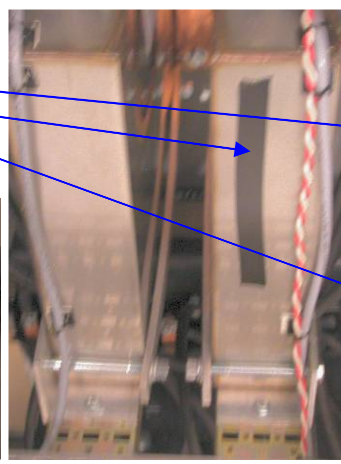

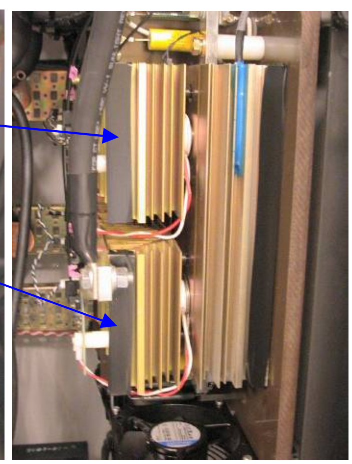

Infrared Images of Converter under Ambient Conditions

IR_0013.jpg 01:19:12 PM Just above the input and output filter capacitor canisters.

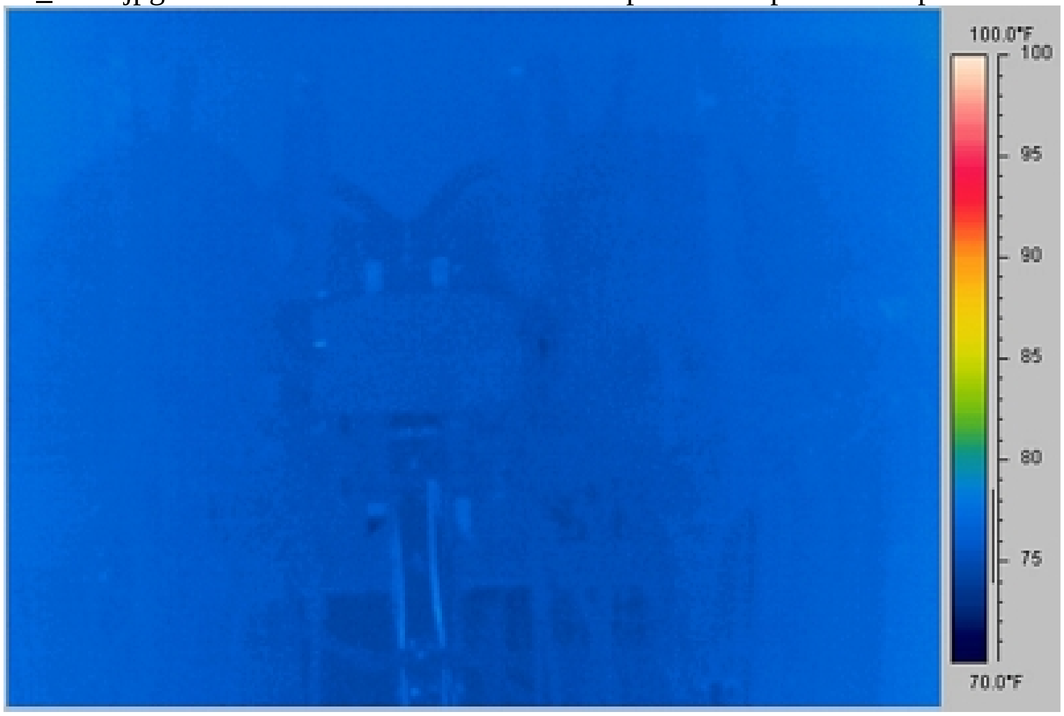

IR_0014.jpg 01:19:34 PM Input and output filter capacitors, SCRs, heat-sinks

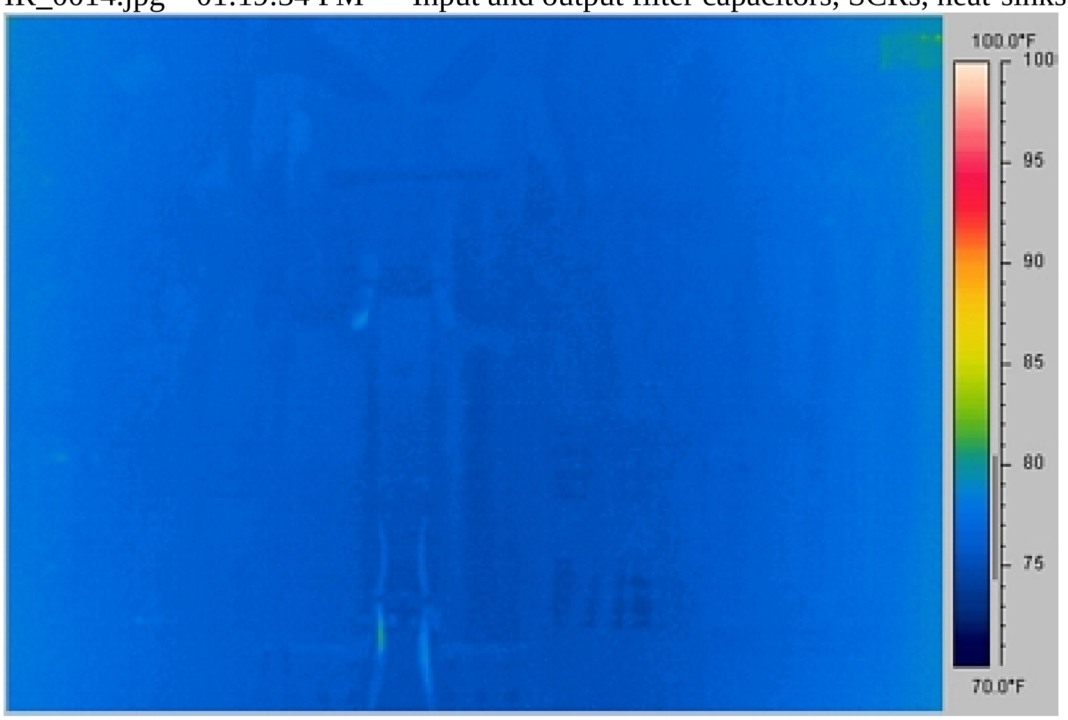

IR_0015.jpg 01:19:54 PM CVTs, connection cables

IR_0016.jpg 01:20:10 PM CVTs, connection cables

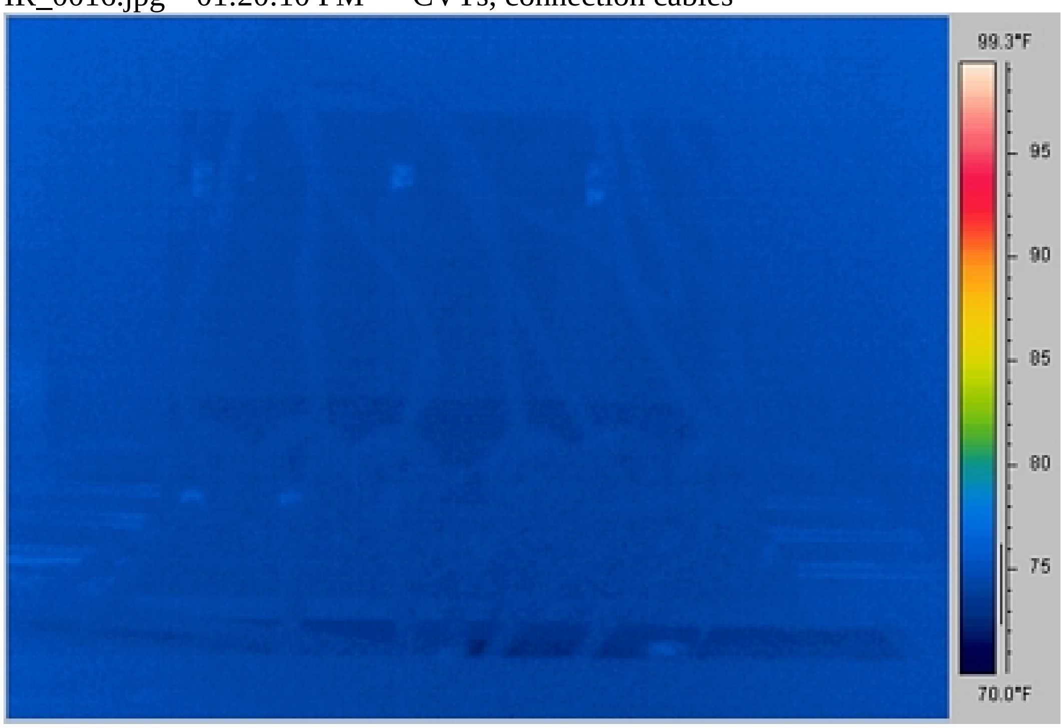

IR_0017.jpg 01:21:32 PM Step-down power transformer for control board

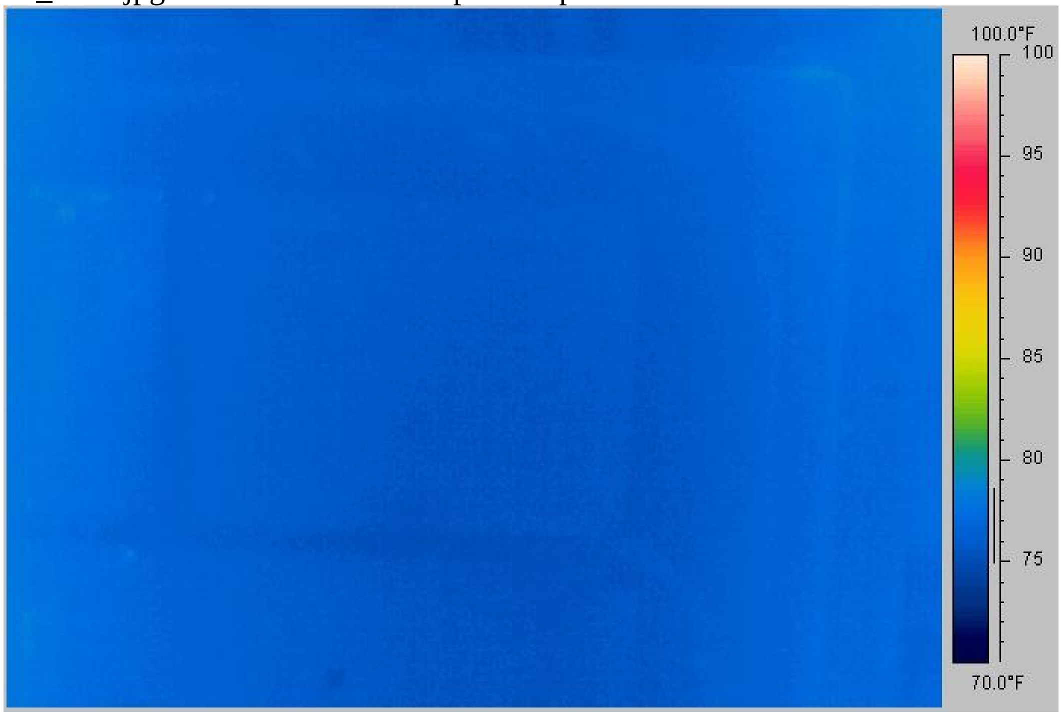

IR_0018.jpg 01:21:40 PM Step-down power transformer for control board

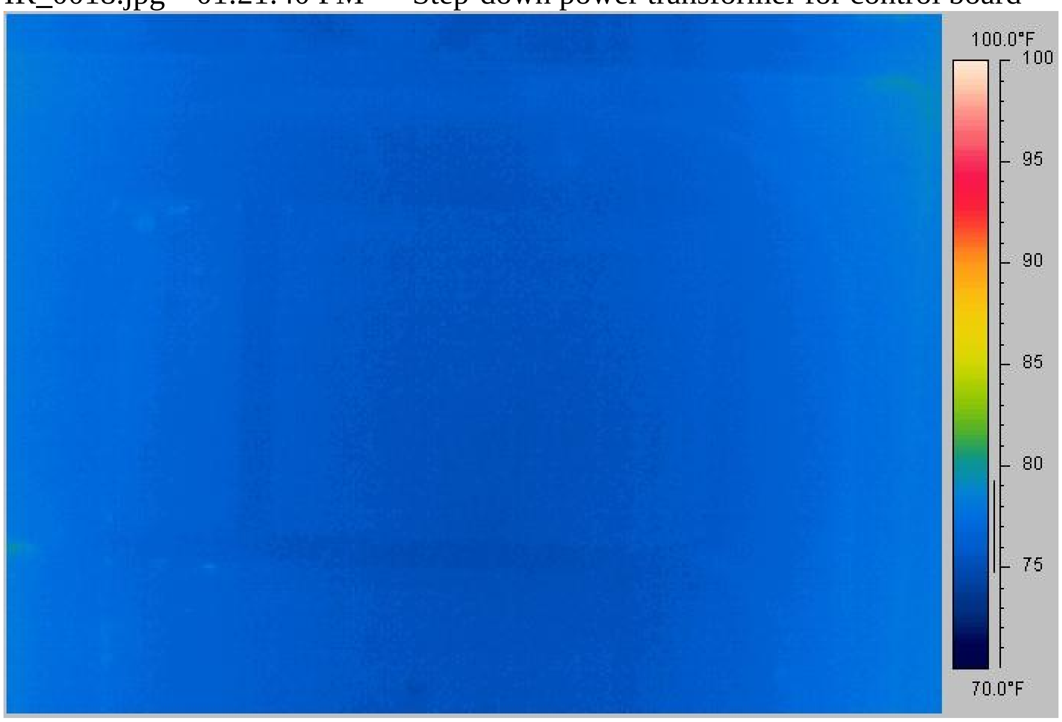

IR_0019.jpg 01:21:52 PM Control board

IR_0020.jpg 01:22:22 PM Control board

IR_0021.jpg 01:23:36 PM Close-up of center capacitors under copper plate

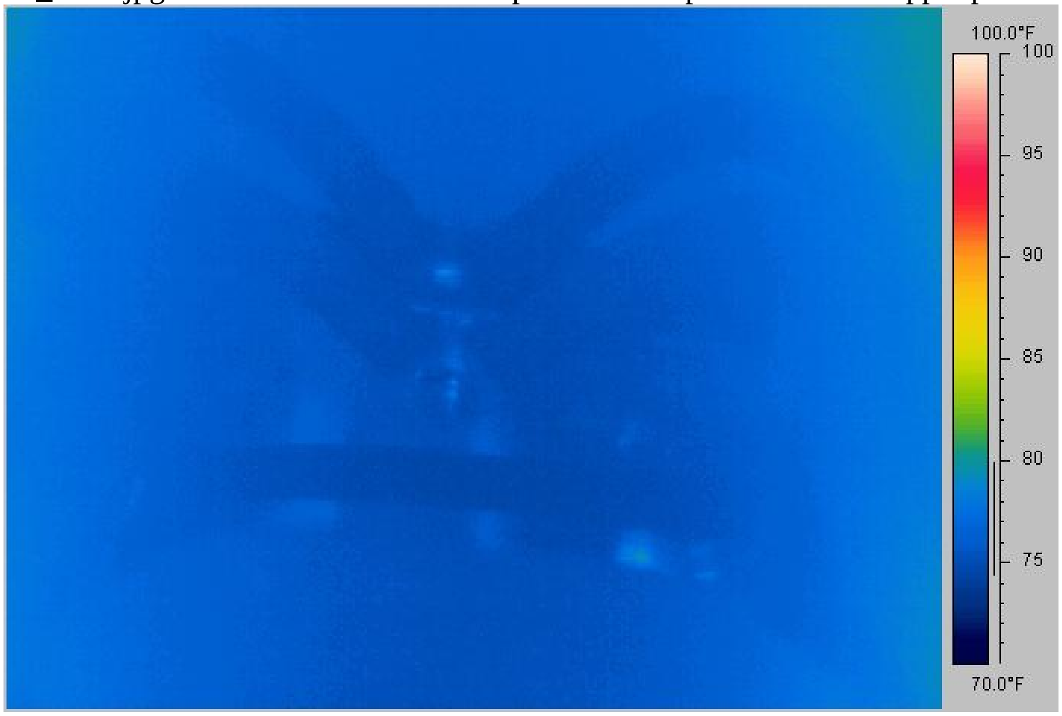

IR_0022.jpg 01:24:38 PM Input inductors

IR_0023.jpg 01:25:32 PM Output inductors

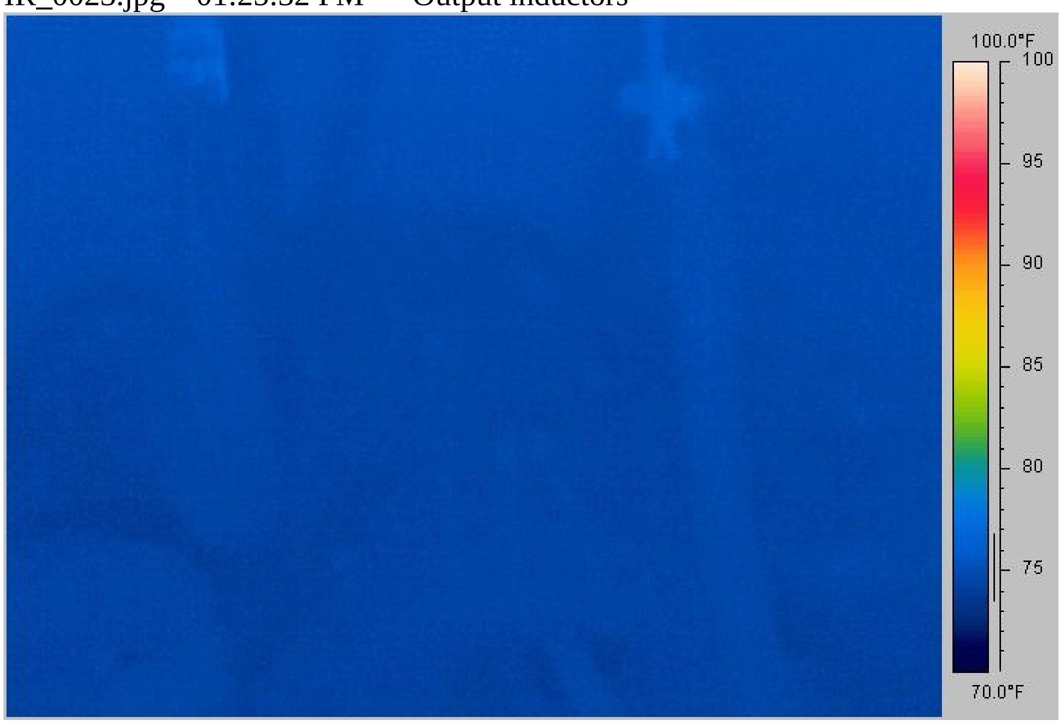

IR Images of the Wind Converter throughout the Test Sequence

IR_0024.jpg 01:25:58 PM Inductors in top of cabinet

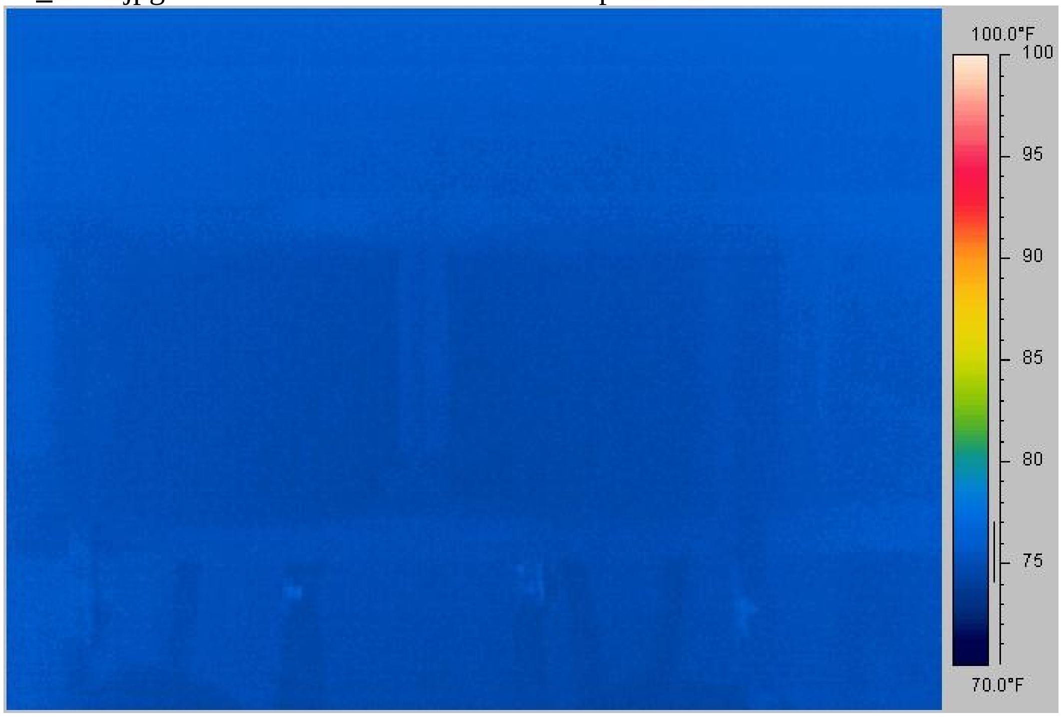

IR_0025.jpg 01:27:34 PM Close-up of an output SCR and heat sink. The small greenish-yellow rectangle on the right side is a thermal reflection of my hand off shiny metal on the converter.

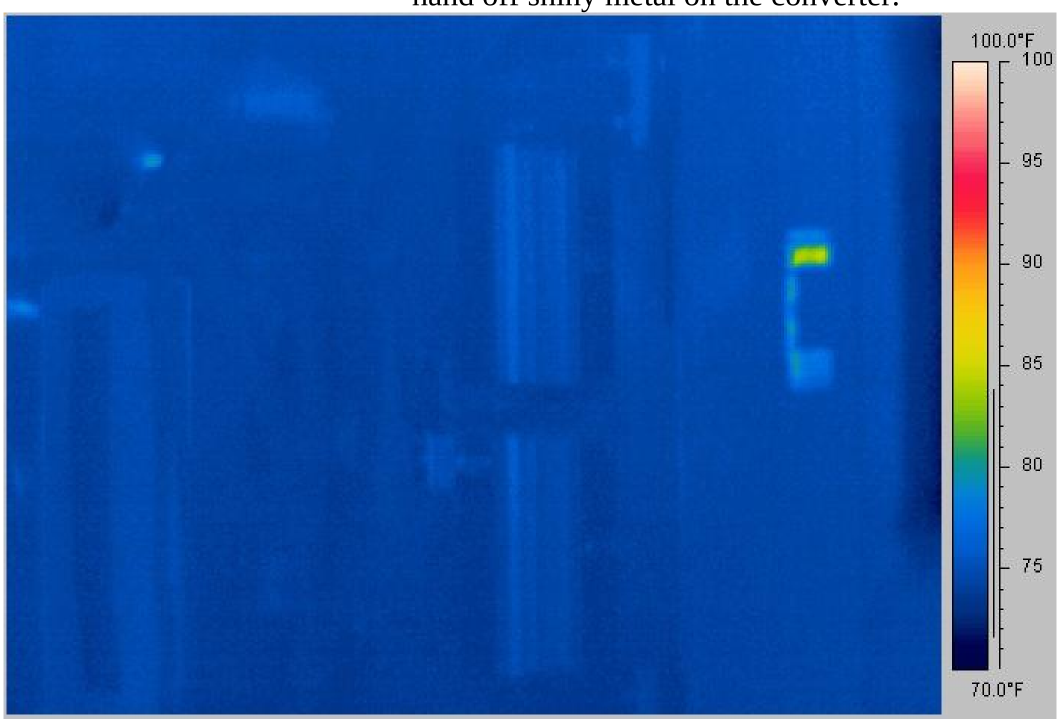

The thermal images, that are about to be shown, are presented in chronological sequence. And for each image, the file creation date is given and unique thermal features are labeled. The authors have noticed that subtle temperature/color detail is loss in the printed IR images in this report; the authors recommend looking at this report on the PC to assess the detail in the IR images.

Immediately below is a list of images that the authors think the reader should take notice.

List of Interesting Images

All of the thermal images show interesting information. However, there are a few images that warrant special attention. Below is a list of images with images that have some kind of detail that the authors think the Princeton Power staff should take notice.

Image file	Page	Comments
IR_0027.jpg	20	There are three components along the bottom center of the control board that heat up immediately, on application of control board power, to a very high temperature (>>270 °F). Also, before the wind converter is actually turned on, there are three heated components on the control board. After the converter is turned on only two components appear to be highly heated. (See also IR_0045 on page 33, IR_0046 on page 34, IR_0079 on page 53, IR_0097 on page 64.)
IR_0032.jpg	23	There is a slight temperature gradient across the heat sink. (The heat sink is cooled by a fan located just below the heat sink and pointing up). (See also IR_0068 on page 46, IR_0104 on page 68.)
IR_0036.jpg	27	Note the uneven heating of the output cables.
IR_0037.jpg	27	Note the uneven heating of the output cables.
IR_0042.jpg	31	Note the uneven heating of the output cables.
IR_0043.jpg	31	Note the uneven heating of the output cables.
IR_0045.jpg	33	After the converter is turned on only two (of three previous) control board components appear to be highly heated. (See also IR_0027 on page 20, IR_0046 on page 34, IR_0079 on page 53, IR_0097 on page 64.)
IR_0046.jpg	34	Close-up of two highly heated components on control board.
IR_0064.jpg	44	Note the uneven heating of the output cables.
IR_0065.jpg	45	Note the uneven heating of the output cables.

IR_0066.jpg	45	Note the slight uneven heating of the input cables.
IR_0068.jpg	46	There is a slight temperature gradient across the heat sink (which is cooled by a fan located just below the heat sink and pointing up). (Compare with IR_0032 on page 23, IR_0104 on page 68.)
IR_0079.jpg	53	Two control board components appear to be highly heated. (Compare with IR_0027 on page 20, IR_0045 on page 33, IR_0046 on page 34, IR_0097 on page 64.)
IR_0097.jpg	64	Two control board components appear to be highly heated. (Compare with IR_0027 on page 19, IR_0045 on page 33, IR_0046 on page 34, IR_0079 on page 53.)
IR_0099.jpg	65	Note the uneven heating of the output cables.
IR_0100.jpg	66	Note the uneven heating of the output cables.
IR_0101.jpg	66	Note the uneven heating of the output cables.
IR_0104.jpg	68	There is a temperature gradient across the heat sink (which is cooled by a fan located just below the heat sink and pointing up). (Compare with IR_0032 on page 23, IR_0068 on page 46.)

IR_0027.jpg 01:34:10 PM Control board. Converter not turned on yet.

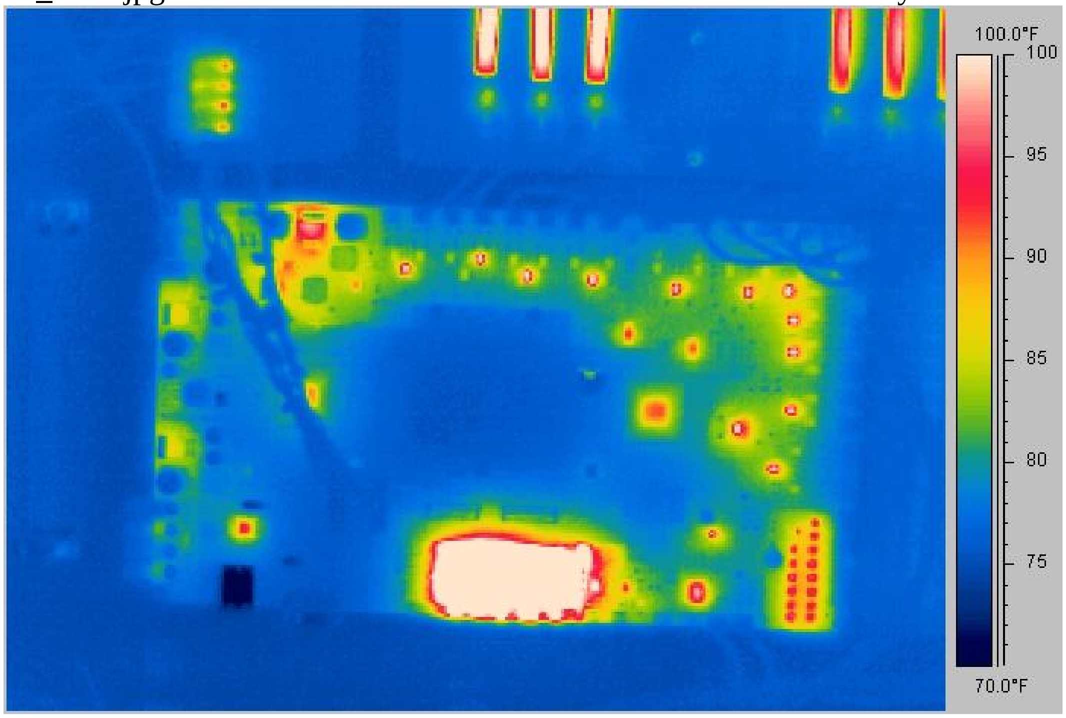

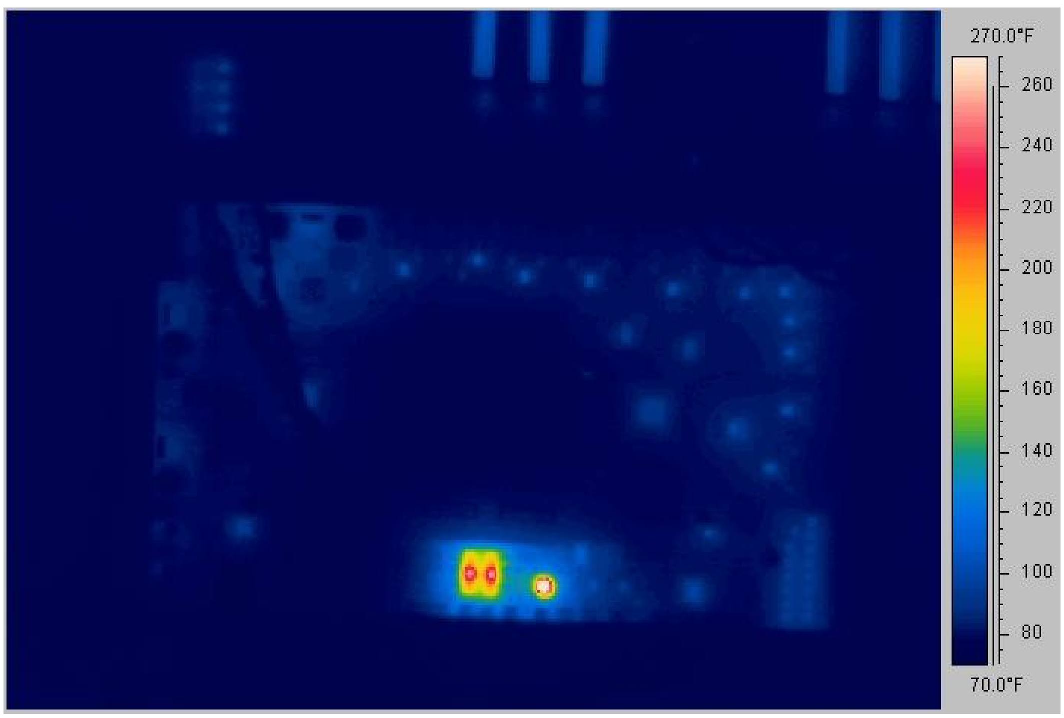

Note: The wind converter was turned on at 1:38:06 PM.

IR_0028.jpg 01:38:52 PM Fans in top of converter.

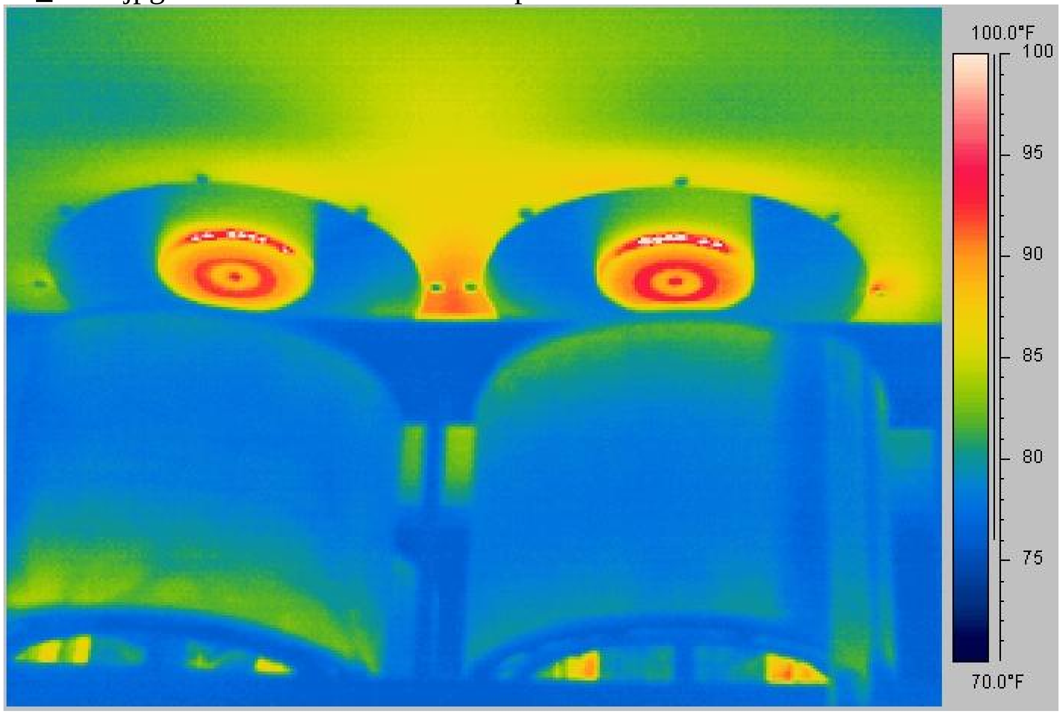

IR_0032.jpg 01:41:36 PM Heat sink and SCRs

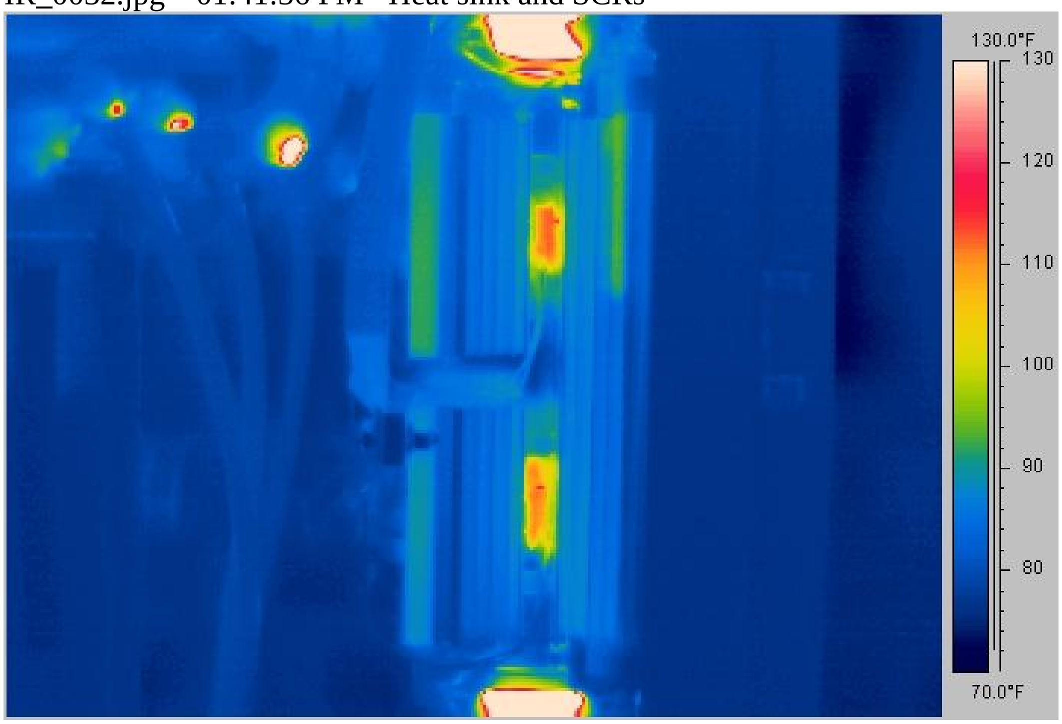

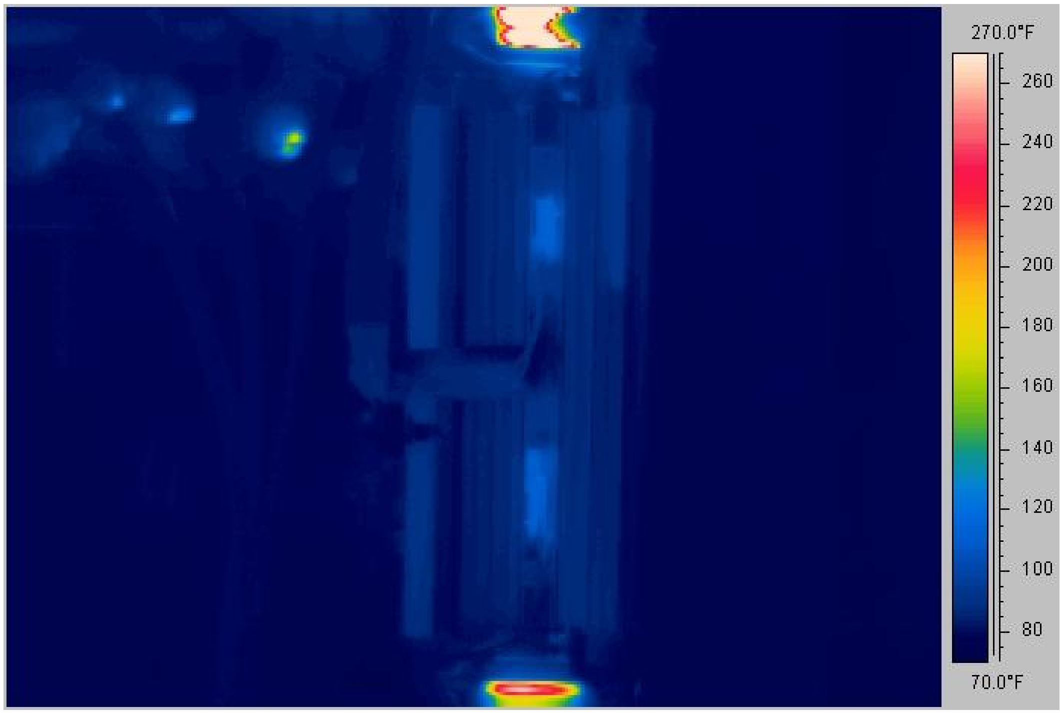

IR_0033.jpg   01:42:16 PM   Horizontal bands are artifacts from the IR camera.

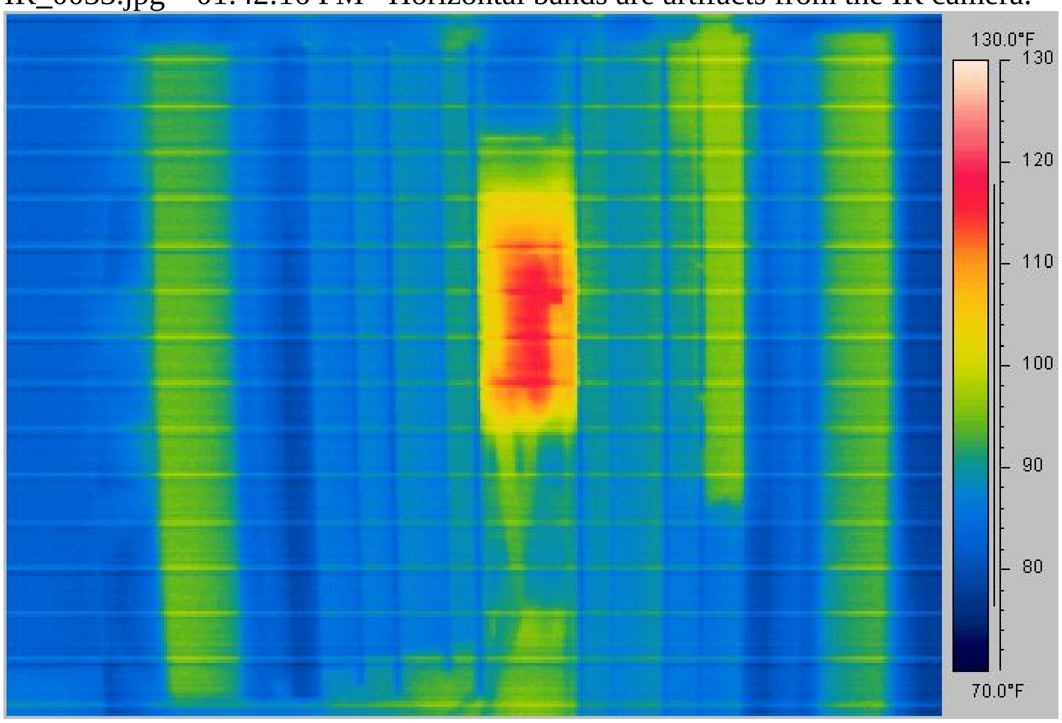

IR_0034.jpg 01:43:58 PM Power resistor (electrical tape placed on one resistor melted)

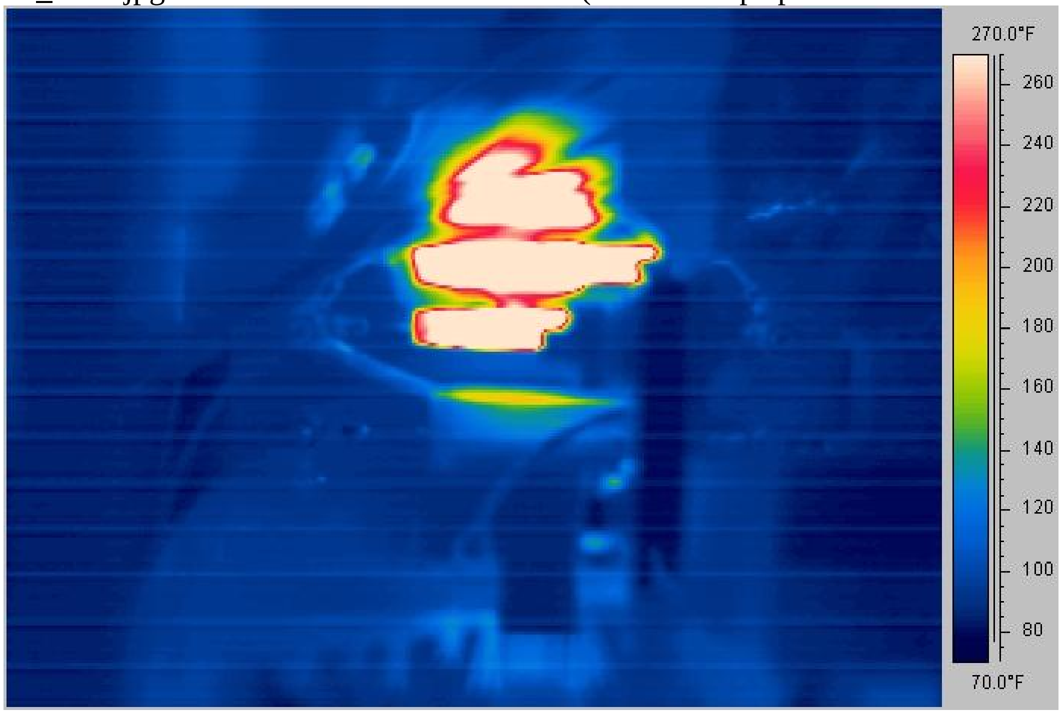

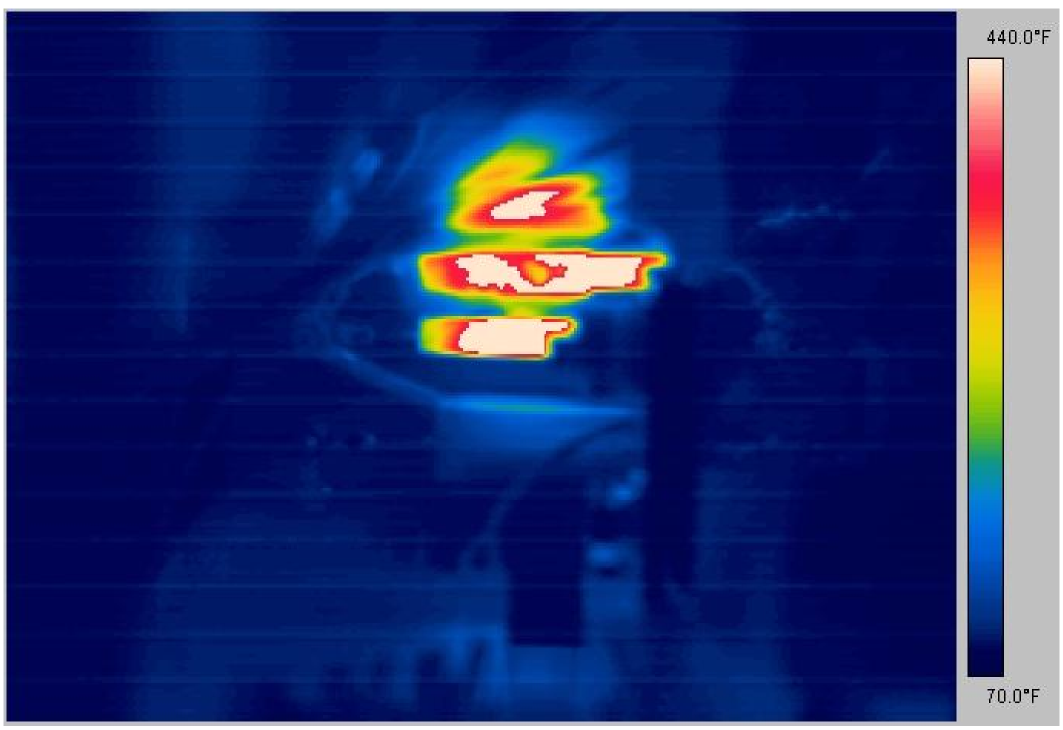

IR_0035.jpg 01:44:50 PM

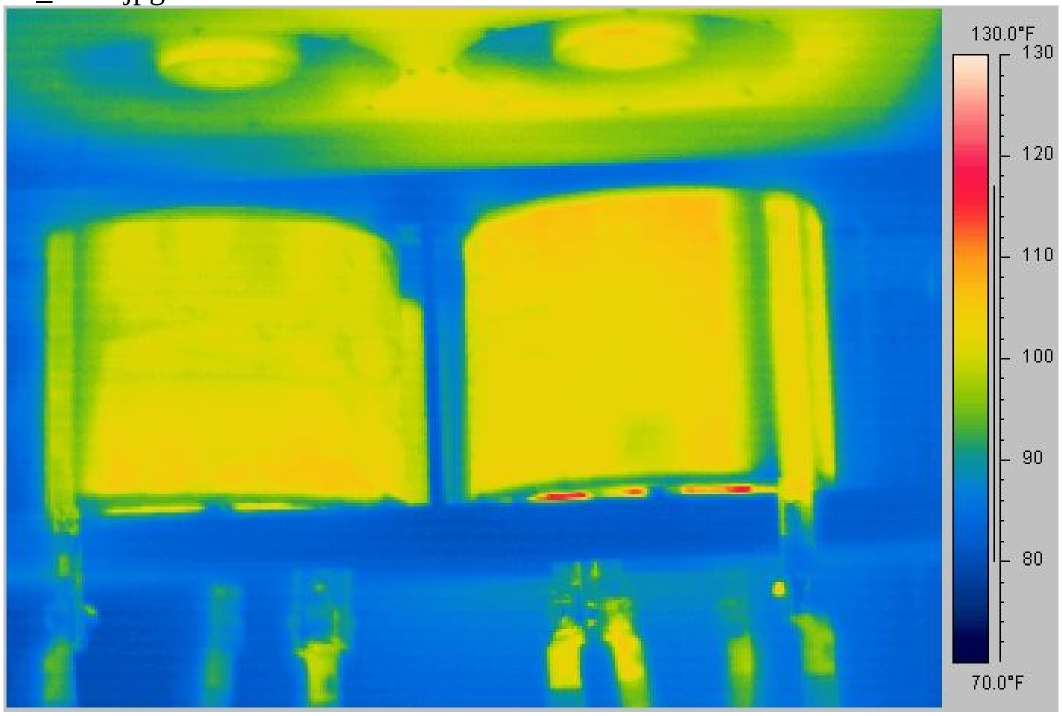

IR_0036.jpg 01:46:06 PM

IR_0037.jpg 01:46:40 PM

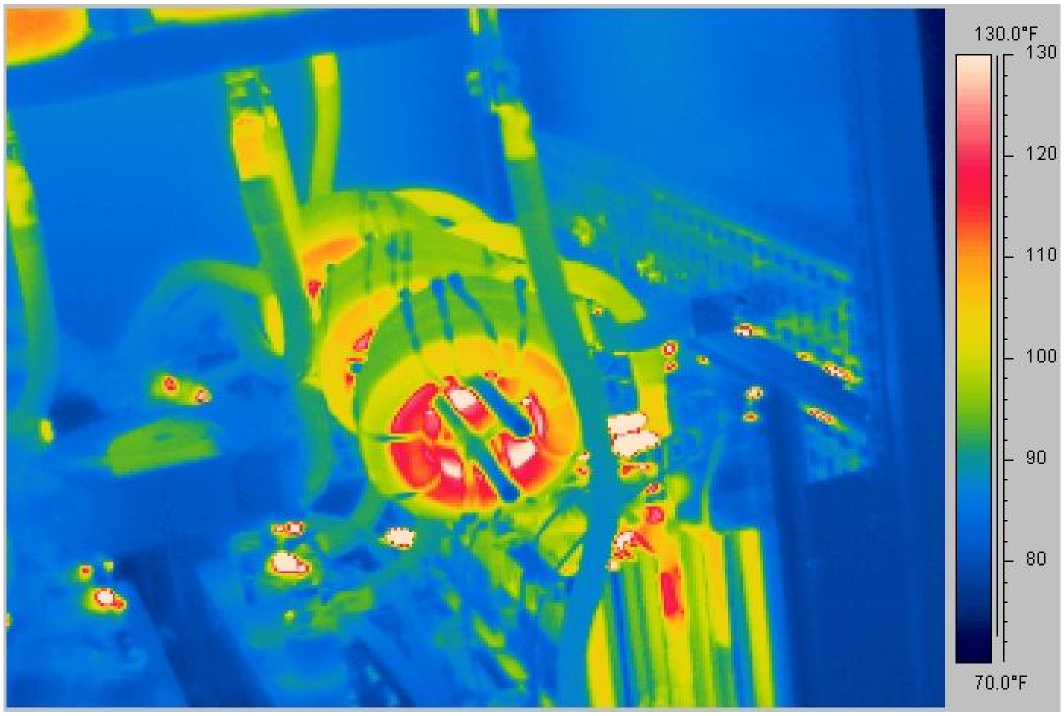

IR_0038.jpg 01:47:20 PM Horizontal bands are artifacts from the IR camera.

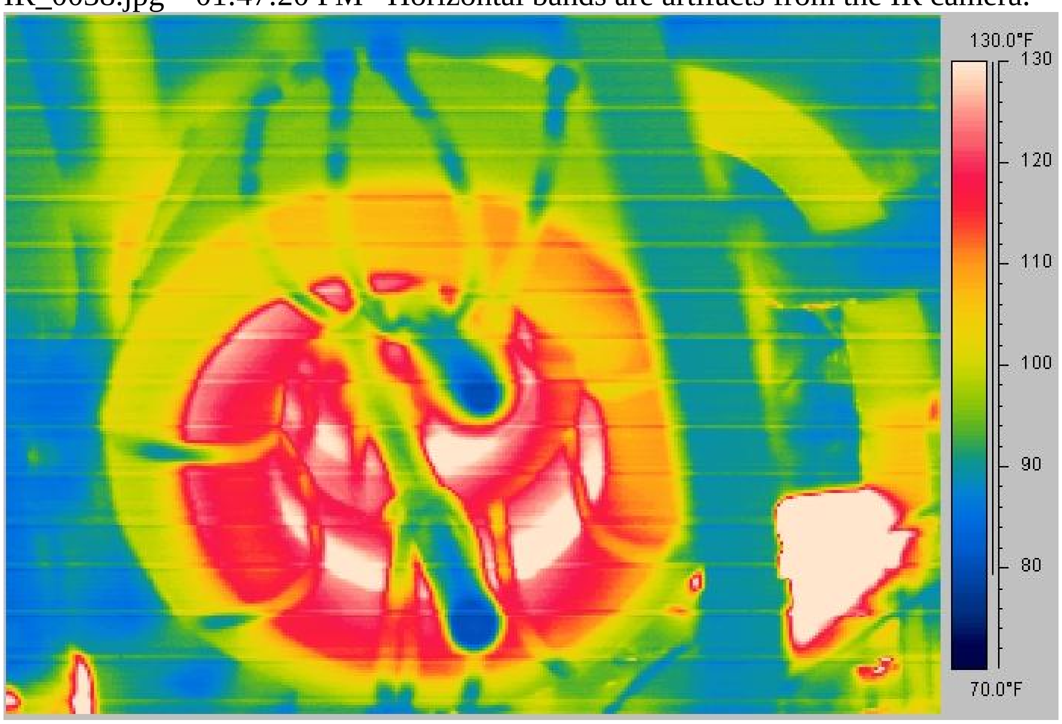

IR_0040.jpg 01:49:34 PM Power resistors

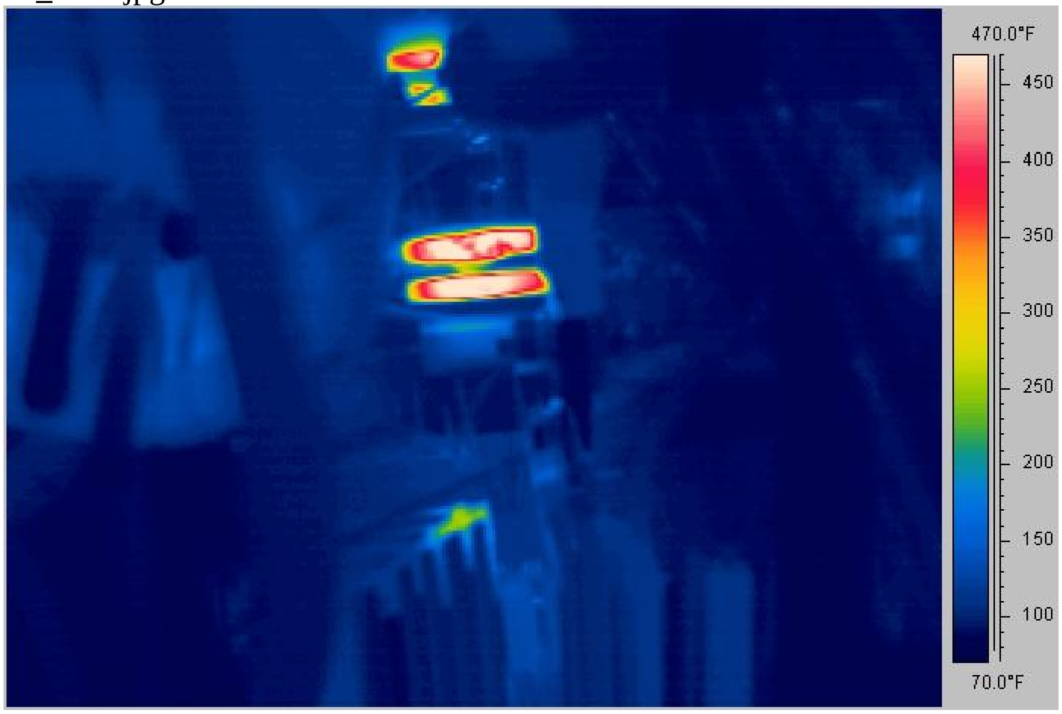

IR_0041.jpg 01:50:20 PM

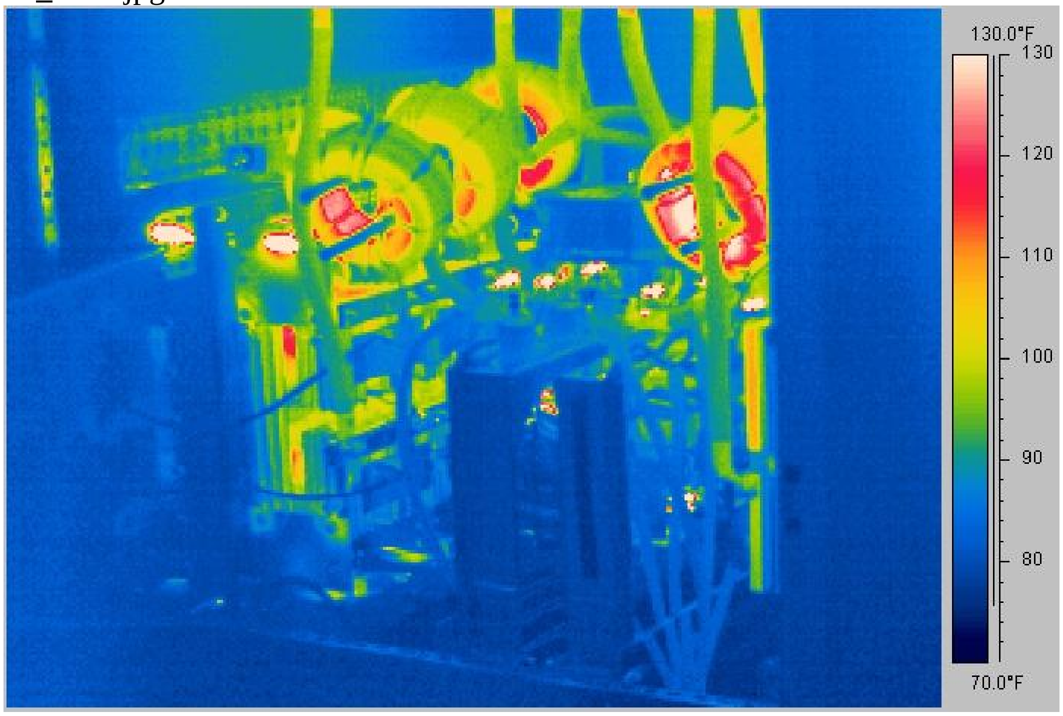

IR_0042.jpg 01:50:42 PM

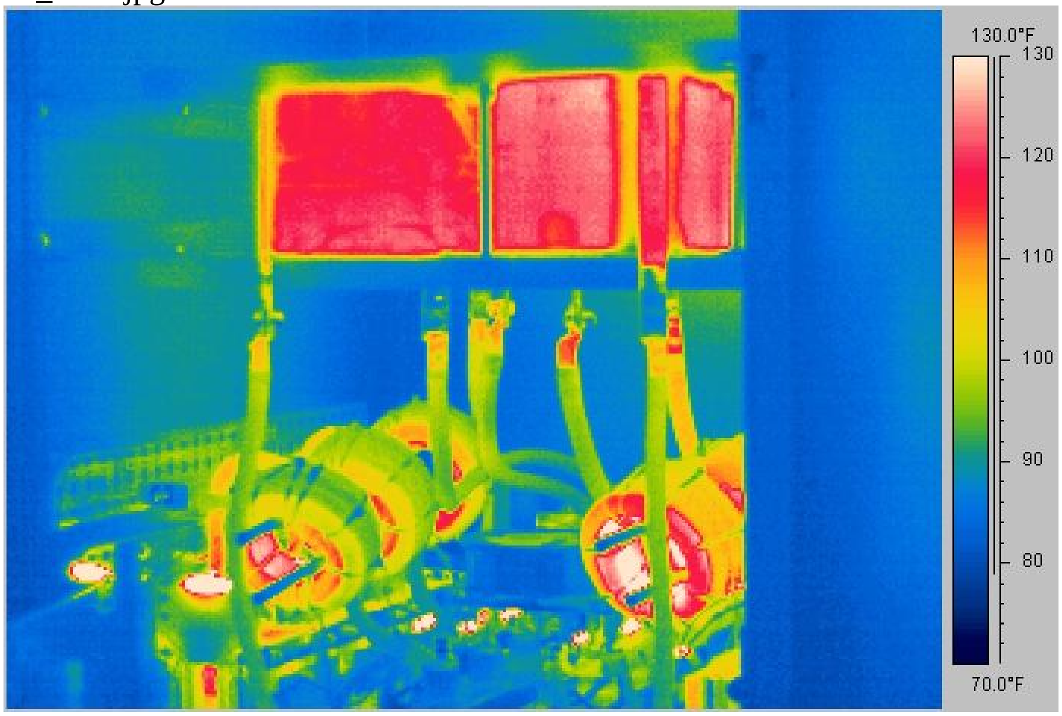

IR_0044.jpg 01:51:10 PM Bottom area of converter

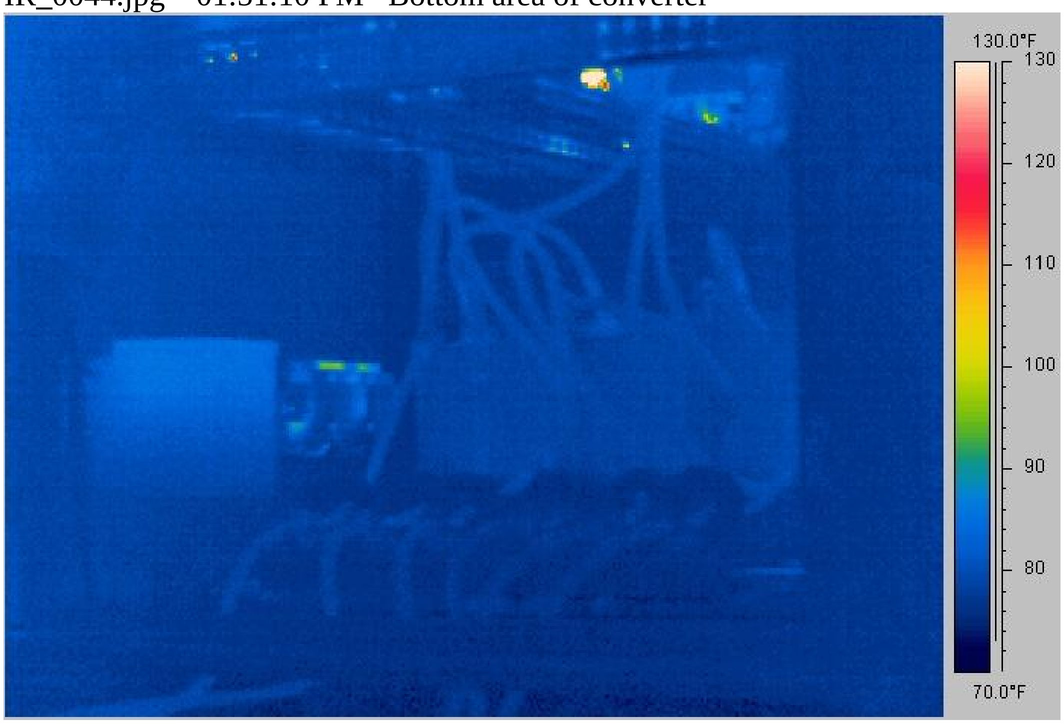

IR_0046.jpg 01:52:34 PM Control board

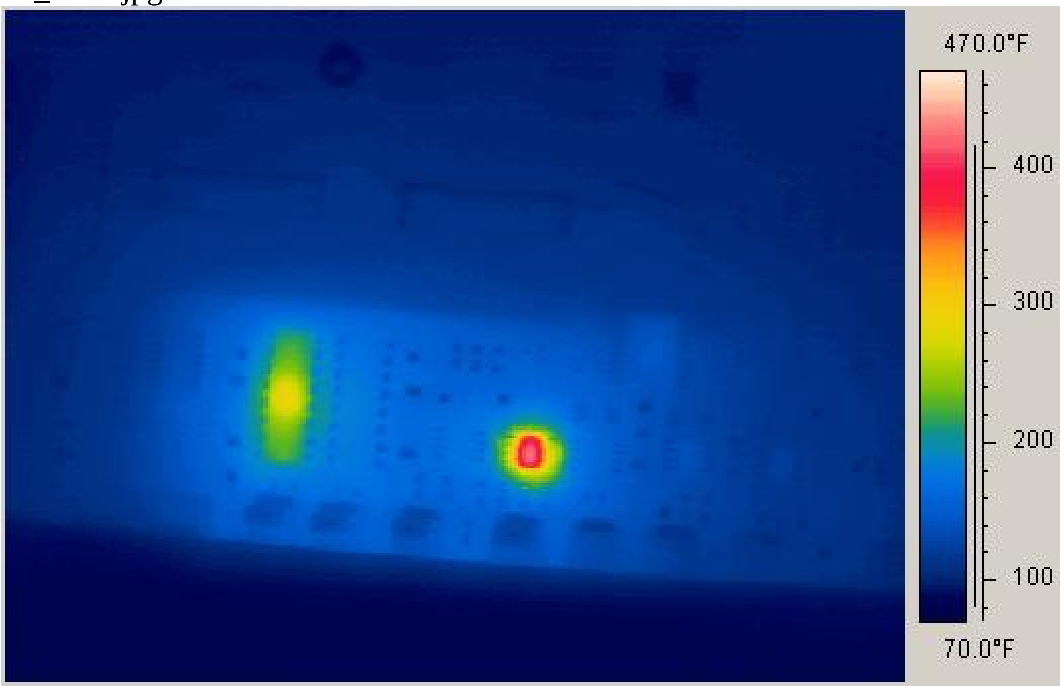

IR_0048.jpg 01:54:28 PM Top backside of wind converter cabinet

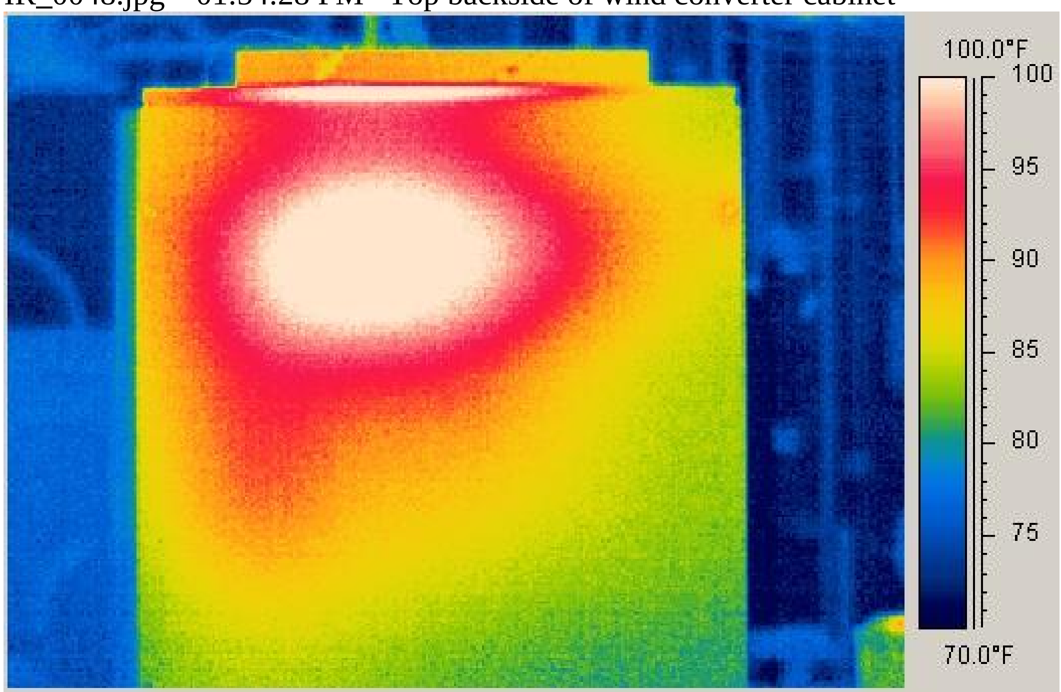

IR_0049.jpg 01:55:18 PM Bottom backside of wind converter cabinet

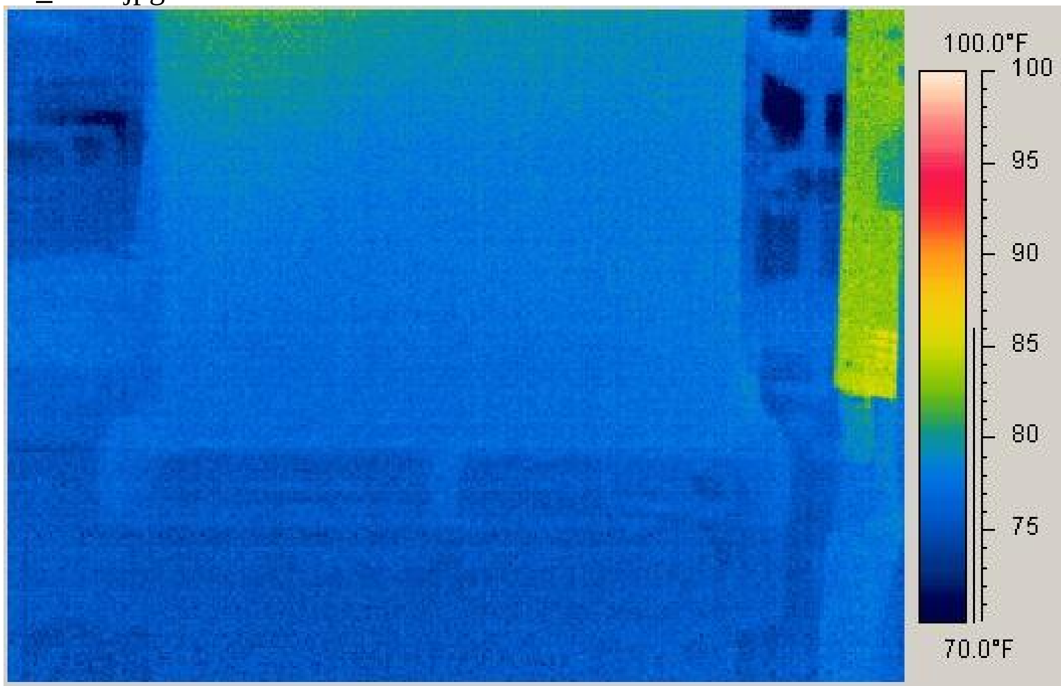

IR_0059.jpg 02:02:12 PM Output inductors

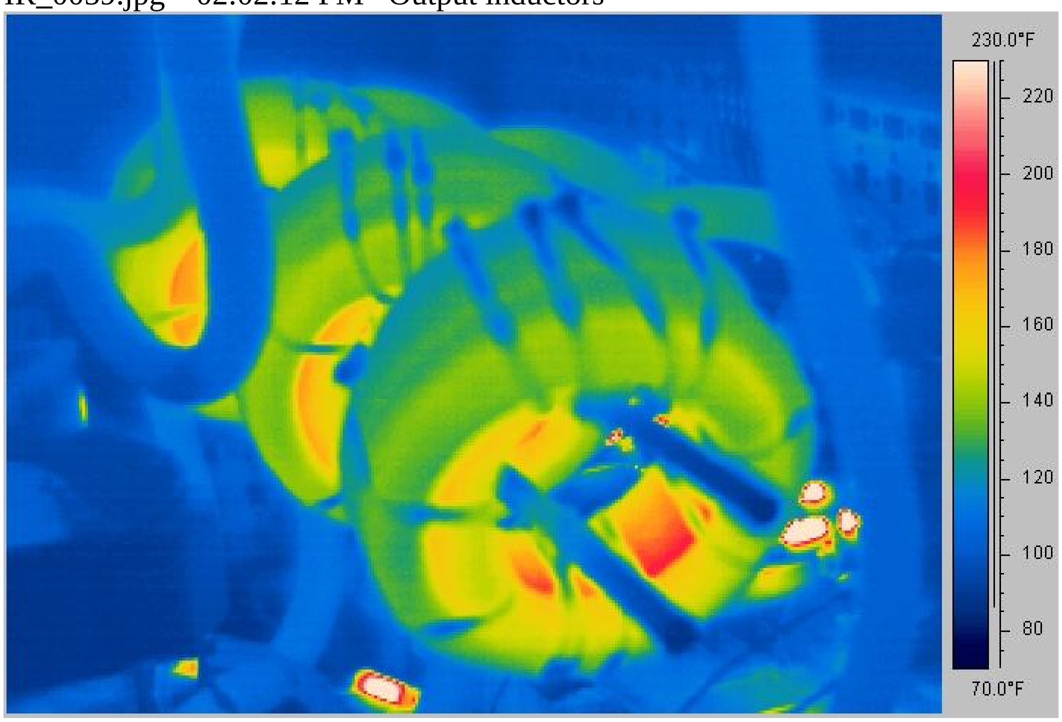

IR_0060.jpg 02:02:48 PM Input inductors

IR_0061.jpg 02:03:12 PM

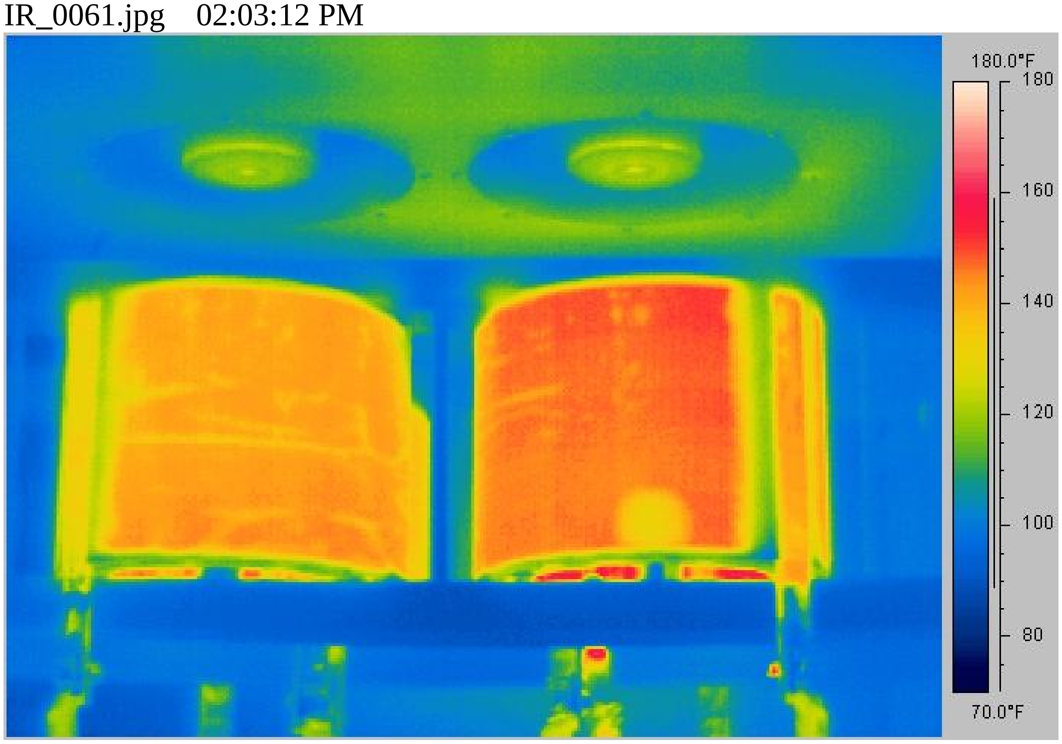

IR_0068.jpg 02:08:30 PM Lower heat sink and SCRs on output side.

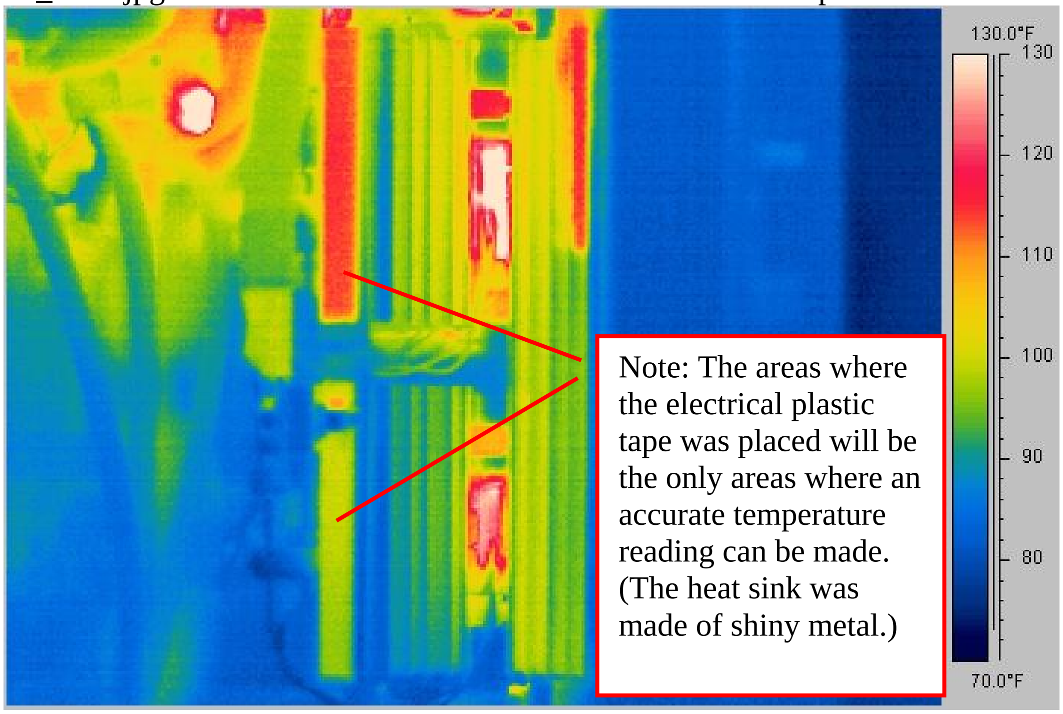

IR_0069.jpg 02:09:34 PM Power resistors

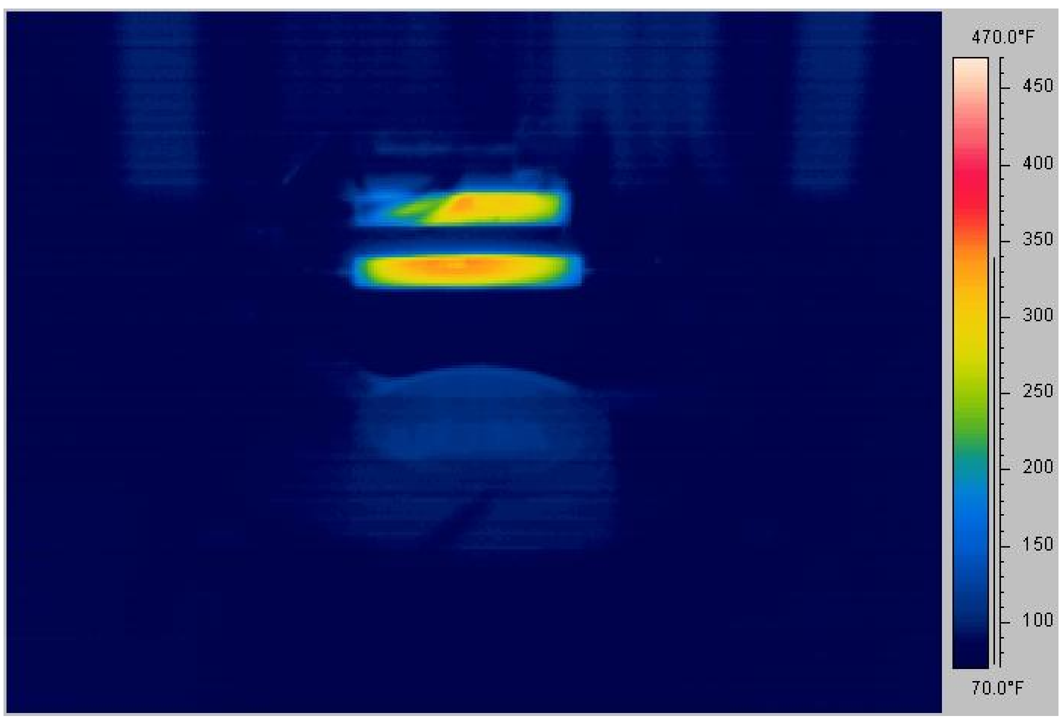

IR_0071.jpg 02:10:32 PM Input and output capacitor canisters.

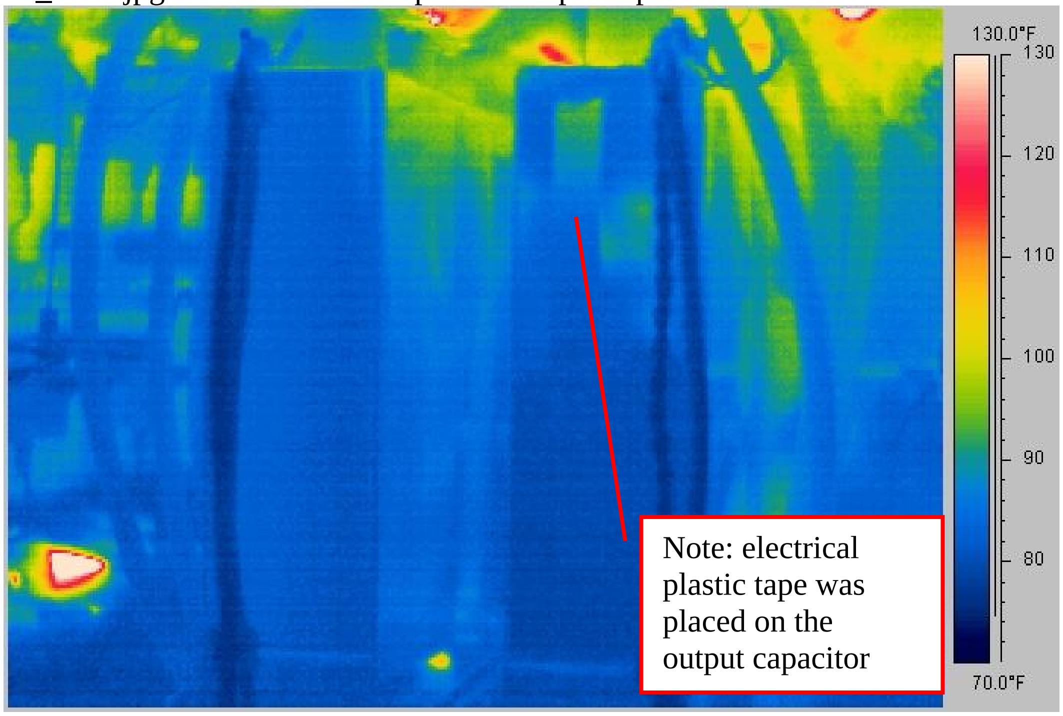

IR_0072.jpg 02:11:04 PM Horizontal bands are artifacts from the IR camera.

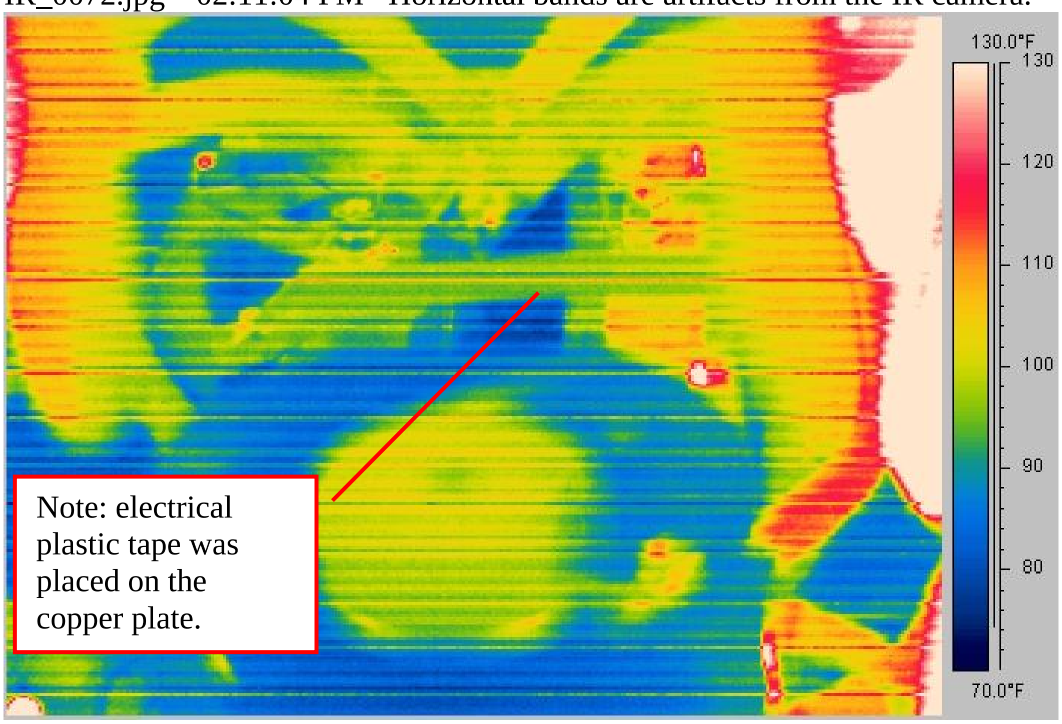

IR_0080.jpg 02:19:20 PM Horizontal bands are artifacts from the IR camera. Output inductor.

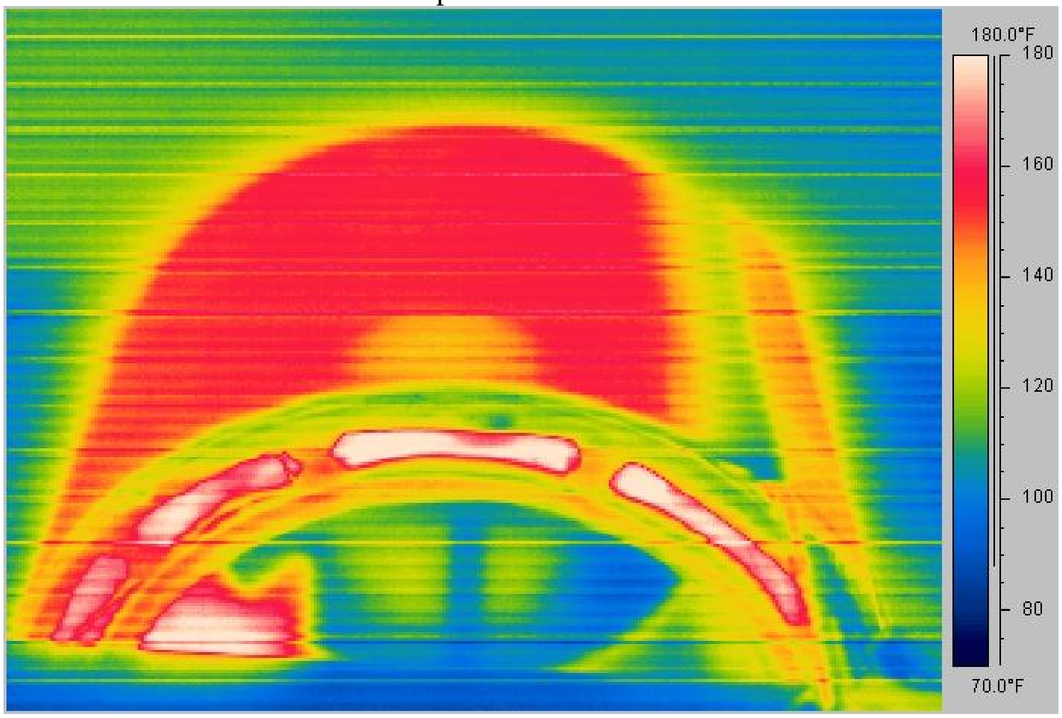

IR_0081.jpg 02:19:34 PM Input inductor.

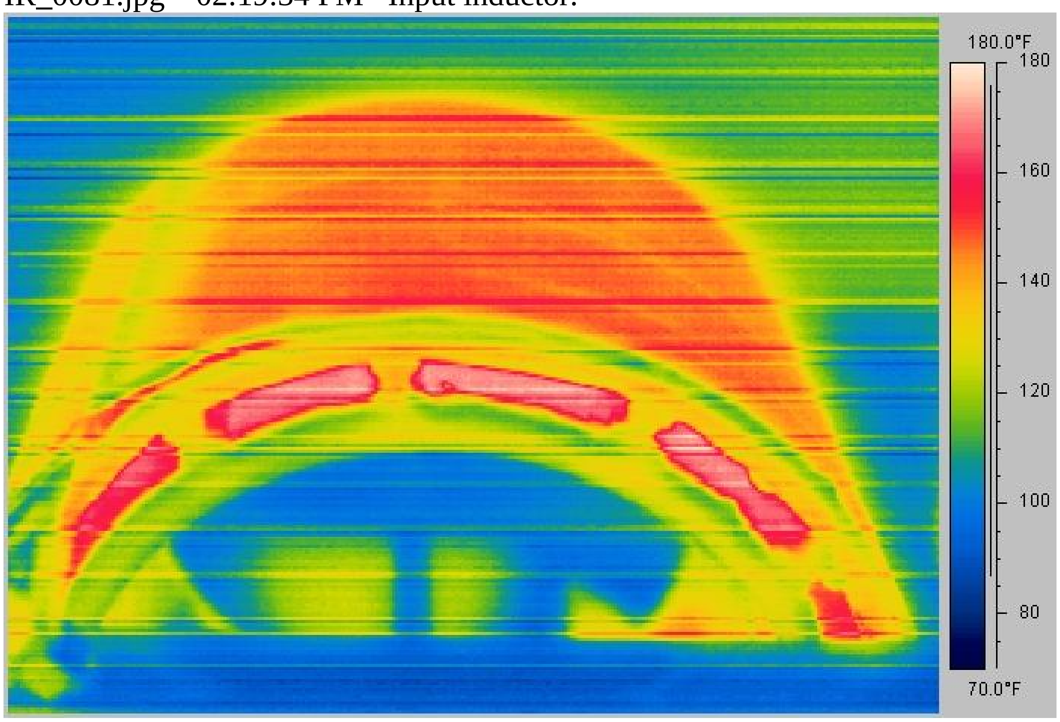

Note: The wind converter was shut off at 2:38:06 PM. However, the control board still received power. From this point in time and on, the wind converter components should be cooling, except for the control board components which still had power.

IR_0099.jpg 02:39:50 PM I/O inductors. Converter cooling.

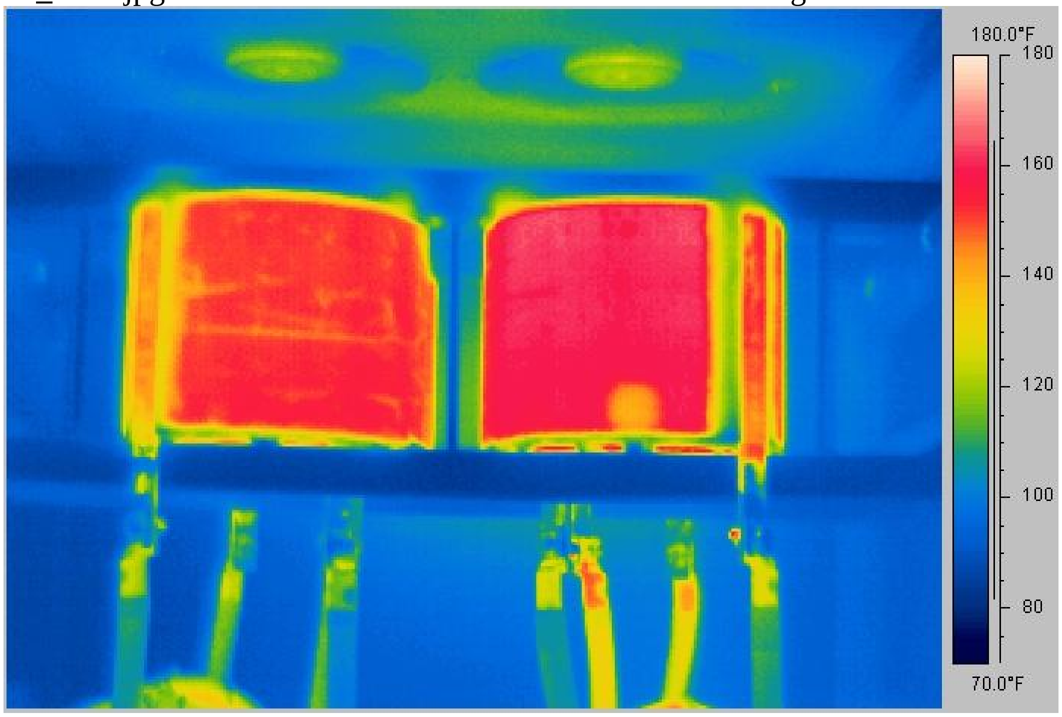

IR_0100.jpg 02:40:42 PM Converter cooling.

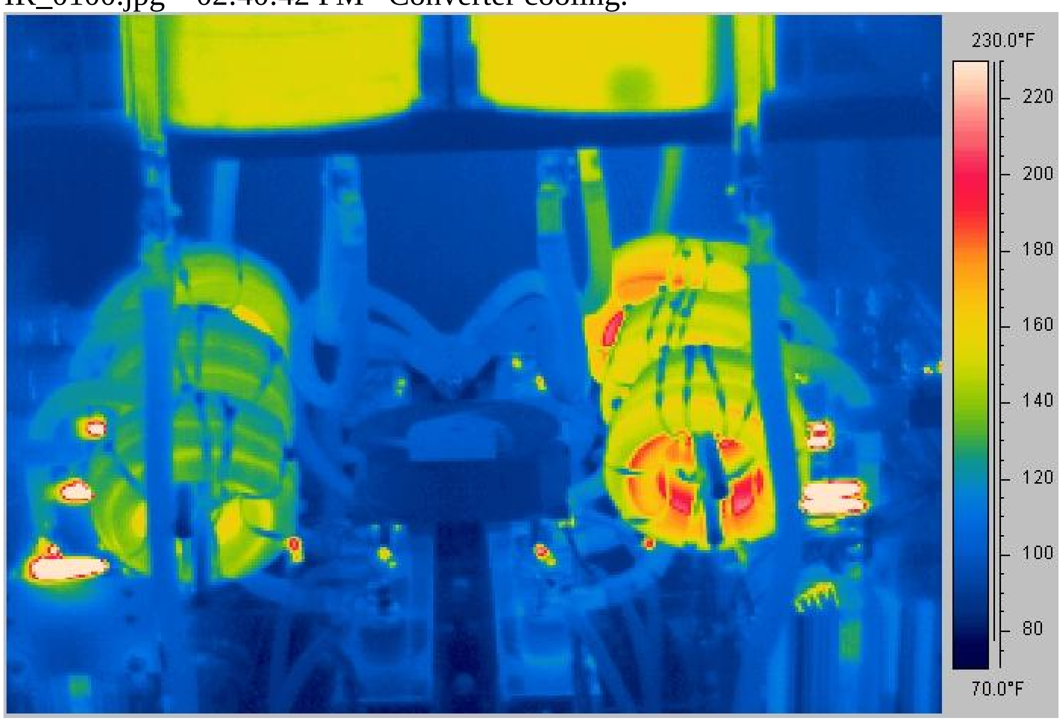

IR_0101.jpg 02:41:30 PM Output inductors. Converter cooling.

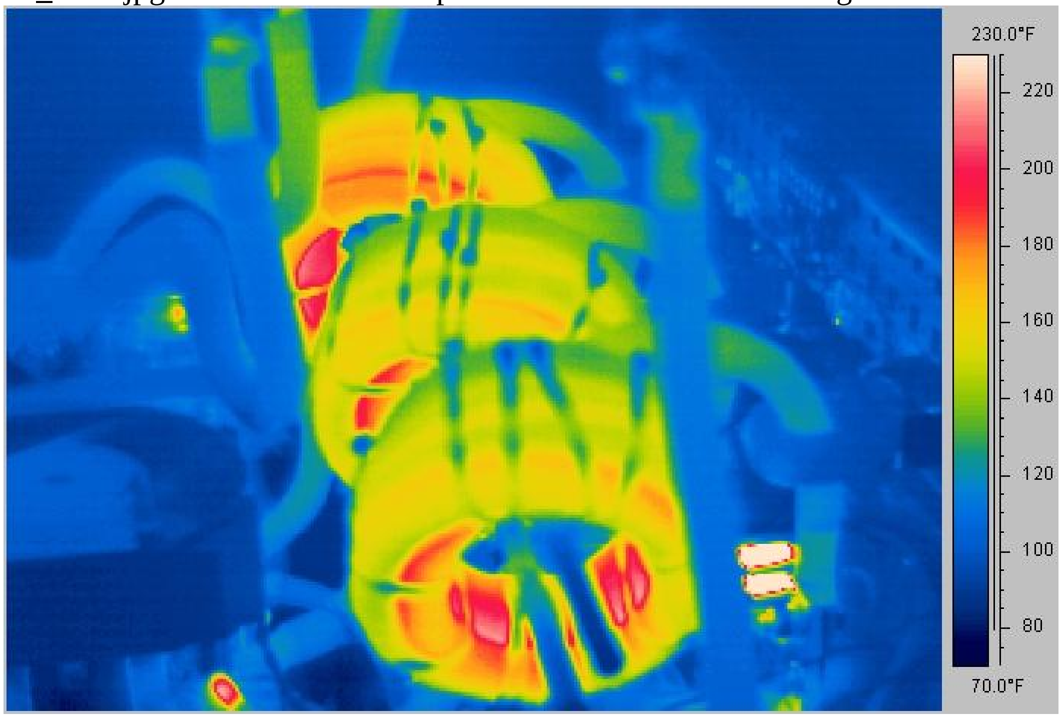

IR_0102.jpg 02:41:58 PM Converter cooling.

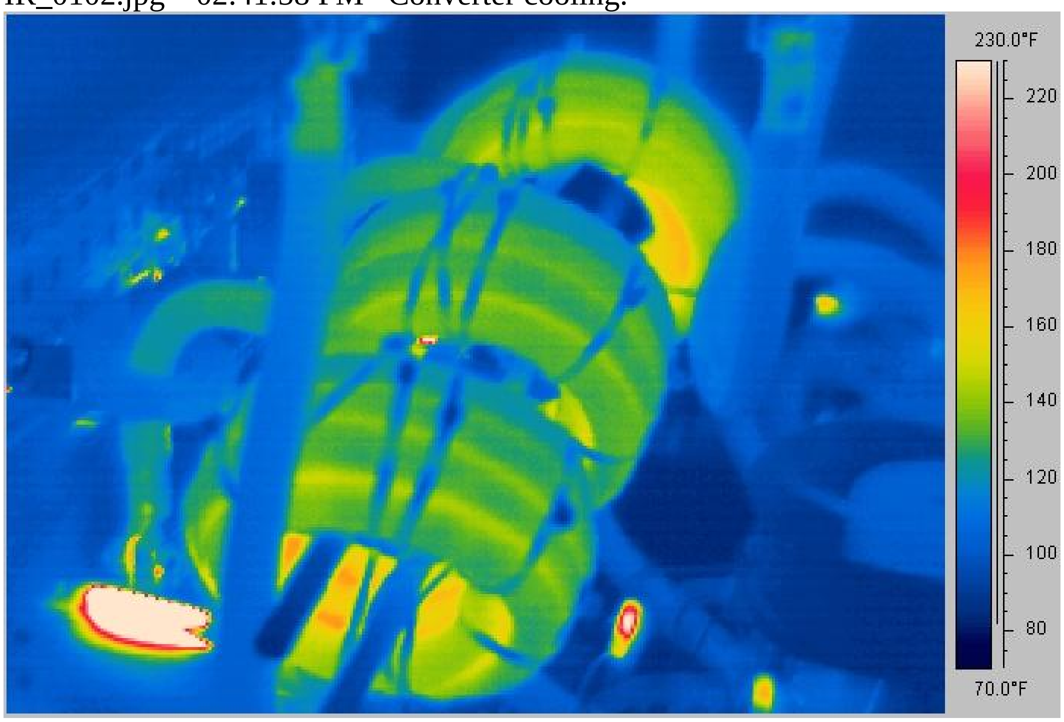

Thermal Testing Staff and Report Authors

IR_0104.jpg 02:43:28 PM Lower heat sink and SCRs on output side.

Converter cooling.

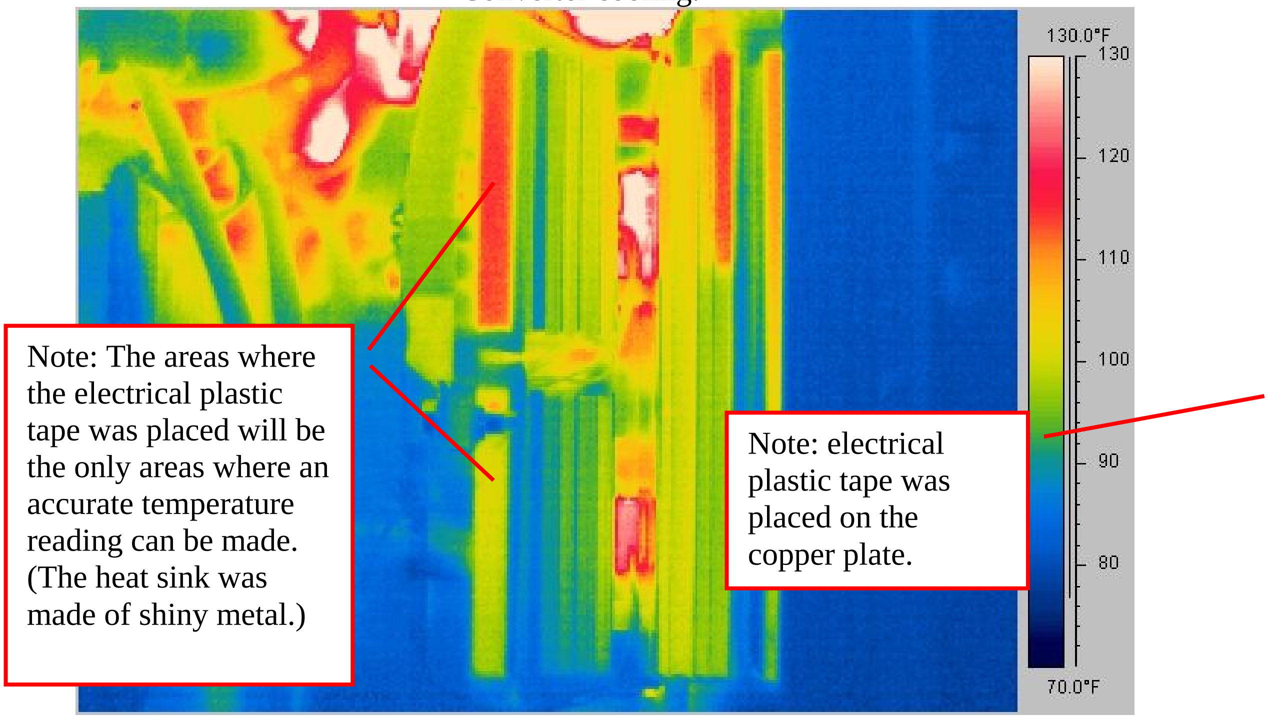

Note: Power to the control board was terminated at 2:47:25 PM.

Mark

Sig

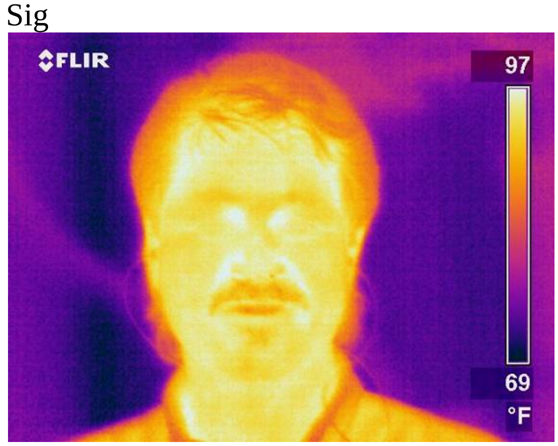

NOTE: The hot-spots on the control system were determined to be from two small jumpers that were connecting the wrong pins. The incorrect connections did not cause malfunctioning of the system, but caused shorts between chip pins and excessive heating. The DETL team was able to remotely modify the jumpers with PPS' help.

Appendix E – Operational Testing Results from Sandia December 12th 2005 (Prototype)

Sandia National Laboratories
Operated for the U.S. Department of Energy by
Sandia Corporation

Sigifredo Gonzalez
SMTS

P.O. Box 5800
Albuquerque, NM 87185-1033

Phone: (505) 845-8942
Fax: (505) 844-2890
Internet: sgonza@sandia.gov

February 14, 2006

Darren Hammell
Princeton Power Systems

Utility interconnection and performance evaluations were conducted on a beta version of Princeton Power Systems (PPS) AC-Link 100kW 480V wind power converter at Sandia National Laboratories Distributed Energy Technologies Laboratory. The PPS AC-Link wind power converter uniquely converts the wind generator's varying frequency/voltage power to utility grade ac power. Since the ac source used to simulate the wind generator has a limit of 50kW/62kVA the PPS converter was configured for 50kW maximum rating. Figure 1 provides a one-line diagram of the converter's input and output connections and transducer locations.

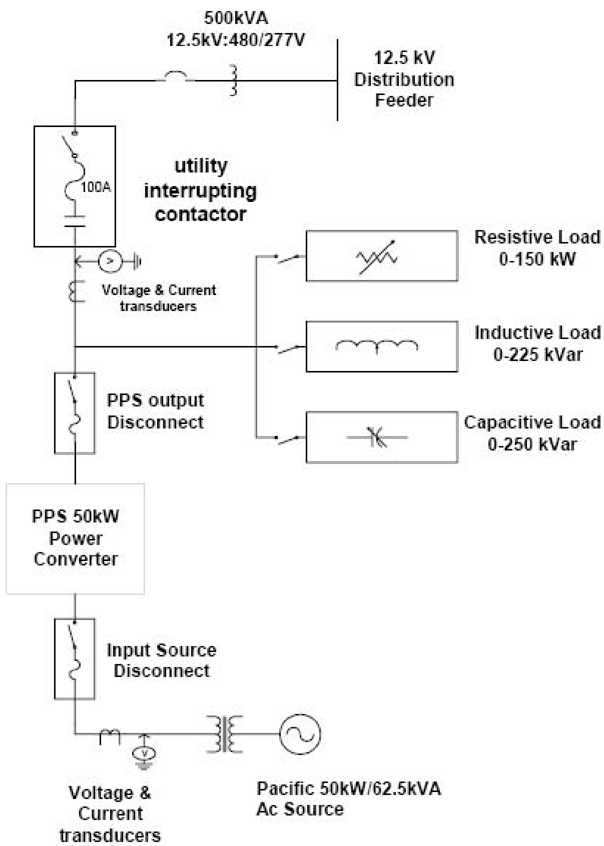

Figure 1. PPS AC Link one-line configuration diagram

Test Configuration

Evaluations on the alpha unit indicated the methods to measure line voltage and frequency were adequate to operate within utility interconnection voltage and frequency operating requirements, therefore, evaluations to determine the voltage and frequency operating range of the beta unit were not conducted. The evaluations conducted on the beta unit consist of islanding tests and converter performance evaluations. Test criteria are specified in UL 1741[1] and IEEE 929-2000[2]. Figure 1 shows a simplified diagram of the test configuration. For these evaluations the AC Link was energized by a Pacific 3060 MS Series power-electronics-based variable ac voltage source. The output of the converter was varied by programming the Pacific ac voltage source to a constant voltage and varying the frequency. A LabView-based data acquisition system utilizing the transducers shown in figure 1 reads the voltages and currents from the transducers, applies the proper scale factors, and uses these values in determining the performance of the device under test.

Anti-islanding Tests

Islanding tests are conducted using the DETL utility feed. Loads are configured and adjusted for each test in accordance with the referenced standards. During an islanding test the contactor disconnects the utility and isolates the loads along with the converter. The time required for the converter to cease energizing its output following loss of utility is monitored and recorded. The most difficult load condition specified by the standards consists of a 60-Hz resonant RLC load matched to the output of the converter. Removal of the utility with this load does not result in any change to the voltage or frequency at the converter terminals that is detectable with passive means. While the probability is very low that such a load would exist at the time the utility was lost, Utility interconnection standards categorize a converter that detects loss of utility with this load condition and ceases to energize its output within two seconds as a "non-islanding converter".

Matched Resonant RLC Load

IEEE 929 and UL 1741 require that the generation source shut down within two seconds following loss of utility with matched 60 Hz resonant RLC loads and the standards require that ten islanding tests be performed at each of four power levels - 25%, 50%, 75% and 100% of rated power. Several islanding tests were performed at 25%, 50% and approximately 100% of rated power. At each power level, the resistive load was adjusted to absorb all real power from the converter, and the reactive loads were adjusted to absorb all reactive power from the converter. The RLC tank circuit was adjusted to have a quality factor (vars/Watts ratio) of 2.5 and tuned for 60-Hz resonance. The 60 Hz resonant tank circuit provides stored energy at 60 Hz and the matched resistive load provides voltage regulation. Initial islanding tests were conducted with the anti-islanding pulse desensitized in order to establish an island. Once the island was established the loads were slightly adjusted to bring the resonant circuit to 60 Hz. The utility was disconnected utilizing a motor contactor that disconnects the utility upon command and a LabView data acquisition system (DAS) records the trigger signal correlating to the removal of the utility and both the voltage and current from the PPS during the island. Figure 6 shows the results of the islanding test at 12.5kW, with anti-islanding detection desensitized. This islanding test resulted in the converter continuing to energize the utility until intervention caused the converter to shutdown. After each islanding event the anti-islanding detection sensitivity was increased until PPS successfully passed the islanding test. Figure 7 shows a successful 12.5kW islanding test. Figure 8 shows the results of islanding tests at 25kW and the anti-islanding detection desensitized resulting in a continuous run on. Figure 9 shows a successful 25kW islanding test. Figure 10 shows the results of islanding tests at 50kW and the anti-islanding detection desensitized resulting in a continuous run on. Figure 11 shows a successful 50kW islanding test.

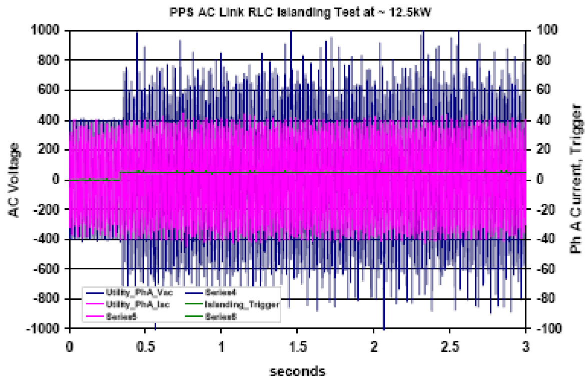

Figure 6. 25% of rated Power Islanding Test with ΔF=1and ΔT=5 on the AI pulse

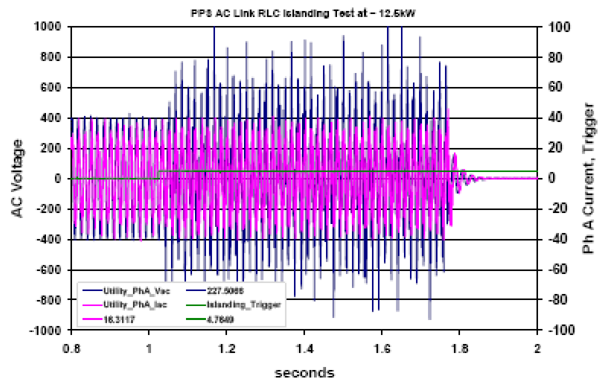

Figure 7. 25% of rated Power Islanding test with ΔF=.05 and ΔT=.66 on the AI pulse

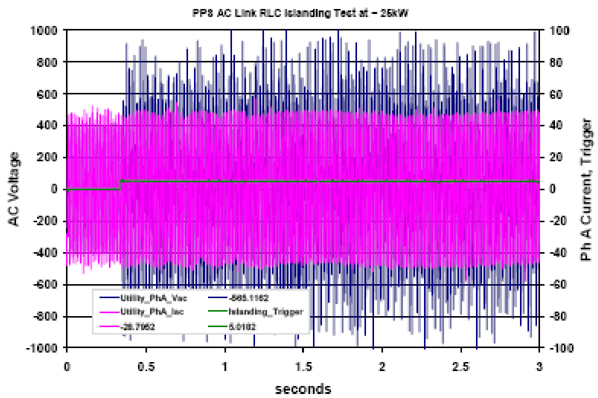

Figure 8. 50% of rated RLC Islanding with ΔF=1and ΔT=5 on the AI pulse

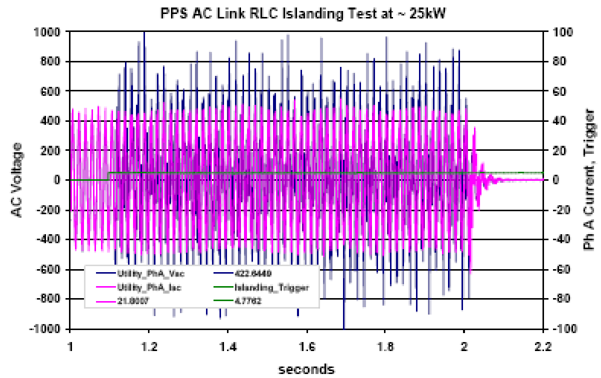

Figure 9. 50% of rated RLC Islanding with ΔF=.05 and ΔT=.66 on the AI pulse

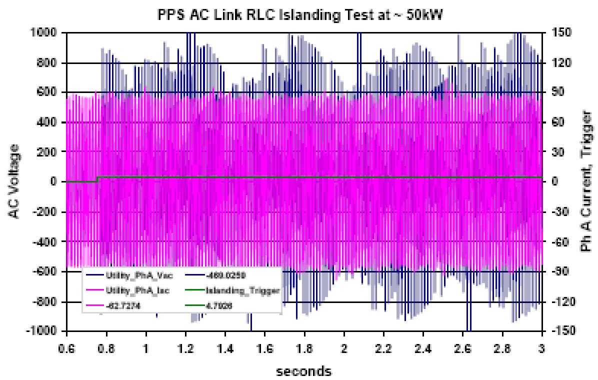

Figure 10. 100% of rated RLC Islanding with ΔF=1and ΔT=5 on the AI pulse

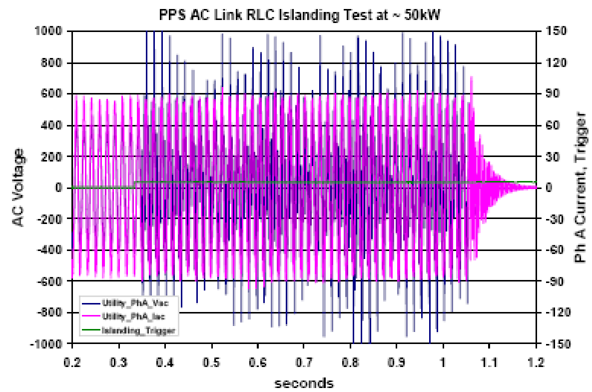

Figure 11. 100% of rated RLC Islanding with ΔF=.05 and ΔT=.66 on the AI pulse

Converter Performance

The performance and power quality of the Princeton Power System converter was analyzed over a range of output power levels. This was accomplished by implementing a watt per Hz profile, where the converter's output power was controlled by ramping the input frequency from 47 to 72 Hz at a fixed input voltage. The frequency is increased linearly from 47 Hz to 72 Hz in 3 minute, held at 72 Hz for 5 seconds, and then reduced to 47 Hz in minute. This process is repeated at different voltages and the results are presented below.

With the output impedance of the Pacific power electronic ac source not having comparable inductance expected on a typical asynchronous generator, the input source voltage and currents experienced high distortic When our DAS is monitoring all three phases, the sampling frequency is reduced enough that the input pow cannot be reliably calculated. Therefore the number of channels was reduced to monitor a single phase on t input and the output to the PPS converter. With the increase in sampling frequency the input and outp calculated power agreed with a Yokogawa Power analyzer, which has a much higher sampling rate. The da presented below is data gathered only on phase C of the PPS converter and phase C of the input source.

Figure 13 shows the converter's output as the frequency is varied. PPS AC Link was programmed to beg energizing the utility when the input frequency exceeded 50 Hz and de-energize the utility when the frequen drops below 50 Hz. Figure 14 shows the efficiency at different power levels. At low power levels, the Paci AC source does not have comparable inductance to a type wind generator. Figure 15 shows our facility's volta THD is slightly above 2.2 % and the converter current THD is slightly above 4% while operating at 47kW a this configuration. Figure 16 shows the power factor values recorded per phase and figure 17 shows the pow (watts) out of each phase

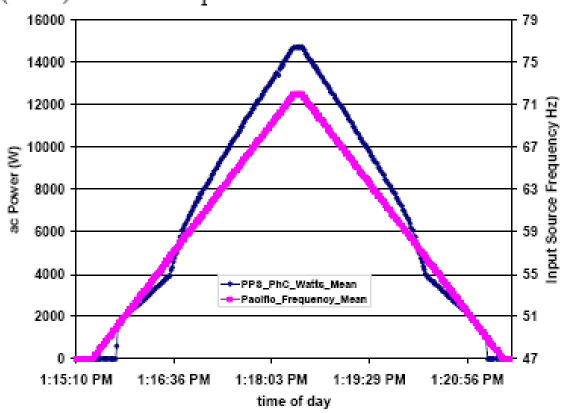

Figure 13. Power Profile of AC-Link

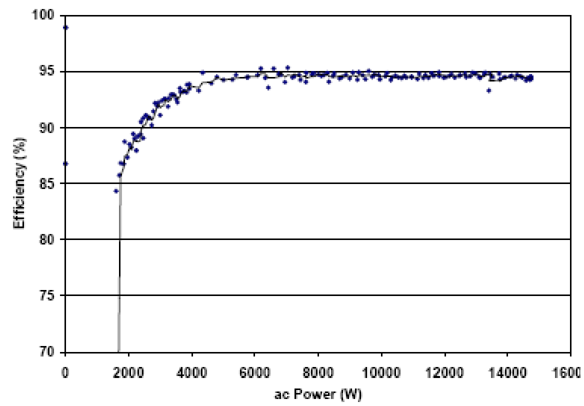

Figure 14. Efficiency (%) with Source voltage =297

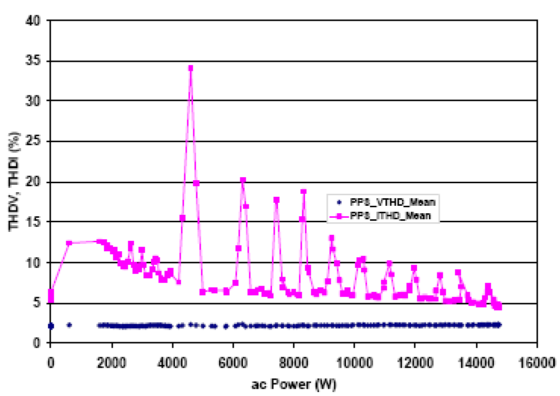

Figure 15. THD on grid voltage and PPS Current

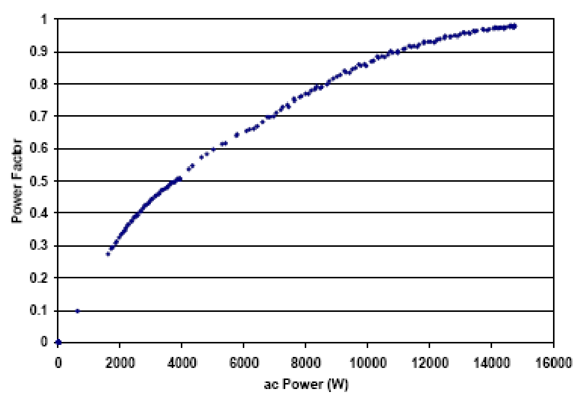

Figure 16. PPS Power factor at various power levels

4

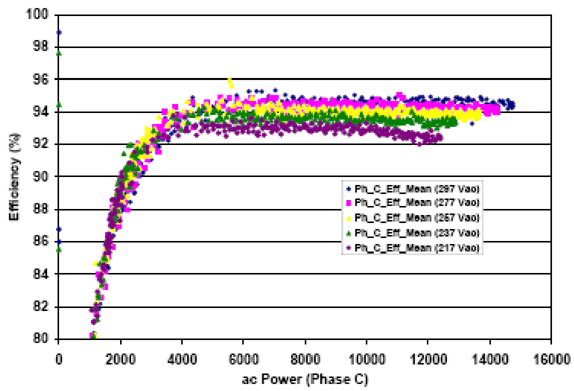

Figure 17. PPS efficiency at various input voltages

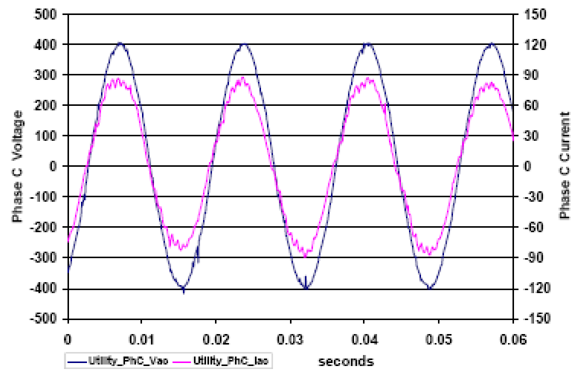

Figure 18. PPS Phase C voltage/current waveforms

Test Summary

Islanding evaluations were conducted at 25%, 50%, and 100% of rated power. At each of the power levels an islanding condition was established by desensitizing the anti-islanding controls and tuning the RLC circuit to resonate at 60Hz. Once the RLC circuit was optimized, the controls were again enabled and an interruption of the utility proved the anti-island method was adequate at preventing an island, even with a finely tuned circuit. The evaluations conducted on the Princeton Power System AC-Link Power Converter indicate adherence to UL 1741 requirements. Additionally, laboratory evaluations demonstrated the flexibility and ease to change and enhance software parameters, enabling compliance to interconnection requirements. The power quality analysis showed the AC-Link's current THD was below 4% at 46kW and the efficiency was > 94% when the source voltage was set to 297.

Below is a list of suggestions where further development and investigation that may increase the performance of the converter.

1. Design circuitry and add hardware to remove the converter from utility interconnection when not exporting power. This will increase daily kWH produced.
2. Investigate high temperature operation at rated power.
3. Investigate voltage levels when the utility is removed and turbine is still contributing energy.

References

[1] UL 1741, Std 1741, Static Inverter and Charge Controllers for Use in Photovoltaic Systems, Underwriters Laboratories Inc, North Brook, ILL

[2] IEEE 929 Std 929-2000, *IEEE Recommended Practice for Utility Interface of Photovoltaic (PV) Systems,* Institute of Electrical and Electronics Engineers, Inc., New York, NY.

Sandia National Laboratories is a multi-program laboratory operated by Sandia Corporation, a Lockheed Martin Company, for the United States Department of Energy under Contract DE-AC04-94AL85000

PV Program Disclaimer

Appendix F – Thermal Imaging Testing Results from Sandia (Prototype)

Input SCRs

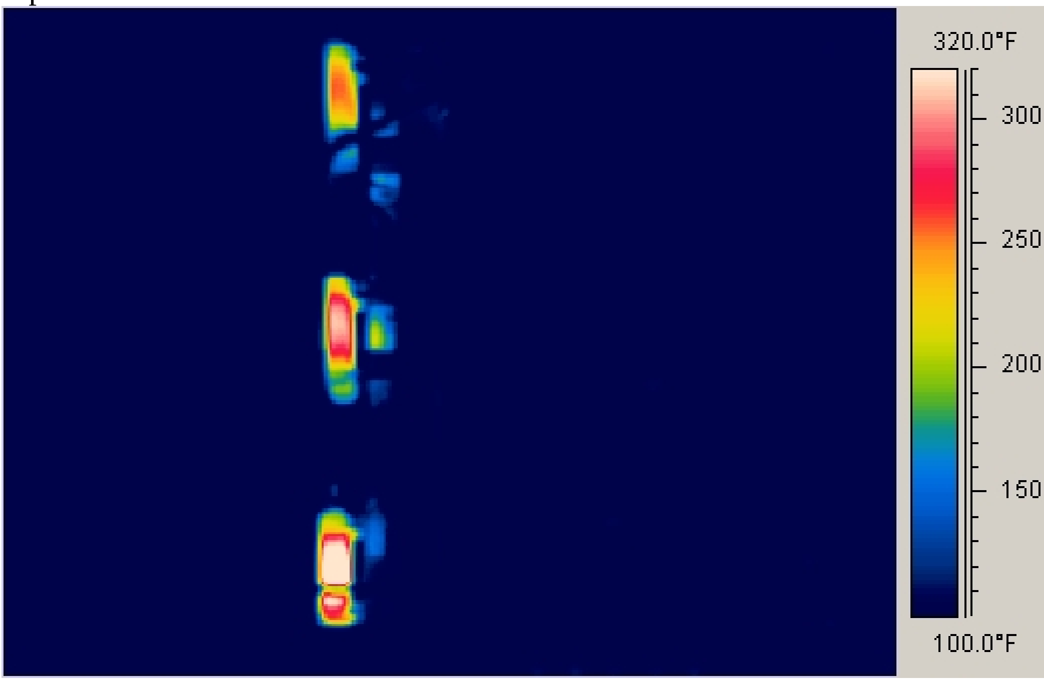

Output SCRs

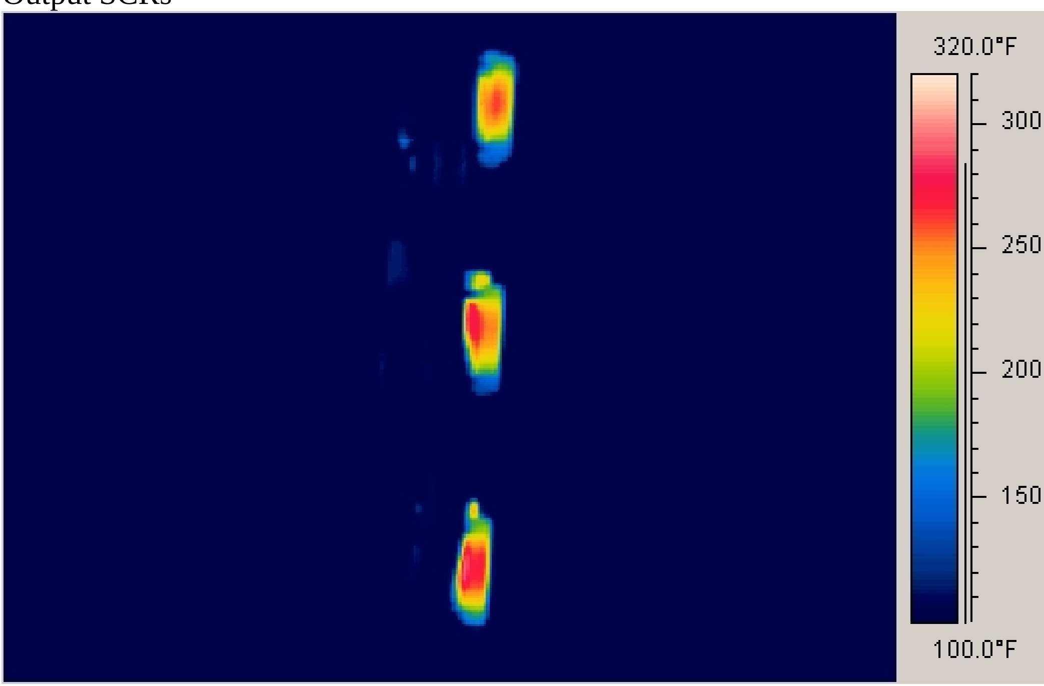

Main Control Board

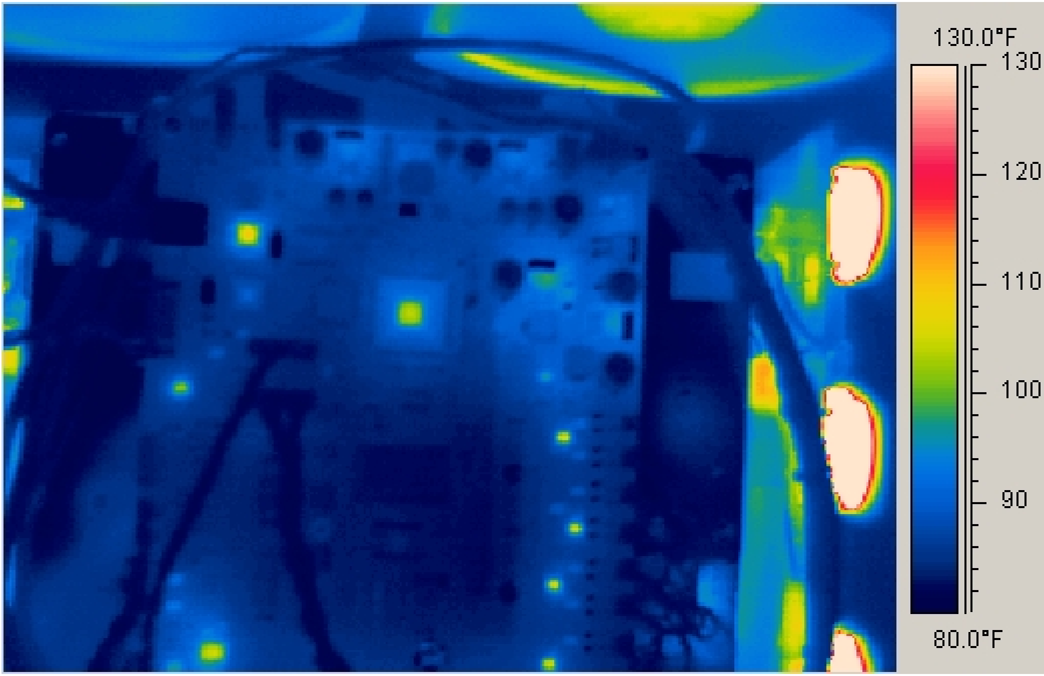

Auxiliary Control Boards (Optical Daughter Card, I/O board, power resistors)

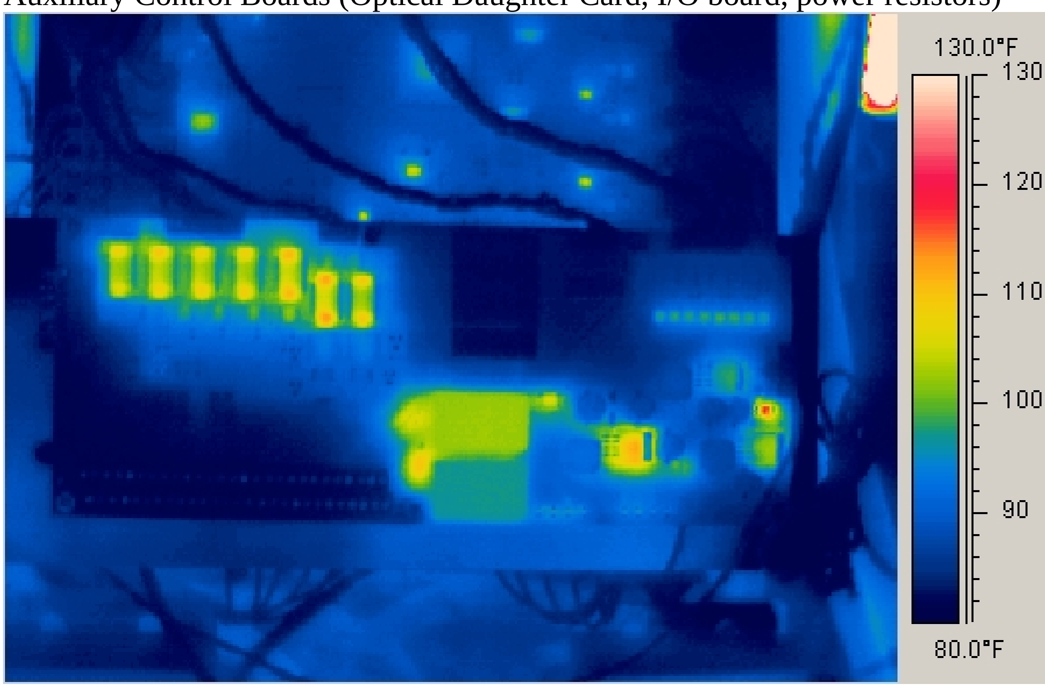

Charging inductor (nanocrystalline core, litz-wire wound)

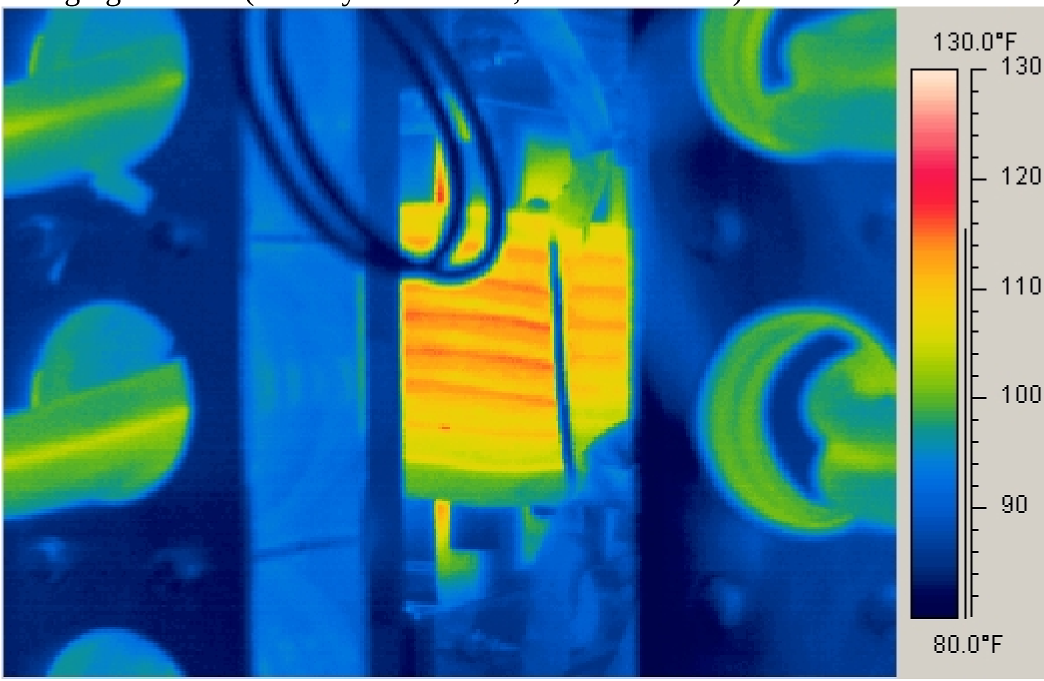

Charging inductor

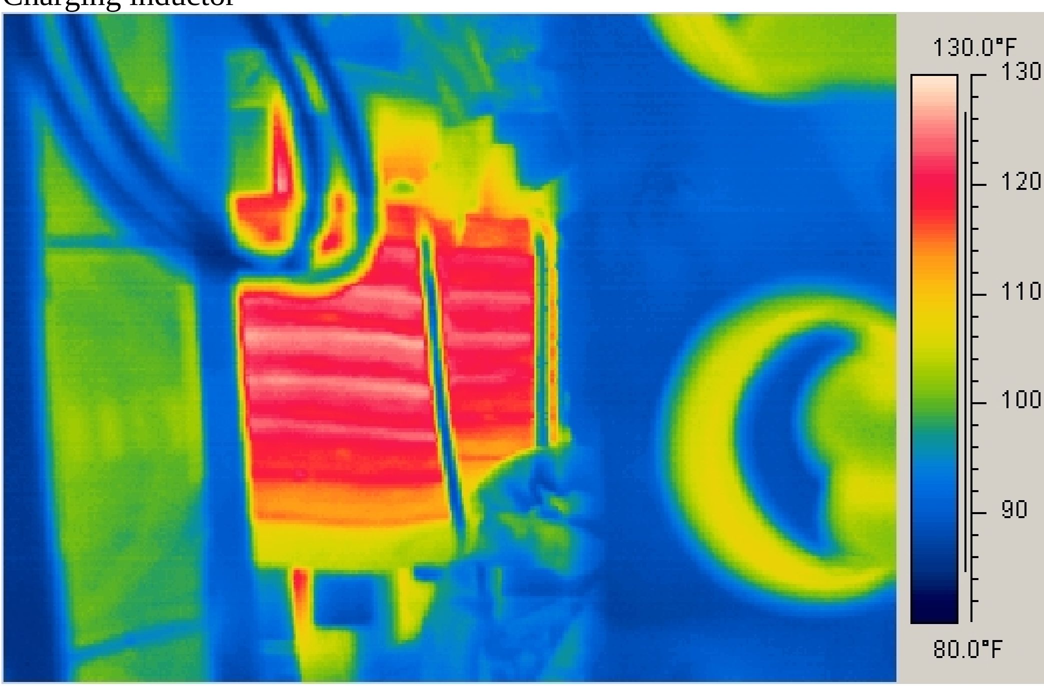

References:

Gonzalez, Sigifredo and Rumsey, Mark, “Thermal Imaging Test of the Princeton Power Systems Wind Power Converter”, October 14, 2005.

Holveck, Mark and Jacobson, Casey, “Sandia DETL Test Results, Princeton Power Systems 50kW Wind Converter”, September 14, 2005.

Holveck, Mark, “Princeton Power Systems Small Wind DETL Testing Plan”, August 11, 2005.

Hammell, Darren et al, “Final Review: Low Wind Speed Technology for Small Turbine Development”, presentation, April 4th, 2006, Broomfield, CO.

END